UNIVERSITY OF PAVIA

Department of Biology and Biotechnology "L. Spallanzani"

XXIX cycle

Doctoral school in Biomedical Sciences - Program in Physiology

Coordinator: Prof. *Egidio D'Angelo*

Oxytocin modulates $GABA_A$ receptor-mediated inhibition onto CA1 pyramidal neurons in mouse

Tutor:

Prof. *Mauro Toselli*

Student:

Dr. *Claudia Maniezzi*

Academic year 2015/2016

TABLE OF CONTENTS

1. ABSTRACT

Oxytocin (OT) is a neuropeptide widely known for its peripheral hormonal effects. However, OT also acts as a neurotransmitter or neuromodulator in the central nervous system controlling processes of attachment, social exploration, recognition and aggression, as well as anxiety, fear conditioning and fear extinction. Some electrophysiological experiments have demonstrated that OT exerts direct effects on specific neuronal populations in the hippocampal formation. In particular, it has been shown that extracellular perfusion of TGOT (Thr^4,Gly^7-oxytocin), a selective OT receptor (OTR) agonist, is able to determine an increase in the frequency and the amplitude of spontaneous inhibitory postsynaptic currents (sIPSC) recorded from CA1 pyramidal neurons (PYR) in rats. More recently, it has been demonstrated that the TGOT-induced increased inhibition arises mainly from fast-spiking GABAergic interneurons (INs) that respond to TGOT with a depolarization. Overall, these literature data indicate that OT is able to modulate the inhibitory synaptic transmission in the hippocampal CA1 field of rats, by targeting a specific class of INs.

Taking the cue from those findings, we planned to characterize in detail the neuromodulatory effects of OT in mouse. In order to exclude any activation of vasopressin receptors by OT, we used the selective OTR agonist TGOT (1 μM). Electrophysiological experiments were performed using the whole-cell patch-clamp technique applied to transversal brain slices. Recordings were carried out on PYRs and GABAergic INs located in CA1 *stratum pyramidale*. For the experiments, three groups of mice were used: i) wild-type that normally express OTRs ($Otr^{+/+}$), ii) knock-out for OTRs in the entire body ($Otr^{-/-}$) and iii) GAD67-GFP^+ (Δneo) in which GABAergic INs are labelled with GFP (Green Fluorescent Protein). After a preliminary analysis of passive membrane properties, performed to assess the overall health of neurons, the effect of TGOT was evaluated on spontaneous inhibitory postsynaptic currents (sIPSC) recorded from PYRs in $Otr^{+/+}$ mice. Our data shown that TGOT caused a significant decrease in the sIPSC interval and a significant increase in the sIPSC amplitude, in agreement with data reported by others. Interestingly, TGOT was able to affect also the sIPSC kinetics properties, causing a significant increase in their time constant of decay: this suggests the involvement of $GABA_A$ receptors ($GABA_AR$) located in a perisynaptic position, i.e., just outside the postsynaptic density, whose distinctive feature is to deactivate slower than synaptic receptors, generating slower sIPSCs. The inhibitory currents modulated by

TGOT were mediated by the activation of $GABA_A$Rs, being blocked by the $GABA_A$R antagonist bicuculline (10 μM). Finally, we demonstrated that the TGOT-induced effects were highly dependent on the activation of OTRs, since were abolished by SSR126768A (0.1 μM), an antagonist selective for the murine isoform of OTRs. Furthermore, TGOT was not able to modulate sIPSCs in $Otr^{-/-}$ mice, emphasizing the necessary presence of OTRs for the induction of responses. In order to understand the mechanism through which TGOT increases the level of the inhibitory transmission onto PYRs, we recorded the miniature inhibitory postsynaptic currents (mIPSC), isolated by applying tetrodotoxin, a voltage-gated Na^+ channel blocker, in order to prevent action potential firing in the presynaptic terminal. TGOT was not able to cause changes in mIPSC interval, amplitude and kinetics of decay, indicating that the effects elicited by the agonist are strictly dependent on the firing activity of the presynaptic neuron. By contrast, TGOT had no significant effects on spontaneous excitatory postsynaptic currents (sEPSC).

After having clarified the action of TGOT on 'phasic' inhibitory transmission, elicited by the activation of synaptic and perisynaptic $GABA_A$Rs, we enquire if the peptide could have some effect on 'tonic' currents, mediated by the activation of extrasynaptic receptors. We demonstrated the presence of tonically active $GABA_A$R-mediated currents by measuring the 'baseline holding current' required to clamp PYRs at a given potential in voltage-clamp mode. Recordings were performed in control conditions and during the application of bicuculline (10 μM), according to the standard method described in literature. We observed an inward shift in the 'baseline holding current' in the presence of bicuculline, consistent with the abolition of tonic currents. Subsequently, we evaluated the effect of TGOT on the 'baseline holding current', in order to investigate a putative modulation elicited by the agonist. Actually, we observed an outward shift in the 'baseline holding current' during perfusion of TGOT, consistent with an increase in tonically active currents.

Since TGOT was able to modulate both phasic and tonic GABAergic transmission onto PYRs, we tried to understand the source of that increased inhibition. We found that TGOT was able to depolarize mainly a specific subpopulation of GABAergic INs. Interestingly, the analysis of the firing pattern revealed that the majority of the responding INs were stuttering fast-spiking cells. The same depolarization was observed in the presence of blockade of both $GABA_A$Rs and glutamatergic receptors, suggesting that the TGOT-induced effect on fast-spiking INs is due to a direct binding to OTRs. Indeed, the perfusion of the antagonist selective for the murine isoform of OTRs completely abolished the depolarization.

Furthermore, in neurons modulated by TGOT the presence of OTRs was confirmed by some single-cell reverse transcription (RT)-PCR experiments. Preliminary experiments were performed as well to investigate the putative ionic mechanism underlying the TGOT-induced depolarization. OTRs are 'promiscuous' G protein coupled receptors, displaying affinity for the $G_{q/11}$ protein. A downstream effector of $G_{q/11}$ is protein kinase C (PKC) that phosphorylates different target proteins, including L-type voltage-gated Ca^{2+} channels. We tested the putative involvement of a Ca^{2+} current in the TGOT-induced depolarization by using nifedipine, a selective L-type channel blocker. Actually, in the majority of INs examined nifedipine was able to abolish the depolarization elicited by TGOT. However, given the considerable heterogeneity of intracellular pathways activated by OTRs, we cannot exclude the involvement of other ionic conductances modulated by TGOT.

Finally, we investigated the consequences of TGOT perfusion on the membrane potential of PYRs. Most of them, examined at their spike threshold, became hyperpolarized by TGOT and their firing rate was significantly decreased. The hyperpolarizing response was completely abolished by the blockade of both $GABA_A$Rs and glutamatergic receptors, indicating that the effect requires the activation of $GABA_A$Rs that generate a hyperpolarizing current. The long duration of the hyperpolarization suggest the involvement of extrasynaptic rather than synaptic $GABA_A$Rs: indeed, extrasynaptic $GABA_A$Rs give rise to a tonic inhibition that is much more prolonged than that mediated by synaptic $GABA_A$Rs.

Since the main consequence of the hyperpolarization is a reduction in cell excitability, we asked if TGOT was able to alter the capability of PYRs to generate action potentials in response to depolarizing current steps. Our analysis revealed that in the presence of the agonist, the firing frequency of PYRs was lower than that obtained in control conditions with the same current injection. This was also evident in the firing rate-to-injected current (F-I) relationship that was shifted to the right during perfusion of TGOT. As described in literature, a rightward shift in the F-I curve is attributable to an increase in tonically active inhibitory currents: this leads to a persistent reduction in the input resistance and therefore in cell excitability. The gain (i.e., the slope) of the F-I relationship was not influenced by TGOT, in agreement with the reported observation that in hippocampal PYRs an increase in tonic inhibition modulates predominantly the neuronal offset but has minimal effects on neuronal gain.

In conclusion, TGOT can influence the activity of hippocampal GABAergic cells and therefore regulate the operational modes of the downstream PYRs.

2. AIM OF THE WORK

The aim of the present work is to provide the electrophysiological characterization of the effects of oxytocin (OT) in CA1 hippocampal region. It takes the cue from some published data showing that:

i) OT acts as a neurotransmitter or neuromodulator in the central nervous system controlling processes of attachment, social exploration, recognition and aggression, as well as anxiety, fear conditioning and fear extinction [Meyer-Lindenberg et al., 2011],

ii) OT affects both consolidation and retrieval of memory [De Wied, 1991], by enhancing long-term potentiation (LTP) at Schaffer's collaterals-CA1 synapses in the hippocampus [Tomizawa et al., 2003],

iii) OT modulates the excitability of specific neuronal populations in the hippocampal formation [Mühlethaler et al., 1983; Tiberiis et al., 1983; Mühlethaler et al., 1984; Raggenbass et al., 1989; Raggenbass, 2001; Owen et al., 2013].

The pivotal study by Zaninetti and Raggenbass on rats [2000] has shown that extracellular perfusion of TGOT (Thr^4,Gly^7-oxytocin), a selective OT receptor (OTR) agonist, is able to increase the inhibition onto CA1 pyramidal neurons (PYR). More recently, Owen and colleagues [2013] have demonstrated that a specific population of GABAergic interneurons (IN) is directly modulated by TGOT.

On this basis, in our work we proposed to investigate in detail the hippocampal network involved in the oxytocinergic system in mice. For this purpose, we evaluated the action of TGOT on the inhibitory and excitatory transmission mediated by synaptic receptors onto CA1 PYRs. To elucidate the importance of OTRs in the TGOT-mediated effects, we used both $Otr^{+/+}$ and $Otr^{-/-}$ mice: the first normally express OTRs, whereas the latter are knock-out for receptors in the entire body. Moreover, we assessed the action of TGOT on tonic inhibitory currents, mediated by the activation of extrasynaptic receptors that are widely described in CA1 PYRs [Banks & Pearce, 2000; Scimemi et al., 2005; Mortensen & Smart, 2006; Prenosil et al., 2006; Pavlov et al., 2009]. Then, we tried to identify the neuronal target of TGOT and the putative ionic mechanisms underlying the TGOT-mediated effects.

Finally, we studied the consequences of TGOT perfusion on the membrane potential of PYRs, focusing on alterations in their capability to generate action potentials in response to depolarizing current steps.

3. INTRODUCTION

3.1 Oxytocin (OT)

3.1.1 OT molecular structure

OT is a nonapeptide organized in a six-amino acid cyclic portion, delimited by two cysteine residues (Cys1 and Cys6) linked by a disulphide bridge, and a carboxyl-terminal α- amidated three-residue tail [Gimpl & Fahrenholz, 2001] (**fig. 1**). OT is structurally similar to the antidiuretic hormone arginine-vasopressin (AVP) which differs from OT in two residues: at the 8th position AVP possesses an arginine (Arg) in most mammals, while OT a leucine (Leu); at 3rd position AVP possesses a phenylalanine (Phe) while OT an isoleucine (Ile). The presence of Arg8 in AVP is essential for stimulating AVP receptors whereas the presence of Ile3 in OT is important for the activation of OT receptors [Gimpl & Fahrenholz, 2001].

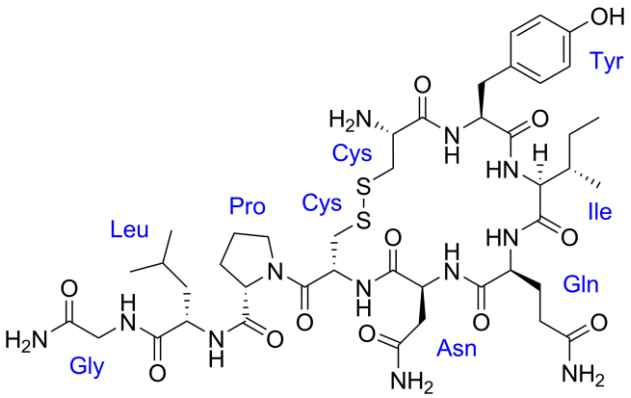

Fig. 1. OT molecular structure.

3.1.2 OT gene expression and post-translational processing

OT and AVP are ancient peptides, members of a phylogenetically conserved family [Donaldson & Young, 2008].

In mouse, rat and human genomes, OT and AVP genes are located on the same chromosomal locus, separated by a short (3,5-12 kbp) intergenic region [Hara et al.,1990; Gainer et al., 2001], but are transcribed in opposite directions. This type of genomic arrangement could result from the duplication of a common ancestral gene, followed by the inversion of one of the genes [Gimpl & Fahrenholz, 2001].

The human gene for OT-neurophysin I is mapped to chromosome 20p13 [Rao et al., 1992] and consists of three exons: the first encodes a translocator signal, the nonapeptide hormone, the tripeptide processing signal (GKR), and the first nine residues of neurophysin; the second encodes the central part of neurophysin (residues10–76); and the third encodes the carboxyl terminal region of neurophysin (residues 77– 93/95) (**fig. 2**) [Gimpl & Fahrenholz, 2001].

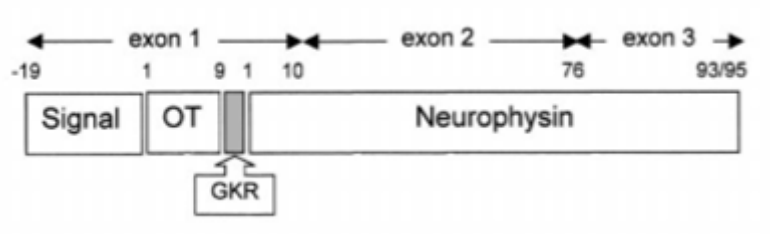

Fig. 2. Domain organization of OT pre-propeptide including the processing sites. The precursor is splitted into the three fragments by enzymatic cleavages, one involving a glycyl-lysylarginine (GKR) sequence. Adapted from [Gimpl & Fahrenholz, 2001].

The expression of the OT gene generates mRNA encoding a pre-propeptide in which OT is complexed in a 1:1 ratio with neurophysin, a small (93-95 residues) disulphide-rich protein. The main function of neurophysin appears to be related to the proper targeting, packaging, and storage of OT within the granules before release into the bloodstream [Gimpl & Fahrenholz, 2001]. Significant processing of the OT pre-preopeptide, such as endoproteolytic cleavages and carboxyl terminal amidation, partly takes place in the granules that contain the enzymes for post-translational modification during the transport to the axon terminal [Stoop, 2012].

3.1.3 OT release and diffusion

In the central nervous system, the OT gene is primarily expressed in *magnocellular* neurons in the hypothalamic paraventricular (PVN) and supraoptic (SON) nuclei. Action potentials in these neurosecretory cells trigger the release of OT from their axon terminals in the neurohypophysis [Poulain & Wakerley, 1982]. The hormone enters the bloodstream together with OT secreted by peripheral tissues (e.g. uterus, placenta, amnion, corpus luteum, testis) and acts on its targets. The typical actions of peripheral OT are stimulation of uterine smooth muscle contraction during labour and milk ejection during lactation [Kiss & Mikkelsen, 2005].

Furthermore, *magnocellular* neurons in the SON release large amounts of OT and AVP in

the central nervous system: interestingly, this release takes place at the level of their dendrites, as evidenced by the ultrastructural visualization of omega fusion profiles that mark sites of exocytosis [Pow & Morris, 1989]. Importantly, dendritic release *in vivo* does not parallel axonal release [Ludwig, 1998]. For example, in rats OT, involved in body fluid homeostasis and systemic osmotic stimulation, promptly activates secretion of the peptide into the blood. The same stimuli also evoke OT release from dendrites in the SON, but not at the same time (dendritic release appears to be delayed by >1 h and persists for much longer) [Ludwig et al., 1994]. Depending on the nature of the physiological stimulus to OT-containing cells, their response might involve an increase in the dendritic release with or without an increase in electrical activity at the cell bodies: in this way, dendritic and axonal release of the peptide can be regulated wholly independently. OT itself is able to elicit dendritic release: the binding of OT to the receptors expressed on dendrites or soma of *magnocellular* neurons elevates intracellular Ca^{2+} concentrations and triggers exocytosis of vesicles; once dendritic peptide release is triggered, because of the peptide feedback, dendritic release can be self-sustaining and, therefore, long-lasting. This generates synchronous pulses of activity, leading to autoregulatory effects. OT also stimulates the production of endocannabinoids, which act on afferent terminals to inhibit glutamate release and, therefore, indirectly inhibit OT neurons [Hirasawa et al., 2004]. Results from *in vitro* studies also indicate that OT acts both pre- and postsynaptically to attenuate the effects of GABA inputs [Brussaard et al., 1996; Koksma et al., 2003; De Kock et al., 2004]. These complex actions suggest that the peptide augments excitatory interactions between OT cells while reducing the effects of external inputs, so facilitating synchronization of their activity. In the PVN another population of OT-staining neurons has been identified: *parvocellular* neurons that terminate elsewhere in the central nervous system. OT-releasing fibers have been described in various brain areas in rats: the dorsomedial hypothalamic nucleus, several thalamic nuclei, the dorsal and ventral hippocampus, *subiculum,* entorhinal cortex, medial and lateral septal nuclei, amygdala, olfactory bulbs, mesencephalic central gray nucleus, *substantia nigra, locus coeruleus*, raphe nucleus, the nucleus of the solitary tract, and the dorsal motor nucleus of the vagus nerve [Gimpl & Fahrenholz, 2001]. The axonal projections of *parvocellular* neurons to the brainstem and spinal cord provide these sites with a rich source of OT, but in other brain areas there is a mismatch between the projection fields of OT neurons and sites where OT exerts its behavioural effects, including the regulation of complex social cognition and behaviors [Heinrichs et al., 2009].

The above documented mismatches suggest that central action of OT is mainly mediated by non-synaptic release of the peptide that reaches its targets by diffusion, indeed high concentrations of OT and AVP have been detected in microdialysis samples from discrete areas in conscious animals [Ludwig & Leng, 2006].
Not all centrally projecting OT neurons are located within the *parvocellular* PVN. Extra hypothalamic OT-synthesizing neurons have been found in the triangular nucleus of the septum, the medial posterior region of the bed nucleus of the *stria terminalis* and the medial preoptic area in rodents and primates [Sofroniew & Weindl, 1978].

3.2 OT receptor (OTR)

3.2.1 OTR molecular structure

OTR is a 389 amino acid polypeptide belonging to the rhodopsin-type (class I) G protein-coupled receptors (GPCR) superfamily, members of which possess seven putative transmembrane domains (TM1-7), three extracellular (ECL1-3) and three intracellular (ICL1-3) loops [Stoop, 2012]. The amino-terminal domain is located on the extracellular side while the carboxyl-terminal domain is facing the cytoplasm (**fig. 3**) [Gimpl et al., 2008]. OTR displays the structural hallmarks characteristic of the class I receptors: the Cys residues connected by a disulphide bridge (located in ECL1 and ECL2); two other well-conserved Cys residues within the carboxyl-terminal domain; the aspartate (Asp) residue in TM2 (Asp85 in human OTR) and two or three potential N-glycosylation sites in the extracellular amino-terminal domain. The disulphide bridge between Cys residues seems to be necessary for the correct OTR folding [Barberis et al., 1998]. Most likely, Cys residues in the carboxyl-terminal domain are palmitoylated and anchor the cytoplasmic tail in the lipid bilayer [Gimpl & Fahrenholz, 2001]. The Asp residue is believed to be important for receptor activation [Bockaert & Pin, 1999]. The glycosylation of asparagine (Asn) residues seems to be involved in increasing the efficiency of OTR trafficking and their expression at the plasma membrane [Kimura et al., 1997].

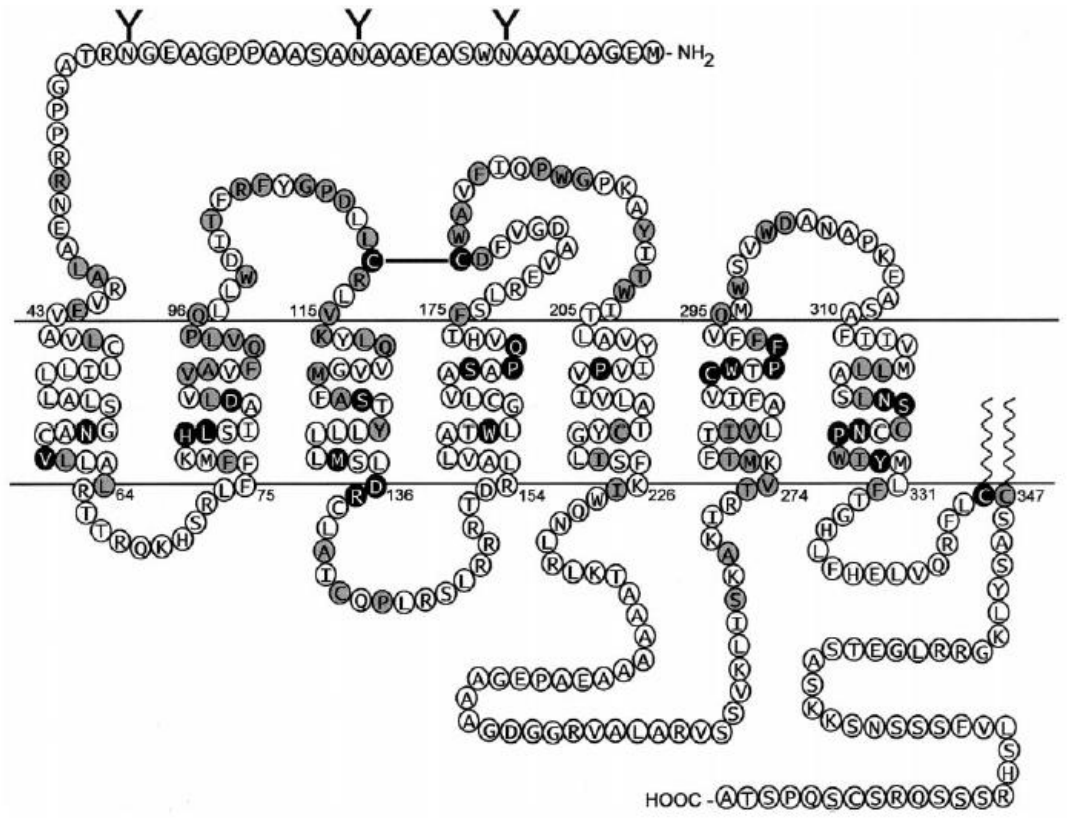

Fig. 3. Schematic structure of the human OTR with amino acid residues shown in one-letter code. The residues conservative within the OTR/AVPR subfamily are outlined in gray, and residues conservative for the whole G protein-coupled receptors (GPCRs) superfamily are outlined in black. The putative N-glycosylation ('Y') and palmitoylation (at C346/C347) sites are marked [Gimpl & Fahrenholz, 2001].

OTR binding pocket is defined by transmembrane helices and surrounded by extracellular loops. In particular, ECL2 binds the cyclic portion of OT [Postina et al., 1996], whereas the linear tail interacts with EL1 which contains a Phe residue (Phe103) that is crucial to determine the ligand selectivity [Chini et al., 1995].

The interaction sites with G proteins are represented by intracellular loops and the carboxyl-terminal [Quian et al., 1998]. Furthermore, the Asp85 residue located in TM2 is involved in mediating the conformational changes that trigger the OTR signalling [Zingg & Laporte, 2003].

3.2.2 OTR signalling pathway

The binding of a selective agonist to GPCRs leads to receptor activation, phosphorylation, and the translocation of β-arrestin to the receptor complex, an event that disrupts the receptor/G protein interaction [Stoop, 2012].

OTR is defined as 'promiscuous receptor' because of its ability to bind different G proteins [Chini et al., 2008; Manning et al., 2008]. This property leads to the involvement of potential activation of different second messengers cascades and consequently to a considerable heterogeneity of responses. For example, OTR is functionally coupled to $G_{q/11}$ protein that stimulates the activity of phospholipase Cβ (PLCβ) isoforms which generate inositol trisphosphate (IP3) and 1,2-diacylglycerol (DAG). IP3 triggers Ca^{2+} release from intracellular stores, whereas DAG stimulates the protein kinase C (PKC) that in turn can phosphorylate different target proteins [Gimpl & Fahrenholz, 2001]. The intracellular Ca^{2+} mobilization initiates smooth muscle contraction [Alberi et al., 1997], increases nitric oxide production which can promote cardiomyogenesis [Danalache et al., 2010] and, in neurons, can modulate inward rectifying conductances [Gravati et al., 2010]. In neurosecretory cells, rising Ca^{2+} levels control cellular excitability, modulate their firing patterns and lead to transmitter release.

In most cell systems studied so far, OT-induced intracellular Ca^{2+} increase is greater in the presence of extracellular Ca^{2+} than that in its absence. This suggests that OT has also effects on Ca^{2+} influx through voltage-gated or ionotropic receptors [Gimpl & Fahrenholz, 2001]. In support of this idea, some data indicate that PKC is able to phosphorylate a subtype of voltage-gated Ca^{2+} channel, the L-type channels, inducing a positive modulation of L-type currents [Yang & Tsien, 1993; Weiss et al., 2012; Satin, 2013]. In neurons, however, OT can also activate inward rectifying currents through a pertussis-sensitive $G_{i/o}$ protein [Gravati et al., 2010].

3.3 The hippocampal formation

3.3.1 Anatomy and connectivity of the hippocampal formation

The hippocampal formation is a bilateral structure located in the medial temporal lobes. In rodents, it appears stretched with a curved crescent-shaped aspect (**fig. 4**). Phylogenetically, the hippocampal formation is the ancient part of the telencephalic cortex, known as archicortex or allocortex, and is divided into three structures: dentate gyrus (DG), Ammon's horn (CA) and subicular complex. Dissecting the hippocampus according to a plane orthogonal to its axis, two C-shaped interlocking cell layers appear (**fig. 5**): the smaller C is

represented by the granular cell layer of DG, whereas the larger C is formed by the pyramidal cell layer of CA and subicular complex [Ramón y Cajal, 1893].

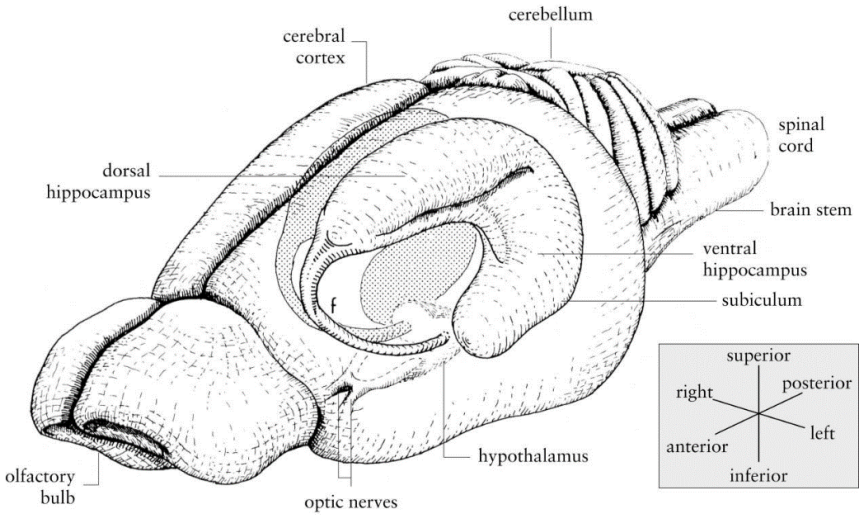

Fig. 4. Hippocampus shape and its localization in rodent brain. Adapted from [Witter & Amaral., 2004].

From a structural point of view, DG maintains a constant cytoarchitecture whereas CA can be further divided into three regions: CA3, the area closest to the *hilus* of DG; CA1, on the other curve of the C continuing to subicular complex, and CA2, between CA3 and CA1. Sometimes, a CA4 area is defined, but it can be taken as the equivalent of the hilar region of DG (**fig. 5**). Subicular complex is divided into *subiculum*, adjacent to CA1, *presubiculum* and *parasubiculum* continuing to enthorinal cortex (EC) (**fig. 5**).

The hippocampal formation is reciprocally connected to subcortical areas (amygdala, mammillary body, hypothalamic nuclei) through the fimbria, a prominent band of white matter along the medial edge of the hippocampus. The connection to the contralateral hippocampus is allowed by commissural fibers. The main cortical afferents to the hippocampus originate from EC through the perforant path, whereas the outputs directed back to the cortex mostly consist of indirect (through the *subiculum*) or direct projections to EC and the parahippocampal regions.

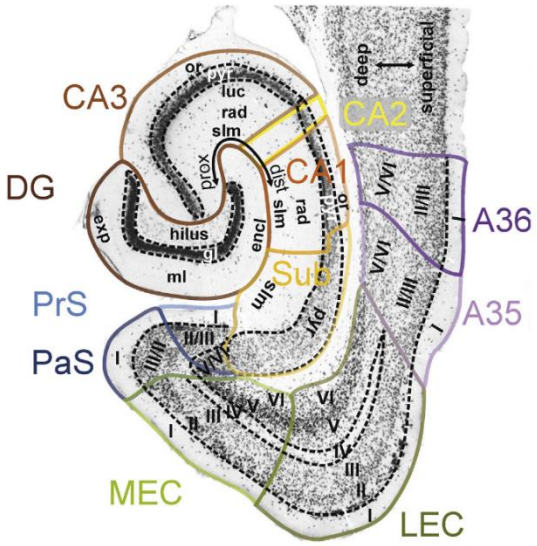

Fig. 5. Transversal section of the hippocampus with the histological subdivision of the hippocampal formation and its surrounding structures. Abbreviations: DG, dentate gyrus; CA3, CA2, CA1, areas of Ammon's horn; Sub, *subiculum*; PrS, *presubiculum*; PaS, *parasubiculum*; MEC, medial enthorinal cortex; LEC, lateral enthorinal cortex; A35 and A36, area 35 and 36 of the perirhinal cortex. Adapted from [Paxinos, 2015].

3.3.1.1 Dentate gyrus (DG)

DG is an allocortex organized into three layers [Andersen et al., 2007]:

- the molecular layer is the most superficial and is composed mainly of fibers. It contains dendrites of granule cells, afferent axons from stellate neurons located in the layer II of EC (in the outer two-thirds of the layer) [Steward, 1976; Steward & Scoville, 1976; Steward & Vinsant, 1983] and axons from mossy cells ascending from the polymorph zone (in the inner one third of the layer) [Gottlieb & Cowan, 1973; Deller et al., 1996]. The molecular layer is also composed of sparse neurons, including axo-axonic cells that project to granular neurons and probably regulate their activity [Soriano & Frotsher, 1989];
- the granular layer is the intermediate portion and contains the cell bodies of granule cells, the principal neurons of DG, and the soma of basket cells. Dendrites of granule cells are distributed into the molecular layer, whereas their axons propagate into the polymorph zone and CA3 region [Claiborne et al., 1986] and form mossy fibers, so named because they present varicosities all along their lengths;
- the polymorph zone (*hilus* of the DG) is the deepest layer of DG and is bordered by CA3 region. It comprises many classes of neurons with different morphologies.

Although these neurons have not yet been completely identified [Amaral, 1978], the most abundant cell types are mossy glutamatergic cells and basket GABAergic cells. Axons of mossy cells propagate into the molecular layer and form synapses with dendrites of granule cells. These neurons seem to be the major source of the glutamatergic associational and commissural projection to DG [Amaral, 1978; Amaral et al., 2007].

The granule cells of DG are the first stage of the tri-synaptic loop for the hippocampal information processing, since they are contacted by perforant path fibers (**fig. 6**). However, they receive also intrinsic projections from the contralateral (commissural) and ipsilateral (associational) hilar neurons. Other sources of extrinsic innervation of DG are the supramammillary nucleus of the hypothalamus [Wyss et al., 1979], the septum and the nucleus of diagonal band of Broca [Kohler et al., 1984; Freund & Antal, 1988 and the brain stem nuclei [Segal & Landis, 1974; Azmitia & Segal, 1978].

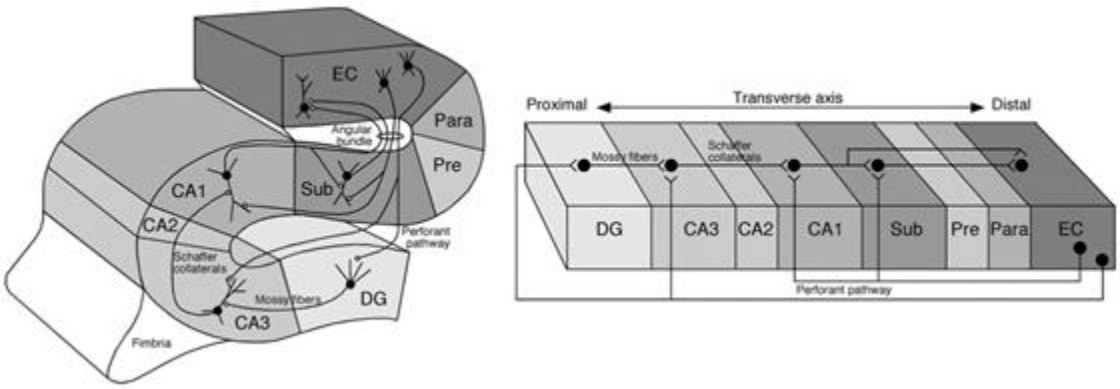

Fig. 6. Model of the tri-synaptic loop for the hippocampal information processing. Abbreviations: EC, enthorinal cortex; Para, *parasubiculum*; Pre, *presubiculum*; Sub, *subiculum*; DG, dentate gyrus. Adapted from [Andersen et al., 2007].

3.3.1.2 Ammon's horn (CA)

CA is an allocortex and is the main part of the hippocampal formation, organized into six layers [Andersen et al., 2007]:

- the *stratum* a*lveus* is the most superficial layer that protrudes into the temporal horn of the lateral ventricle and continues medially to form the fimbria. It contains efferent axons of pyramidal neurons;

- the *stratum oriens* is the layer immediately below the *alveus*, containing the cell bodies of basket and horizontal cells, the septal and commissural fibers coming from the contralateral hippocampus and basal dendrites of pyramidal cells;
- the *stratum pyramidale* includes the cell bodies of pyramidal cells, the principal excitatory neurons of the hippocampal formation. The soma of these neurons has a triangular shape with the base facing the surface layers (**fig. 7**). Basal dendrites originate from the base of the cell body and propagate into the overlying layer (*oriens*), whereas a robust apical dendrite originates in the opposite position and branches in underlying layers (*lacunosum* and *moleculare*) (**fig. 7**). Axon originates in the opposite position respect to the apical dendrite, but in CA3 region it forms axon collaterals (named Schaffer's collaterals) that move towards the inner portion and run parallel to the layers up to CA1 area;
- the *stratum radiatum* in CA3 area contains axons arising from granule neurons of DG (mossy fibers), while in CA1 it contains septal and commissural fibers and Schaffer's collaterals;
- the *stratum lacunosum* contains the apical dendrite of pyramidal neurons, Schaffer's collaterals and perforating fibers coming from EC;
- the *stratum moleculare* is the innermost and contains few neurons. It can be reached by the most distal portions of apical dendrites of pyramidal neurons. The molecular layer of CA blends with that of DG.

Despite pyramidal neurons are the main cells, CA contains a great variety of non-pyramidal neurons located primarily in the *strata oriens, radiatum* and *lacunosum-moleculare* but also in the *stratum pyramidale*. These cells are almost exclusively GABAergic interneurons [Ribak *et al.*, 1978] and contribute to the signal processing by modulating the flow of information through feedforward and feedback inhibition. Interneurons can be classified based on their soma localization, dendritic and axonal morphology, secondary neurotransmitter or other neurochemical marker, as well as electrophysiological properties [Freund & Buzsáki, 1996; Maccaferri & Lacaille, 2003; Klausberger & Somogyi, 2008]. They include: basket cells, chandelier (or axo-axonic) cells, O-LM neurons (*Oriens Lacunosum-Moleculare* associated cells), horizontal trilaminar cells, radial trilaminar cells, bistratified neurons, LM cells (*Lacunosum-Moleculare* interneurons) and IS interneurons (Interneuron-Selective interneurons) **(fig. 7**). Dwelling on basket cells, they are located in or

near the *stratum pyramidale*. They target the soma and proximal dendrites of pyramidal neurons; furthermore, in CA3 region they can often form recurrent inhibition loops with pyramidal cells that can help dampen excitatory responses. Like their counterparts in the cortex [Conteras, 2004] the majority of hippocampal basket cells are also parvalbumin (PV)-expressing and fast-spiking neurons.

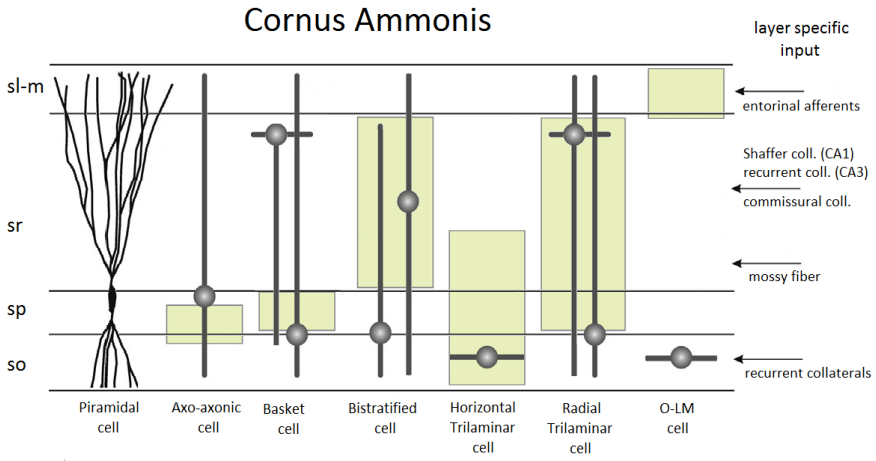

Fig. 7. Morphological classification of CA interneurons in rodents. Black circles represent the position of the cell body; black lines indicate the orientation and the laminar distribution of the dendritic tree; green squares represent the axonal arborisation. Pyramidal neurons are also indicated. On the right, different excitatory inputs to CA are shown. Adapted from [Freund & Buzsaki, 1996].

Regarding the connectivity, mossy fibers arising from granule cells cross the hilar region of DG and form 'giant' synapses with proximal dendrites of CA3 pyramidal cells at the level of *stratum lucidum*, a sub-layer between the *stratum pyramidale* and the *stratum radiatum*. This synapse represents the second stage of the tri-synaptic loop for the hippocampal information processing (**fig. 6**). The third element of the loop is represented by the synapse between Schaffer's collaterals and CA1 pyramidal neurons.

The main output from CA1 is to the *subiculum*, but some axons also terminate in EC and prefrontal cortex [Amaral & Witter, 1989; Van Groen & Wyss, 1990], other limbic cortical areas, the lateral septum, the *nucleus accumbens*, and the olfactory bulb [Van Groen & Wyss, 1990].

3.3.1.3 Subicular complex

Subicular complex includes three structures: *subiculum*, adjacent to CA1, *presubiculum* and *parasubiculum*.

Subiculum is arranged in three layers:

- the *stratum moleculare*, the most superficial, contains apical dendrites of subicular pyramidal cells;
- the *stratum pyramidale* contains the cell bodies of pyramidal efferent neurons. However, subicular pyramidal cells are more dispersed than that of CA3 and CA1 fields;
- the *stratum multiforme* is the innermost and comprises neurons with different morphologies, whose function is probably to modulate output signals.

Axons from CA1 pyramidal cells form synapses with dendrites of subicular pyramidal cells: this can be considered as the 'fourth' stage of the hippocampal tri-synaptic loop (**fig. 6**). Subicular pyramidal cells send extended projections to the deeper layers of the caudal medial EC, closing the loop [Van Groen et al., 1986]. Other projections arising from the deepest subicular pyramidal cells are directed to the anterior nuclei of the thalamus; furthermore, projections coming from superficial neurons reach the mammillary bodies, the septum, *nucleus accumbens* and prefrontal cortex [O'Mara et al., 2001].

3.3.2 Electrophysiological and neurochemical features of hippocampal neurons

The electrophysiological classification of the hippocampal neurons is mainly based on their firing. First of all, pyramidal cells and interneurons differ in their firing rate: interneurons display a firing rate higher than that of pyramidal neurons [Eccles, 1969]. Secondly, while pyramidal cells are mainly characterized by a regular discharge [Markram *et al*., 2004], interneurons are very heterogeneous [Kawaguchi, 1993; Macaferri & McBain, 1996]. Indeed, based on their steady-state voltage response to depolarizing current steps, interneurons can be classified in five main groups (**fig. 8**):

- non-accomodating (NAC) are characterized by a repetitive discharge without frequency adaptation;
- accomodating (AC) exhibit a frequency adaptation and a firing rate lower than that of NAC;
- stuttering (STUT) are characterized by a discharge with clusters of action potentials separated by a unpredictable periods of silence;

- irregular-spiking (IS) fire action potentials randomly during the discharge;
- bursting (BST) give rise to a cluster of 3-5 action potentials riding on a slow depolarizing wave and followed by a strong slow afterhyperpolarization.

In addition to the electrophysiological classification, interneurons can be grouped based on the expression of secondary neurotransmitter or other neurochemical marker. For example, there are basket cells and chandelier neurons that express PV as well as basket cells that express cholecystokinin (CCK) [Szabó et al., 2010]. The PV-expressing cells exhibit predominantly a STUT discharge, whereas the CCK-expressing neurons are largely characterized by a regular firing [Pawelzik et al., 2002]. The PV- and CCK- positive interneurons express different types of receptors and are thus sensitive to different neuromodulators, playing specific functional roles within the hippocampal network [Pawelzik et al., 2002].

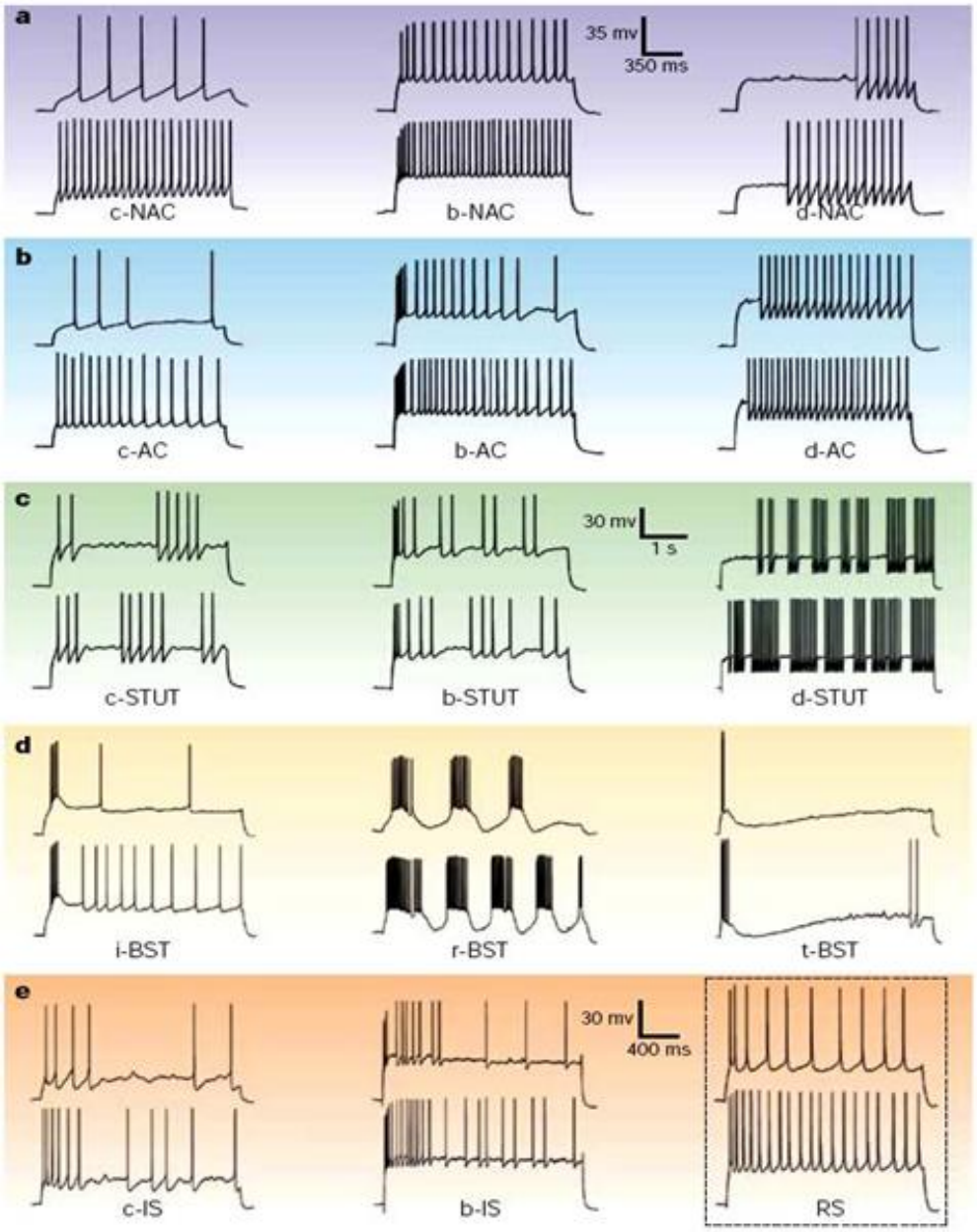

Fig. 8. Different electrophysiological classes of inhibitory interneurons. Based on the steady-state voltage response to depolarizing current steps, five principal classes of interneurons have been identified: non-accommodating (NAC); accommodating (AC); stuttering (STUT); bursting (BST); irregular-spiking (IS). According to the type of response at the onset of the depolarizing current, most classes can be subdivided into three subclasses: delay (d); classic (c) and burst (b). For bursting interneurons, the three types are repetitive (r), initial (i) and transient (t). Regular-spiking (RS) is an example of a classic discharge of pyramidal cell [Markram et al., 2004].

3.3.3 The role of OT in the hippocampal formation

Using *in vitro* light microscopic autoradiography, the presence of binding site for OT has been widely demonstrated in the hippocampal formation, in particular at the level of CA1

region and *subiculum* [Freund-Mercier et al., 1989; Tribollet et al., 1988; Barberis & Tribollet, 1996]. Since the hippocampus is involved in several functions, including learning and memory consolidation [Ribot, 1881; Wernicke, 1881; Korsakov, 1889], spatial navigation [Scoville & Milner, 1957; Teng & Squire, 1999; Rosenbaum et al., 2000] and emotional processes [Papez, 1937; MacLean, 1949], questions have been raised about the role of OT in the hippocampus.

The first indications of the involvement of neurohypophysial peptides in cognitive processes were reported in 1965. Then, De Wied found that the removal of the posterior pituitary, a procedure that disrupts the pituitary-adrenal responsiveness, also impaired the maintenance of an avoidance behavior in the rat. This deficit could be restored by treatment with AVP [De Wied, 1965]. On this basis, the author hypothesized that AVP positively modulated the active avoidance behavior. By contrast, in the 1970s studies with central and peripheral administration of OT indicated that this hormone accelerated the extinction of conditioned avoidance responses in the rat. Hence, OT became recognized as an amnesic neuropeptide [Bohus et al., 1993]. Further works revealed that AVP and OT affected both consolidation and retrieval of memory [De Wied, 1991], by modulating long-term potentiation (LTP) [Dubrovsky et al., 1996; Morimoto & Goddard, 1985; Kaminska et al., 2000; Urbanoski et al., 2000]. In particular, it has been shown that OT can enhance LTP at Schaffer's collaterals-CA1 synapses and improve long-lasting spatial memory function during motherhood [Tomizawa et al., 2003]. Moreover, OT-induced paired-pulse facilitation, in terms of decrease in synaptic failure and increase in the number of activated synapses, has been described in synapses between a subclass of CA1 GABAergic interneurons and pyramidal neurons [Jiang et al., 2000].

According to these evidences, some authors tried to understand the cellular target of OT in CA1 field [Zaninetti & Raggenbass; Owen et al., 2013] and in DG [Harden & Frazier, 2016]. In CA1 area, Zaninetti and Raggenbass have demonstrated that TGOT (Thr^4,Gly^7-oxytocin), a selective OTR agonist, is able to increase the excitability of a specific subpopulation of GABAergic interneurons (basket cells) that innervate the cell bodies and proximal dendrites of pyramidal neurons [Zaninetti & Raggenbass]. From a physiological perspective, these TGOT-responsive interneurons were fast-spiking cells [Owen et al., 2013]. In the *hilus* of the DG, Harden and Frazier have described a population of GABAergic fast-spiking interneurons that innervate mossy cells at perisomatic locations and are directly depolarized by acute application of TGOT [Harden & Frazier, 2016].

Overall, these electrophysiological data indicate that in the hippocampus OT causes a facilitation in the GABAergic transmission that could be involved in shaping spike timing in local excitatory circuits [Harden & Frazier, 2016]. From this perspective, well timed activation of OTRs could be neuroprotective and help control runaway hyperexcitability that leads to epileptogenesis [Harden & Frazier, 2016]. Indeed, consistent with this idea Owen and colleagues have demonstrated that TGOT decreases spontaneous action potential firing of CA1 pyramidal neurons and increase the spike fidelity [Owen et al., 2013].
More generally, by influencing the activity of hippocampal GABAergic cells, OT can play a role in the regulation of the operational modes of excitatory neurons, not only by modulating inhibition/disinhibition, but possibly also by inducing and maintaining network oscillation or synchronization or by promoting plasticity [Freund & Buzsaki, 1996].

3.4 The GABAergic system

3.4.1 General properties of $GABA_A$ receptors ($GABA_AR$)

GABA (γ-aminobutyric acid) is the main inhibitory neurotransmitter in the adult mammalian central nervous system. Its action is mediated by the interaction with GABA receptors (GABAR) that were identified by both electrophysiological and pharmacological points of view in all brain regions. Using selective blockers, two classes of GABARs were described, $GABA_A$Rs and $GABA_B$Rs, that differ in pharmacological, biochemical and electrophysiological properties [Sigel et al., 2006].

$GABA_A$Rs belong to the family of Cys-loop ligand-gated ion channels, members of which (e.g. nicotinic acetylcholine, glycine and 5-hydroxytryptamine type 3 (5-HT3) receptors [Lester et al., 2004]) possess a characteristic loop formed by a disulphide bridge between two Cys residues. $GABA_A$Rs are pentameric assemblies of subunits that form a central ion channel. Nineteen $GABA_A$Rs subunits (α1–6, β1–3, γ1–3, δ, ε, θ, π and ρ1–3) have been cloned from the mammalian central nervous system, with further variations resulting from alternative splicing (e.g. the γ2 subunit) [Simon et al., 2004].
Each subunit is assembled in four transmembrane domains (TM1-4) linked by intracellular and extracellular loops (**fig. 9**). Both amino-terminal and carboxyl-terminal domains are located on the extracellular side. The amino-terminal domain contains different glycosylation sites, while the carboxyl-terminal domain possess the Cys-loop motif.

The intracellular loop between TM3 and TM4 is important for the phosphorylation operated by intracellular protein kinases and for the interaction with other cellular molecules [Wang et al., 1999; Siegel et al., 2006]. The channel pore is mainly constituted by TM2 of each subunit and contains positively charged amino acids which confer to receptors a permeability to anions, in particular Cl^- (**fig. 9**). On the extracellular side and in the channel pore of $GABA_A$Rs there are several binding sites for agonists (e.g. barbiturates, benzodiazepines, neurosteroids and imidazopyridines) and antagonists (e.g. bicuculline, picrotoxin, flumazenil and gabazine).

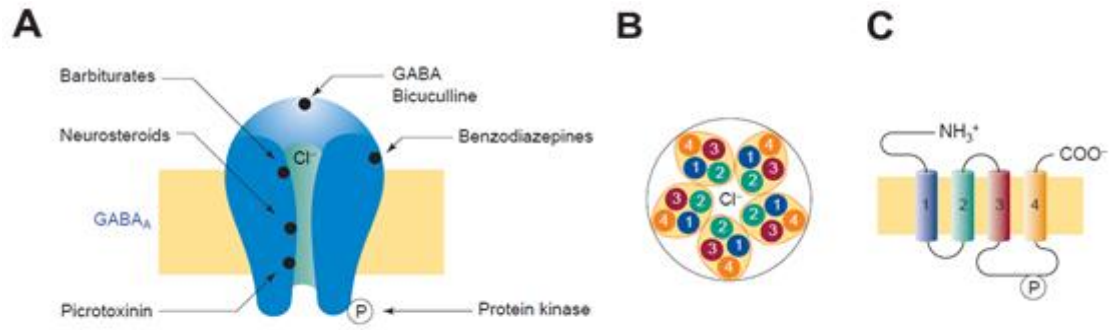

Fig. 9. (A) Structural model of a $GABA_AR$. The central pore, the main binding sites and their respective ligands are indicated. **(B)** Section of the $GABA_AR$. The pentameric assembly is shown. **(C)** Molecular structure of a single subunit. The subunit is composed of four (1-4) transmembrane domains linked by intracellular and extracellular loops. Amino-terminal, carboxyl-terminal and the intracellular phosphorylation sites are indicated. Adapted from [Bormann, 2000].

3.4.1.1 $GABA_AR$ subunit composition and localization

The most abundantly expressed receptor subtype in the brain is formed by α1, β2 and γ2 subunits [Mckernan & Whiting, 1996; Sieghart & Sperk, 2002; Whiting, 2003]. The likely stoichiometry is two α, two β and one γ subunit [Tretter et al., 1997; Farrar et al., 1999]. Other common assemblies also contain α, β and γ2 subunits (for example α2β3γ2 α3β3γ2, α4βxγ2, α5β3γ2 and α6βxγ2), whereas receptors in which the γ2 subunit is replaced by γ1, γ3 or δ are less abundant. Further variability arises from the fact that individual pentamers might contain two different α or two different β subunit isoforms [Sieghart & Sperk, 2002]. In some cases, the γ subunit can be replaced by ε, δ or π subunits, and the π and θ subunits might also be capable of co-assembling with α, β and γ [Neelands et al., 1999; Neelands & Macdonald, 1999]. Finally, the ρ1 subunit can form homomeric receptors defined $GABA_C$Rs, a subfamily of ionotropic GABARs [Bormann, 2000; Johnston, 2002], but it can

also form receptors with γ2 subunit [Qian & Ripps, 1999] or with both α1 and γ2 subunits [Milligan et al., 2004]. This molecular heterogeneity has important functional consequences for $GABA_AR$ subtypes: the subunit composition dictates not only the properties of receptors, but also their cell surface distribution and dynamic regulation [Hevers & Luddens, 1998].

In the late 1980s light-microscopic immunofluorescence and EM immunogold methods allowed precise subcellular localization of $GABA_ARs$. In particular, α1, α2, α3, α6, β2/3 and γ2 subunits were found within the postsynaptic specialization of GABA-containing synapses of many brain regions, including cerebellum, *globus pallidus*, hippocampus and neocortex [Craig et al., 1994; Nusser et al., 1995; Somogyi et al., 1996; Fritschy et al., 1998; Nusser et al., 1998]. At that time, each of these receptor subunits was also found in extrasynaptic plasma membranes, and no $GABA_AR$ subunit type has yet been found to have an exclusively synaptic location.

However, later on it has been found that some $GABA_ARs$ did not seem to be expressed at synaptic junctions. For example, in cerebellar granule cells the δ subunit was shown to be present exclusively in extrasynaptic somatic and dendritic membranes, i.e., hundreds of nanometres away from the edge of the nearest postsynaptic density [Nusser et al., 1998]. In DG granule cells, the δ subunit was found in a perisynaptic position, i.e., just outside the postsynaptic density (within 30 nm) [Wei et al., 2003]. In general, the δ subunit forms receptors specifically with α6 and β2/3 subunits (α6β2/3δ and α1α6β2/3δ) in cerebellar granule cells and with α4 and βx subunits (α4βxδ) in several areas of the forebrain, including DG [Barnard et al., 1998]. For each of these receptor subtypes, the lack of a γ subunit is probably responsible for their failure to be incorporated at the synapse.

In addition to the δ subunit, other subunit subtypes might also be present predominantly, if not exclusively, outside synapses. In hippocampal pyramidal cells, the α5 subunit (which probably forms α5β3γ2 receptors) shows diffuse surface labelling at the light microscopic level without detectable synaptic clustering. In this case, the presence of the α5 subunit seems to override the ability of the γ2 subunit to promote synaptic localization [Farrant & Nusser, 2005].

Overall, these findings indicate that receptors containing a γ2 subunit in association with α1,α2 or α3 subunits are the predominant synaptic receptor subtypes, whereas receptors that contain α4, α5 or α6 subunits (α6βxδ, α4βxδ and α5βxγ2) are predominantly or exclusively extrasynaptic [Farrant & Nusser, 2005]. .

3.4.1.2 $GABA_AR$ biophysical properties

The diversity in the location and subunit composition endows $GABA_ARs$ with distinct biophysical properties, particularly those associated with agonist binding and gating [Farrant & Nusser, 2005]. A key property of any ligand-gated ion channel is its sensitivity to endogenous agonist that reflects both the affinity of the receptor for its ligand and the efficacy of the ligand, i.e., how effectively it promotes ion channel gating [Colquhoun, 1998]. For recombinant receptors that contain α, β and γ subunits, sensitivity to GABA is most strongly affected by the type of α subunit that is present: α5-containing extrasynaptic receptors have a higher affinity than α3-containing synaptic receptors [Bohme et al., 2004]. Moreover, replacing the γ2 subunit in α4β3γ2 assemblies with a δ subunit increases the sensitivity to GABA [Brown et al., 2002]. Overall, these data indicate that extrasynaptic receptors display a high affinity for GABA that allows them to respond to the low levels of neurotransmitter present in the extracellular space [Bright & Smart, 2013].

Activation, deactivation and desensitization of recombinant receptors are also greatly affected by their subunit composition. As regard deactivation, the insertion of a γ2 subunit into αβ receptors increases the deactivation speed about 2-fold [Boileau et al., 2003]. Moreover, for both αβγ and αβδ assemblies, the rate of deactivation depends on the type of α subunit present; for example, α1-containing αxβ1γ2 receptors deactivate about 5-fold faster than those containing the α2 subunit [McClellan & Twyman, 1999] and α1-containing αxβ3δ receptors deactivate about 4-fold faster than those containing the α6 subunit [Bianchi et al., 2002]. In the hippocampus, α5-containing perisynaptic receptors deactivate about 3-fold more slowly than synaptic receptors [Prenosil et al., 2006]. As regard the degree of desensitization, it affects the ability of postsynaptic receptors to respond to repetitive high frequency activation [Mellor & Randall, 2001], being also important for the effect of a persistent low concentration of GABA. Ambient GABA can promote entry of receptors into partially bound, slowly desensitizing states, which potentially reduces the availability of synaptic receptors [Overstreet et al., 2000]. Consistent with the interrelation between deactivation and desensitization, the addition of a γ2 subunit to αβ receptors slows down the macroscopic desensitization [Boileau et al., 2003]. For αβγ assembly, the rate and the extent of desensitization are influenced by the type of α subunit: receptors containing the α1 subunit desensitize more rapidly than those containing an α5 [Caraiscos et al., 2004] or α6 subunit [Tia et a., 1996].

In summary, data from recombinant receptors show that all macroscopic and microscopic functional properties of $GABA_AR$s depend strongly on their subunit composition and are wholly consistent with distinct mode of $GABA_AR$ activation.

3.4.2 Modes of $GABA_AR$ activation

3.4.2.1 Phasic activation

$GABA_AR$-mediated synaptic communication is tailored to allow the rapid and precise transmission of presynaptic activity into a postsynaptic signal. On the arrival of an action potential at the nerve terminal, a local Ca^{2+} influx triggers the fusion of synaptic vesicles with the presynaptic membrane at the release site. Each vesicle is thought to liberate several thousands of GABA molecules into the synaptic cleft, generating a peak in GABA concentration [Mody et al., 1994]. The binding of neurotransmitter to synaptic $GABA_AR$s, clustered opposite the release site, triggers the near-synchronous opening of their ion channels and thus the influx of Cl^-. This mode of activation is defined 'phasic' because of the short duration of the GABA transient to which synaptic receptors are exposed: indeed, experiments using low-affinity competitive antagonists indicate that the synaptic GABA concentration decays with a time constant of <500 µs [Overstreet et al., 2002]. The phasic activation generates postsynaptic currents whose activation and deactivation kinetics depend on the time constant of GABA clearance and the biophysical properties of synaptic $GABA_AR$s. Indeed, spontaneous inhibitory postsynaptic currents (sIPSC), generated by the spontaneous release of neurotransmitter occurring when the presynaptic terminal fires spontaneous action potentials, have a rapid onset with rise times of a few hundreds of microseconds (**fig. 10A**) [Nusser et al., 1997; Brickley et al., 1999; Burkat et al., 2001]. This reflects the proximity of receptors to the site of GABA release and the speed of the closed to-open channel transition [Jones et al., 1995; Burkat et al., 2001; McClellan & Twyman, 1999]. If the time course of the GABA concentration transient is brief, the decay of sIPSCs is dominated by the ion channel deactivation, whose speed is determined by the microscopic kinetics of receptors [Jones & Westbrook, 1995]. The expression of $GABA_AR$ subtypes that incorporate different subunits is proposed to contribute to the differences observed in the decay of sIPSCs at different stages of development [Okada et al., 2000] and in different cell types [Nusser et al., 1999; Bacci et al., 2003].

The phasic receptor activation addresses only the most straightforward situation, in which the released neurotransmitter activates only those receptors that are located just in front of the postsynaptic density. However, there are further levels of complexity, which might include the activation of receptors located in adjacent postsynaptic densities within the same synaptic bouton, or interactions between multiple vesicles that are released from a single synaptic specialization at a short interval. Indeed, if a repetitive discharge of action potentials triggers the release of several number of vesicles at a single active zone, $GABA_A$Rs will be exposed to a different GABA concentration transient. Following diffusion from its release site (a phenomenon called 'spillover'), GABA might activate receptors located in a perisynaptic position, just outside the postsynaptic density (**fig. 10B**). In this case, the GABA waveform to which receptors are exposed will be determined by their location relative to the release site, the geometry and spatial arrangement of the neighbouring cellular elements, diffusional barriers and the proximity of GABA transporters in neurons and astroglia [Overstreet et al., 2002; Barbour & Hausser, 1997; Kullmann, 2000]. It is important to note that currents resulting from GABA spillover can still be considered phasic, in the sense that they are temporally related to the release event. However, the kinetic properties of phasic currents mediated by perisynaptic receptors are different from those of currents mediated by synaptic receptors. For example, in the hippocampal formation it has been shown that sIPSCs recorded from CA1 pyramidal neurons can be subdivided into $GABA_{A,fast}$ and $GABA_{A,slow}$ currents based on their deactivation rate [Prenosil et al., 2006]. The former are mediated by α2-containing synaptic $GABA_A$Rs expressed on the soma and by α1-containing synaptic receptors expressed on dendrites, whereas the latter are mainly mediated by α5-containing perisynaptic $GABA_A$Rs [Prenosil et al., 2006].

In general, one important function of phasic inhibition is the generation of rhythmic activities in neuronal networks. For example, cortical and hippocampal basket cells synchronize the activity of a large population of pyramidal neurons, generating and maintaining ϑ and γ frequency network oscillations [Somogyi & Klausberger, 2005; Jonas et al., 2004; Cobb et al., 1995]. The exact location of GABA-releasing synapses is also important in the control of regenerative electrical activity in dendrites [Miles et al., 1996; Spruston et al., 1995] or in the synaptic integration. For example, the selective activation of somatically terminating interneurons during feed-forward inhibition of hippocampal pyramidal cells produces a

requirement for precise coincidence detection of excitatory input at the soma [Pouille & Scanziani, 2001].

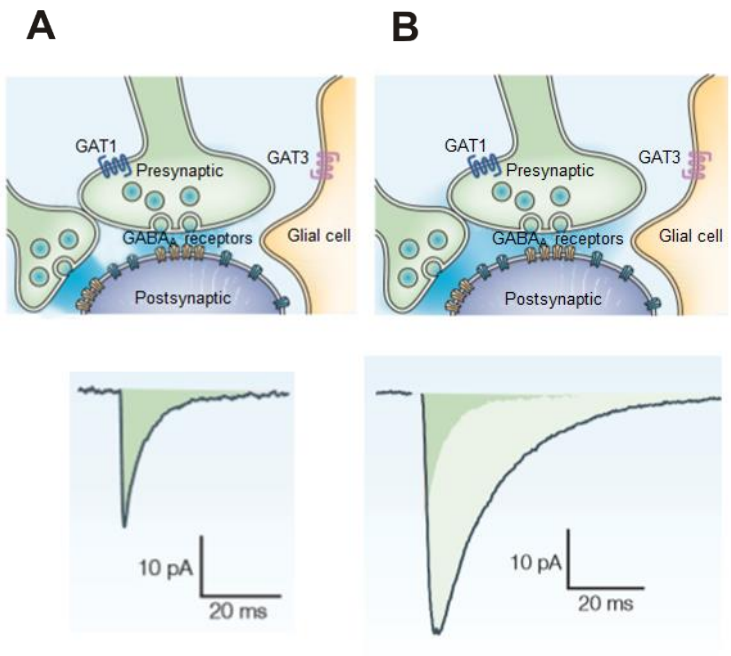

Fig. 10. (A) Representative GABAergic synapse (upper panel) in which two presynaptic elements contact a single postsynaptic neuron. A glial cell in the proximity of one release site is also indicated. The spontaneous fusion of synaptic vesicles with the presynaptic membrane, elicited by the arrival of an action potential, causes the neurotransmitter release in the extracellular space. The binding of GABA to synaptic $GABA_ARs$ (yellow), clustered opposite the release site, triggers a spontaneous inhibitory postsynaptic current (sIPSC) (lower trace) whose amplitude depends on the number of synaptic $GABA_ARs$ activated, whereas its kinetics depend on the time constant of GABA clearance and the biophysical properties of receptors. This mode of activation is defined 'phasic'. **(B)** A repetitive discharge of action potentials triggers the release of several number of vesicles at a single active zone, promotes GABA spillover and activates both synaptic and perisynaptic $GABA_ARs$ (blue). The phasic activation of perisynaptic receptors generates a larger and much slower sIPSC (lower trace, dark green): the increased amplitude is explained by the activation of a greater number of postsynaptic receptors, whereas the slower deactivation is related to the kinetics properties of perisynaptic receptors. The area of synaptic $GABA_AR$-mediated sIPSC (light green) is superimposed for comparison. Adapted from [Farrant & Nusser, 2005].

3.4.2.2 Tonic activation

The phasic activation of synaptic and perisynaptic receptors is fundamental to information transfer in the brain. However, neurotransmitters that are traditionally considered to participate in rapid point-to-point communication can also participate in slower forms of signalling [Mody, 2001]. At the extreme, this might include the 'tonic' activation of receptors located in somatic, dendritic and axonal regions of the neuronal membrane that are distant from sites of neurotransmitter release [Kullmann et al., 2005]. The tonic activation of $GABA_ARs$ is evident in certain embryonic neurons before the synapses formation

[Valeyev et al., 1993; Loturco et al., 1995; Owens et al., 1999]. In mature neurons that display sIPSCs, the tonic activation of $GABA_A$Rs was first identified in voltage-clamp recordings from rat cerebellar granule cells [Kaneda et al., 1995]. The application of a saturating concentration of $GABA_A$R antagonists, usually bicuculline and gabazine (SR-95531), not only blocked sIPSCs, but also decreased the 'baseline holding current' required to clamp the cells at a given membrane potential (**fig. 11**). This shift in the 'baseline holding current' was explained by an increase in the input resistance and was associated with a reduction in the current variance, consistent with a decrease in the number of open $GABA_A$ channels [Kaneda et al., 1995; Brickley et al., 1996; Wall & Usowicz, 1997]. The amplitude of the tonic current was estimated by the difference between the 'baseline holding current' recorded during perfusion of $GABA_A$R antagonists and that recorded in control conditions. Subsequent studies have indicated that GABA-mediated tonic conductances exist in granule cells of DG [Nusser. & Mody, 2002], layer V pyramidal neurons in the somatosensory cortex [Yamada et al., 2004], CA1 pyramidal cells [Banks & Pearce, 2000; Scimemi et al., 2005; Mortensen & Smart, 2006; Prenosil et al., 2006; Pavlov et al., 2009] and CA1 inhibitory interneurons [Semyanov et al., 2003].

The most parsimonious explanation for the presence of a tonic conductance is that GABA must be present in the extracellular space at a sufficiently high concentration to cause persistent activation of extrasynaptic receptors. The extracellular GABA concentration reflects the number of GABA-releasing neurons and their firing activity: indeed, during periods of intense synaptic activity the extracellular GABA concentration rises [During & Spencer, 1993]. Accordingly, when the ambient GABA concentration increases, also the magnitude of the tonic current potentially increases. This has been shown in the hippocampus, where the application of kainate produces robust firing of interneurons (and thus GABA release), causing an increase in extrasynaptic $GABA_A$R-mediated currents in both hippocampal pyramidal cells [Frerking et al., 1999] and interneurons [Kullmann & Semyanov, 2002].

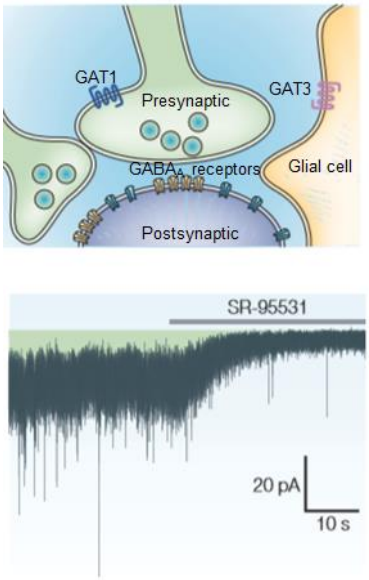

Fig.11. Representative GABAergic synapse (upper panel) in which two presynaptic elements contact a single postsynaptic neuron. A glial cell in the proximity of one release site is also indicated. Following an intense GABA release, a certain amount of neurotransmitter persists in the extracellular space despite the activity of neuronal and glial transporters (GAT1 and GAT3) and tonically activates high-affinity extrasynaptic $GABA_ARs$. The stochastic opening of these receptors triggers a 'noisy' steady-state current, with superimposed phasic currents (lower trace). A high concentration (10 μM) of the $GABA_AR$ antagonist gabazine (SR-95531) blocks both phasic sIPSCs and the tonic channel activity, causing a change in the 'baseline holding current' required to clamp the cell at a given membrane potential. The shaded area beneath the current recorded before SR-95531 application (green) represents the charge carried by tonically active $GABA_ARs$. Thus, the amplitude of the tonic current can be estimated by the difference between the 'baseline holding current' recorded during perfusion of $GABA_AR$ antagonists and the current recorded in control conditions. All the recordings were performed using whole-cell patch-clamp technique in voltage-clamp mode. The holding potential was -70 mV and the Nernst equilibrium potential for Cl^- (E_{Cl-}) was is set to be close to 0 mV, so the phasic events appear as inward currents. Adapted from [Farrant & Nusser, 2005].

The tonic activation of $GABA_ARs$ has one straightforward outcome on neurons: a persistent reduction in the input resistance. This phenomenon, known as 'shunting' (or silent) inhibition [Mitchell & Silver, 2003], affects the magnitude and duration of voltage responses to injected currents and consequently modulates cell excitability. Several groups have investigated how tonic inhibition acts on the excitability of cerebellar granule cells [Brickley et al., 1996; Hamann et al., 2002; Chadderton et al., 2004]. To that purpose, current steps of increasing intensity were injected into neurons in order to evoke action potentials (**fig. 12A**): in the presence of $GABA_AR$ antagonists that blocked tonic inhibition (e.g. bicuculline), the current required to achieve a given firing rate decreased and cell excitability increased. This behavior was evident in the firing rate-to-injected current (F-I) relationship (**fig. 12B**), characterized by two parameters: the offset (i.e., the minimal intensity of injected current required to attain a response) and the gain (i.e., the slope of the relationship). In the presence of bicuculline (10 μM), the curve was shifted to the left (**fig. 12B**), indicating a reduction in

the offset; the slope, an index of the sensitivity of neurons to changes in excitatory input [Mitchell & Silver, 2003)], was not significantly altered (**fig. 12B**). Thus, in cerebellar granule cells as well as in hippocampal pyramidal cells, tonic inhibition performs a subtractive operation that decreases cell excitability without changing the neuronal sensitivity to input [Pavlov et al., 2009].

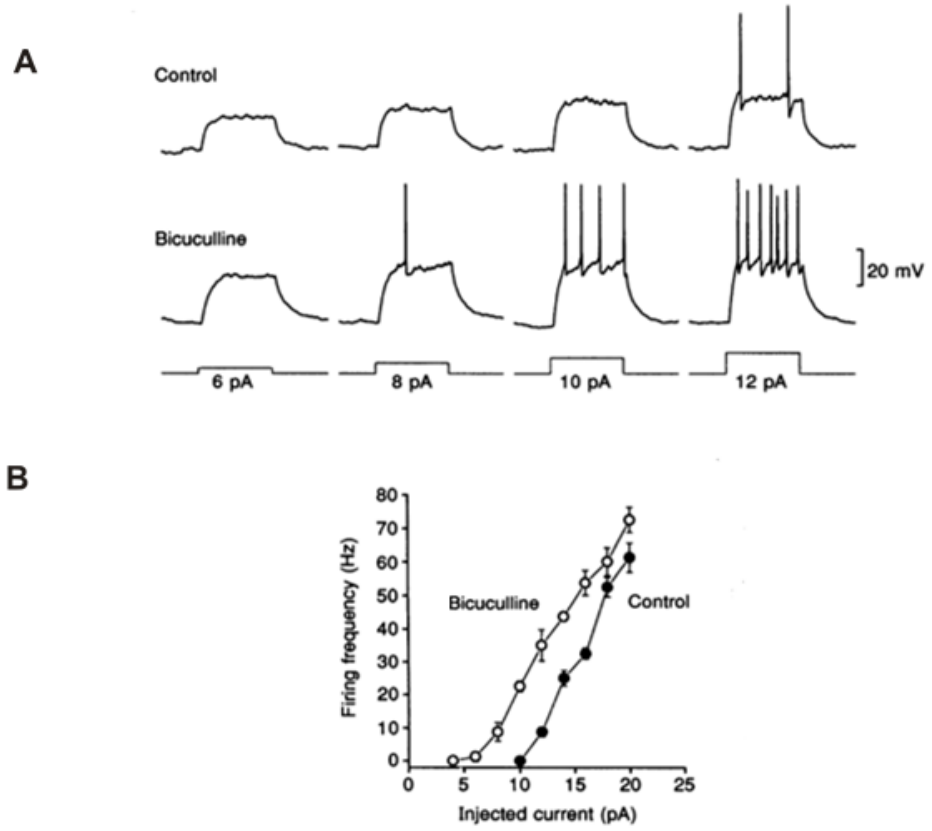

Fig. 12. (A) Representative voltage traces recorded from a cerebellar granule cell, in response to the injection of depolarizing current steps of increasing intensity (6, 8, 10 and 12 pA). In control conditions (upper traces) spiking was initiated by a 12 pA depolarizing current pulse (step; 200 ms). In the presence of bicuculline (10 μM) (lower traces) spiking first occurred with 8 pA injection, indicating an increase in cell excitability elicited by bicuculline. **(B)** Graph showing the firing rate-to-injected current (F-I) relationship referred to the traces of panel A. Data are the mean of 4 trials. The curve obtained in the presence of bicuculline (white dots) is shifted to the left compared to that obtained in control conditions (black dots), indicating a reduction in the offset (i.e., the minimal intensity of injected current required to attain a response). The gain (i.e., the slope of the curve) is not significantly altered by the blockade of tonic inhibition. Adapted from [Brickley et al., 1996].

3.4.3 Modulation of phasic and tonic $GABA_AR$-mediated inhibition

The pattern of phasic inhibition that a neuron receives is obviously determined by the number, variety and activity of presynaptic GABA-releasing neurons, but whether tonic inhibition is similarly determined by neuronal activity is less clear. In theory, both phasic and tonic inhibition could be modulated by changes in GABA release, changes in the number

and properties of $GABA_A$Rs and changes in endogenous neuromodulators (in particular neurosteroids).

As regard changes in GABA release, the facilitation in the exocytosis of vesicles elicited by a co-release of acetylcholine is able to causes a Ca^{2+}-dependent increase in the tonic conductance of cerebellar granule cells [Rossi et al., 2003]. As cerebellum receives cholinergic innervation, this mechanism could provide a physiologically relevant modulation of cell excitability. Furthermore, the blockade of action potentials with tetrodotoxin has also been shown to reduce the tonic conductance in cultured neurons from the hippocampus [Petrini et al., 2004] and cerebellum [Leao et al., 2000], indicating a correlation between the firing activity of the presynaptic element and the magnitude of the tonic current recorded from a postsynaptic neuron.

In addition, many physiological processes are known to modulate the number of $GABA_A$Rs and their functions that are likely to be relevant for both phasic and tonic inhibition. For example, post-translational modifications (such as phosphorylation or palmitoylation) [Wang et al., 2003; Rathenberg et al., 2004] or the interaction with various cytosolic proteins [Luscher & Keller, 2004] can affect both the subcellular location of the receptors and the kinetic behavior or single-channel conductance [Chen et al., 2000].

Finally, many studies demonstrate that tonic currents can be boosted by the addition of either a selective $GABA_A$R agonist or a positive allosteric modulator. For example, THIP (4,5,6,7-tetrahydoisoxazolo[5,4-c]pyridin-3(2H)-one) has been extensively characterized as a 'super-agonist' of extrasynaptic αβδ receptors [Brown et al., 2002; Mortensen et al., 2010] whilst displaying only partial agonist activity at synaptic αβγ receptors [Mortensen et al., 2004]. Furthermore, endogenous neurosteroids act as potent positive allosteric modulators of tonic currents [Belelli et al., 2002; Brown et al., 2002; Wohlfarth et al., 2002]. More recently, a novel compound, DS2, has been identified as a selective modulator of δ-containing $GABA_A$Rs [Wafford et al., 2009; Jensen et al., 2013], increasing the tonic current in thalamic relay neurons with no effect on phasic currents [Wafford et al., 2009; Jensen et al., 2013].

Overall, these data indicate that $GABA_A$R-mediated inhibition can undergoes physiological and pharmacological modulatory processes. It is likely that the modulation of tonic currents has a functional significance different from that of phasic currents, since tonic currents provide a form of signalling over a timescale of seconds to days, whereas phasic currents participate to rapid point-to-point communication, including the maintaining of rhythmic activities in neuronal networks.

4. MATERIALS AND METHODS

4.1 Animal models

4.1.1 $Otr^{-/-}$ mice

Some experiments described in this thesis were performed on young (P17-P26) male and female $Otr^{-/-}$ mice, lacking oxytocin receptors (OTR) in the entire body. This model was kindly donated by the lab of Dr. Bice Chini at the CNR Institute of Neuroscience in Milan. $Otr^{-/-}$ mice were generated by removing the gene coding for OTR (Otr). Briefly, 129/Sv mouse genomic DNA fragments were amplified by PCR (Polymerase Chain Reaction). A 3.4 kbp 5' fragment containing the Otr promoter and exon 1 was inserted upstream of a neomycin resistance cassette (pkg-neo^r) flanked by two FRT (Flp Recognition Target) sites that are recognized by FLP recombinase. For the 3' homology part of the construct, a 1.3 kbp of fragment containing Otr exons 2 and 3 was inserted between two loxP sites, and a 2.9 kbp fragment was added to its 3'end. A diphtheria toxin A gene was used to select against random insertion. The construct (**fig. 13**) was inserted into embryonic stem (ES) cells (129/Sv R1 cell line) using electroporation. Then, ES cells were injected into blastocysts to generate chimeras. The pkg-neo^r cassette was removed by crossing the chimeras with a transgenic mouse expressing FLP recombinase. This procedure generated mice with one Otr allele flanked by two loxP sites ($Otr^{+/flox}$) (**fig. 13**). Homozygous floxed mice ($Otr^{flox/flox}$) did not differ from wild-type littermates and expressed normal amounts of OTRs. To generate forebrain-specific Otr knock-out mice, L7ag13 transgenic line that expresses Cre recombinase under the control of the Camk2a (calmodulin kinase 2a) promoter was crossed with $Otr^{flox/flox}$ or $Otr^{+/flox}$ mice. $Otr^{flox/flox}$ male mice were crossed with $Otr^{+/flox}$ female mice that contained one transgenic allele expressing Cre recombinase ($Otr^{+/flox,cre}$). The offspring $Otr^{flox/flox,cre}$ was forebrain-specific Otr knock-out. To generate whole-body Otr knock-out mice, $Otr^{+/flox,cre}$ male mice which express Cre recombinase in the germ line were crossed with female $Otr^{flox/flox}$ female mice. This led to heterozygous progeny with one Otr allele inactivated throughout ($Otr^{+/-}$). These mice were crossed to get homozygous total Otr knock-out ($Otr^{-/-}$) [Lee et al., 2008].

From a phenotypic point of view, $Otr^{-/-}$ mice display a resistance to change in a learned pattern of behavior, comparable to restricted interests and repetitive behavior in autism and

an increased susceptibility to seizures, a frequent and clinically relevant symptom of autism [Sala et al., 2011]. They also show increased aggression and reduced ultrasonic vocalization of pup upon separation from mother [Sala et al., 2011].

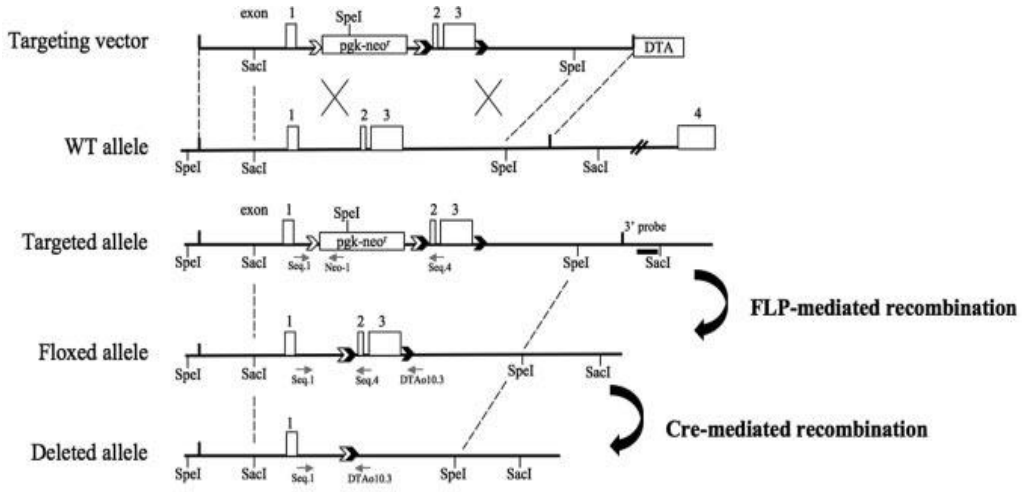

Fig. 13. Schematic diagram of targeting strategy used for the generation of $Otr^{flox/flox}$ and $Otr^{-/-}$ mice. Arrows indicate the primers used for genotyping. Black chevrons indicate loxP sites and white chevrons FRT sites. A neomycin resistance cassette (pkg-neo^r) was inserted in intron 1 and was flanked by FRT; it could be excised by FLP recombinase to obtain the Otr floxed allele. Exons 2 and 3 (open boxed 2 and 3) were flanked by loxP sites and could be excised by Cre recombinase to obtain the Otr knock-out allele. Adapted from [Lee et al., 2008].

4.1.2 GAD67-GFP$^+$ (Δneo) mice

Part of the experiments described in this work were performed on young (P17-P26) male and female GAD67-GFP$^+$ (Δneo) mice. The model was kindly donated by the Japanese group that first generated it [Tamamaki et al., 2003].

To obtain GAD67-GFP$^+$ (Δneo) mice, a cDNA-encoding EGFP (Enhanced Green Fluorescent Protein) was targeted to the locus encoding the enzyme GAD67 (Glutamate Decarboxylase 67) using homologous recombination (**fig. 14**). Homologous recombinant ES cells were used to generate chimeric male mice by 8-cell stage injection. GAD67-GFP$^+$ mice were obtained by breeding chimeric male mice with C57BL/6 or ICR females. These animals retained the EGFP cDNA and a loxP-flanked PKG-Neo cassette in the GAD67 locus (**fig. 14**). The PGK-Neo cassette, used as a positive selection marker for screening homologous recombinant ES cells, was excised *in vivo* by mating GAD67-GFP$^+$ mice with CAG-Cre transgenic mice (**fig. 14**). GAD67-GFP$^+$ mice without the PKG-neo cassette were referred to as GAD67-GFP$^+$ (Δneo) mice.

Since the alteration of both GAD67 alleles is lethal at birth [Asada et al., 1997], mice heterozygous for the altered GAD67 allele were used for all the observations in this study.

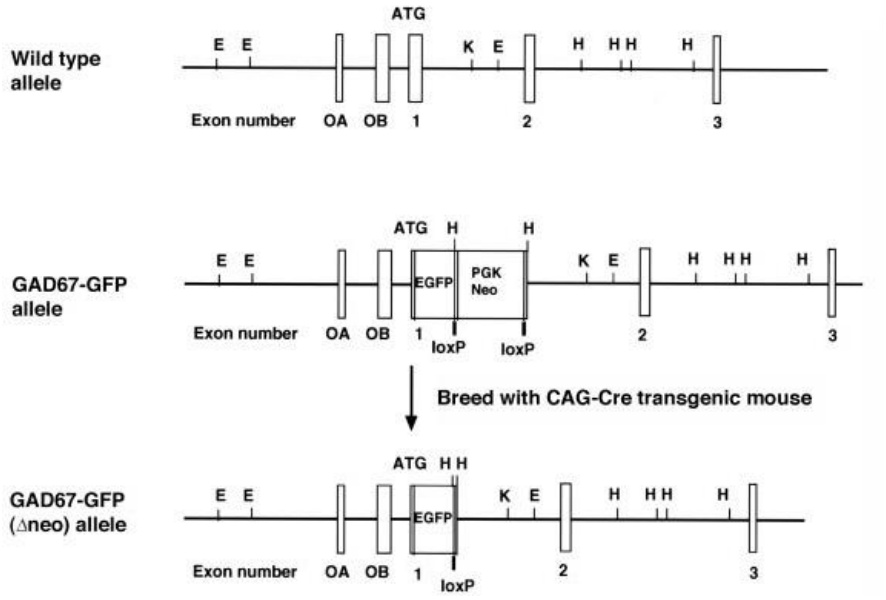

Fig. 14. Schematic representation of the wild-type, targeted, and recombinant alleles of GAD67. The original GAD67-GFP$^+$ mice retained a loxP-flanked neomycin resistance cassette (PGK-Neo). The knock-in mice were bred with CAG-Cre transgenic mice to eliminate the PGK-Neo cassette from the GAD67 locus. The recognition sites of EcoRI (E), HindIII (H), and KpnI (K) are indicated. Adapted from [Tamamaki et al., 2003].

GAD67-GFP$^+$ (Δneo) mice were phenotypically identified during the first three days of their life by placing animals under a fluorescent lamp: blue light was able to excite EGFP revealing a green fluorescent of the entire brain (**fig. 15**).

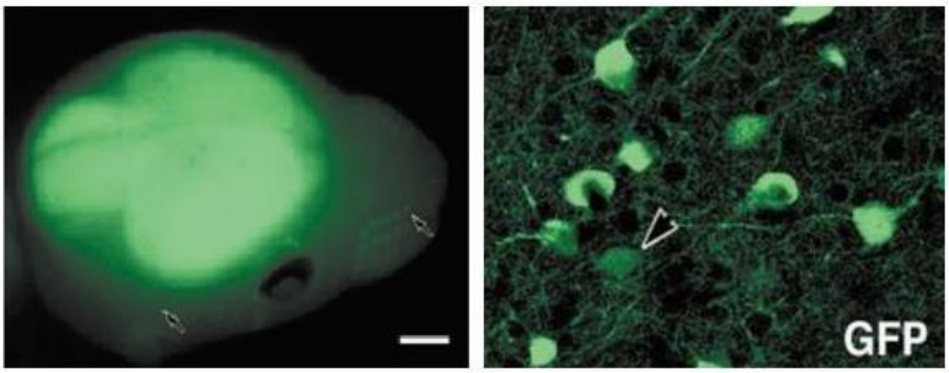

Fig. 15. Head of a GAD67-GFP$^+$ (Δneo) new-born mouse observed with a fluorescence microscope (left). Distribution of GAD67-expressing neurons, recognized thanks to the green fluorescence of EGFP (right). Adapted from [Tamamaki et al., 2003].

4.2 Submerged brain slices preparation

All the electrophysiological experiments described in this thesis were performed on submerged brain slices. The first experiments on brain slices were introduced in 1966 by Henry McIlwain [Yamamoto & McIlwain, 1966a; Yamamoto & McIlwain, 1966b] and they are useful to study the functional mechanisms of neural circuits.

Brain slices were obtained through a standard dissection of young mice. Animals were anesthetized by inhalation of isoflurane (MATERIAL©), a volatile anesthetic. After anesthesia, evidenced by slow respiration and lack of movements and specific reflexes, they were decapitated using a large and sharp pair of scissors. The head was rapidly submerged in ice-cold (~ 4°C), carboxygenated (95% O_2 - 5% CO_2) cutting solution containing (in mM): Sucrose 70; NaCl 80; KCl 2.5; $NaHCO_3$ 26; Glucose 15; $MgCl_2$ 7; $CaCl_2$ 1; NaH_2PO_4 1.25. The carboxygenation ensures an appropriate O_2 supply, whereas low temperatures reduce the excitotoxic damage caused by anoxia.

After a brief period of incubation, the scalp was removed and the skull was completely exposed. Subsequently, a caudal-to-rostral cut along the sagittal suture was performed using fine-pointed scissors, and the two bone flaps of the skull covering each hemisphere were gently removed using a pair of tweezers. After the exposure, the brain was finally isolated performing two coronal cuts at two different rostro-caudal levels: one between the telencephalic hemispheres and the olfactory bulbs and one between the hemispheres and the cerebellum. Then, the two hemispheres were separated through a sagittal cut, carefully extracted from the skull using a spatula and finally submerged in ice-cold cutting solution. Following a brief incubation, transversal brain slices containing the hippocampus were prepared as described by Stoop and Pralong [Stoop & Pralong, 2000]. Briefly, each hemisphere was positioned flat on its medial surface and the dorsal side of the brain was cut along a plane, which was tilted at a 20° posterosuperior-anteroinferior angle from a plan passing between the lateral olfactory tract and the base of the brainstem. This cut ensures good health and functionality of hippocampal neurons because it preserves the integrity of the tri-synaptic circuitry. The exposed dorsal side of the brain was then glued onto a cutting block and 350-µm-thick slices containing the region of interest were obtained using a vibratome (DTK-1000, Dosaka EM, Kyoto, Japan). During the preparation of slices, the tissue was submerged in ice-cold cutting solution. Slices were transferred to an incubation chamber filled with warm (37°C), carboxygenated artificial cerebrospinal fluid (aCSF)

containing (in mM): NaCl 125; KCl 2.5; $NaHCO_3$ 26; Glucose 15; $MgCl_2$ 1.3; $CaCl_2$ 2.3; NaH_2PO_4 1.25. In order to recover the optimal conditions after the cutting process, slices were kept for 30 minutes at 37°C and for 30 minutes at room temperature (~ 23°C) before the electrophysiological analysis.

4.3 Electrophysiological analysis

All the electrophysiological experiments described in the present work were performed using the conventional patch-clamp technique, developed by Sakmann and Neher in 1976 [Neher & Sakmann, 1976a; Neher & Sakmann, 1976b].

4.3.1 Whole-cell patch-clamp recordings

After the recovery, brain slices were transferred to a submerged-style recording chamber and continuously perfused with carboxygenated aCSF at room temperature (~ 23°C). The flow rate was adjusted to 1.4 ml/min. The recording chamber was mounted on a traditional differential interference contrast (DIC) microscope (Nikon E600FN), equipped with a 4X objective (NikonPlan Fluor 4X/0.13) and a 40X water-immersion objective (Nikon Fluor 40X/0.80) and connected to a near-infrared charge-coupled device (CCD) camera that allowed cells visualization. Electrophysiological experiments were performed on hippocampal CA1 pyramidal neurons and GABAergic interneurons located in the *stratum pyramidale*. The former were visually recognized by the triangular shape of their soma, whereas the latter were identified by using a fluorescent system consisting of an Hg-Arch lamp and an appropriate filter set. The cell selected for recording was approached with a patch pipette produced from borosilicate glass capillary tubes (Hilgenberg GmbH, Malsfeld, Germany) using a horizontal puller (P-97, Sutter instruments, Novato, CA, USA). The pipette was filled with a solution iso-osmotic with cytosol (intracellular solution). For some recordings, intracellular solution contained (in mM): K-gluconate 130; NaCl 4; $MgCl_2$ 2; EGTA 1; Hepes 10; CP 5; Na_2ATP 2; Na_3GTP 0.3 (pH adjusted to 7.3 with KOH). For other recordings, the solution contained (in mM): Cs-methanesulphonate 120; KCl 5; $CaCl_2$ 1; $MgCl_2$ 2; EGTA 10; Na_2ATP 4; Na_3GTP 0.3; lidocaine N-ethylbromide 5; Hepes 8 (pH adjusted to 7.3 with KOH). When filled with the above solutions, patch pipettes had a resistance of 4-5 MΩ. A silver chloride electrode connected to a MultiClamp 700B amplifier (Axon Instruments Molecular Devices, Sunnyvale, CA) was inserted into the pipette to

deliver and record electrical signals. During the approach of the pipette to the cell, controlled by a system of mechanical and piezoelectric micromanipulators (Burleigh® PCS-6000), a positive pressure was applied inside the pipette in order to prevent clogging of the tip. When the tip was in close proximity to the neuron, a suction was gently applied to the back of the pipette, in order to create a very high resistance seal (1 GΩ or more - 'giga seal') between the cell membrane and the tip. This configuration is called cell-attached (**fig. 16A**). The correct formation of the 'giga seal' is important to ensure the electrical isolation of the patched area and therefore to minimize leakage currents. The whole-cell configuration (**fig. 16B**), used in all the experiments described in this work, was achieved by applying a brief strong suction inside the pipette, in order to cause the rupture of the membrane patch under the tip. In this configuration, the interior of the pipette becomes continuous with the cytoplasm of the cell, allowing the measurement of electrical potentials and currents flowing through the entire cell membrane.

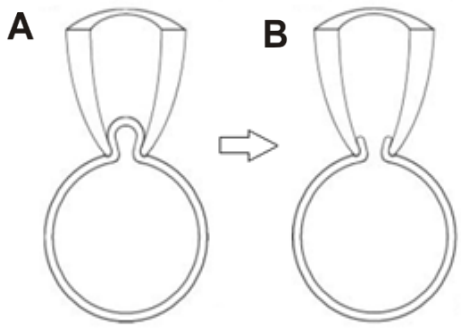

Fig. 16. (A) Schematic representation of cell-attached configuration in which the tip of the pipette is in close contact with the cell membrane. **(B)** After the rupture of the membrane patch under the tip, the interior of the pipette becomes continuous with the cytoplasm of the cell (whole-cell configuration). Adapted from [Molleman, 2003].

Experiments were performed in voltage- and current-clamp modes. Voltage-clamp allows to measure transmembrane currents flowing through ion channels, while holding the cell membrane potential at a set value. Current-clamp allows to evaluate the variations of voltage in response to currents that can be injected or pharmacologically evoked. All the electrical signals generated by the cell were digitized with a Digidata 1322 computer interface (Digitata, Axon Instruments Molecular Devices, Sunnyvale, CA) and then acquired using the software Clampex 9.2 (Molecular Devices, Palo Alto, CA, U.S.A.). Data were sampled at 20 kHz and filtered at 10 kHz before the off-line analysis.

4.3.2 Drugs and chemicals

The effects of specific chemicals were studied upon external perfusion of the slice. All drugs were dissolved in distilled water and stored at -20°C in stock solutions. Before the experiment, drugs were added to aCFS in order to reach an appropriate experimental concentration.

The stimulation of OTRs were performed through the application of TGOT (Thr^4,Gly^7-oxytocin, Bachem, Bubendorf, Switzerland; 1 μM), an OT analogue that selectively activates OTRs without stimulating vasopressin receptors. The appropriate concentration of the agonist was chosen following some voltage-clamp experiments in which the effect of different concentrations of TGOT (1 nM, 10 nM and 1 μM) was assessed on spontaneous inhibitory postsynaptic currents (sIPSC) recorded from CA1 pyramidal neurons. sIPSCs are the consequence of the spontaneous release of neurotransmitter occurring when the presynaptic terminal fires spontaneous action potentials. Our data shown that on average TGOT (1 nM) caused a reduction of 12.4 ± 3.2 % in the sIPSC interval (the reciprocal of the instantaneous event frequency) in 13 neurons examined and an increase of 3.5 ± 1.4 % in the sIPSC amplitude in 15 cells tested. TGOT (10 nM) caused a reduction of 27.2 ± 3.3 % in the sIPSC interval in 13 neurons and an increase of 7.4 ± 1.9 % in the amplitude in 18 cells. Finally, TGOT (1 μM) caused a reduction of 36.6 ± 6.4 % in the sIPSC interval and an increase of 29.3 ± 11.9 % in the amplitude in 21 cells. Since TGOT (1 μM) evoked the maximal responses (**fig. 17**), this concentration was used for all the experiments.

sIPSCs were isolated by blocking the ionotropic glutamate receptor-mediated synaptic transmission with NBQX (2,3-Dioxo-6-nitro-1,2,3,4 tetrahydrobenzo[f]quinoxaline-7-sulfonamide, Tocris Cookson, Bristol, UK; 10 μM), an AMPA receptor antagonist and (RS)-CPP ((RS)-3-(2-Carboxypiperazin-4-yl)-propyl-1-phosphonic acid, Tocris Cookson, Bristol, UK; 30 μM), an NMDA receptor antagonist.

For the recording of miniature inhibitory postsynaptic currents (mIPSC), which are the result of a stochastic release of neurotransmitter by the presynaptic terminal, the genesis of action potentials was prevented by blocking voltage-gated Na^+ channels with TTX (tetrodotoxin, Tocris Cookson, Bristol, UK; 1 μM).

In other experiments, the effect of TGOT was assessed on spontaneous excitatory postsynaptic currents (sEPSC) that were isolated by blocking the ionotropic $GABA_A$

receptor ($GABA_AR$)-mediated synaptic transmission with bicuculline (SigmaAldrich, Oakville, Ontario, Canada; 10 μM).

To investigate the involvement of OTRs in the TGOT-mediated effects, receptors were blocked using SSR126768A (4-chloro-3-[(3R)-(+)-5-chloro-1-(2,4-dimethoxybenzyl)-3-methyl-2-oxo-2,3-dihydro-1H-indol-3-yl]-N-ethyl-N-(3-pyridylmethyl)-benzamide, hydrochloride, Sigma-Aldrich, Oakville, Ontario, Canada; 0.1 μM), an antagonist selective for the murine isoform of OTRs.

Finally, to evaluate the putative role of L-type voltage-gated Ca^{2+} channels in the responses elicited by TGOT, the channels activity was selectively blocked using nifedipine (Sigma-Aldrich, Oakville, Ontario, Canada; 5 μM).

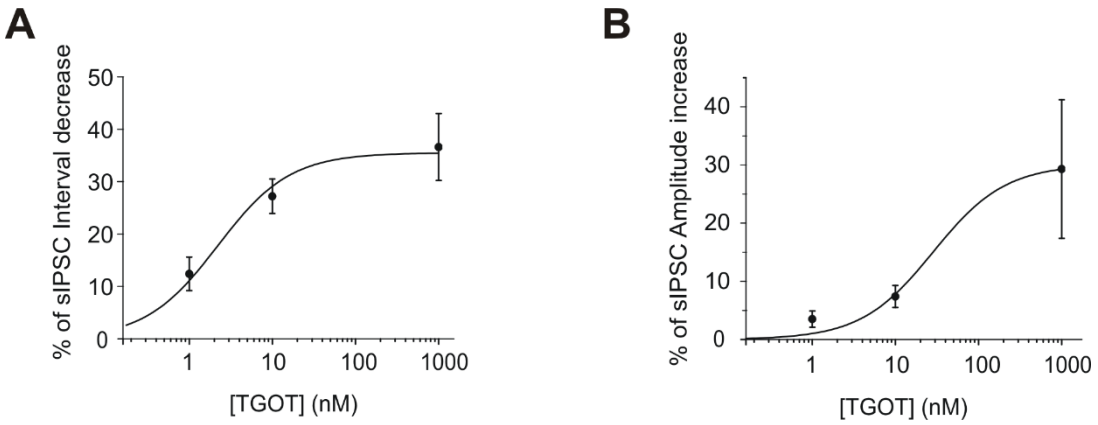

Fig. 17. (A) Sigmoidal relationship between the percentage of sIPSC interval decrease and TGOT concentration ([TGOT]). The mean values were obtained in 13 experiments with TGOT (1 nM and 10 nM) and in 21 experiments with TGOT (1 μM). Note that the maximal decrease in the sIPSC interval was elicited by TGOT (1 μM). **(B)** Sigmoidal relationship between the percentage of sIPSC amplitude increase and [TGOT]. The mean values were obtained in 15 experiments with TGOT (1 nM), 18 experiments with TGOT (10 nM) and in 21 experiments with TGOT (1 nM). Note that the maximal increase in the sIPSC interval was elicited by TGOT (1 μM).

4.3.3 Data analysis

Electrophysiological data were analyzed off-line using the software Clampfit 10.2 (Molecular Devices, Palo Alto, CA, U.S.A.) and NeuroMatic, a collection of Igor Pro (WaveMetrics Inc., Oswego, Oregon USA) functions. Statistical analysis were made with Microsoft Office Excel 2010 and graphs were created using Microcal Origin 6.0 (OriginLab, Northampton, MA) and CorelDRAW 12. All measurements throughout the text are expressed as mean ± standard error; N indicates the number of neurons studied for each

experimental procedure. The results obtained were compared with the two-tailed Student's t-test and were considered statistically significant for $p<0.05$ or $p<0.005$.

4.3.3.1 Analysis of passive membrane properties

Membrane capacitance (C_m) is a passive membrane property that results from the fact that the plasma membrane acts as a capacitor: the phospholipid bilayer is a thin insulator separating two electrolytic media, the extracellular space and the cytoplasm. In this work, C_m was estimated from the capacitive current (I_c) evoked by a -10 mV pulse commanded just after obtaining the whole-cell configuration (**fig. 18**). The relationship between C_m and I_c is the following:

$$I_c = \frac{q}{dt} = C_m \frac{dV_m}{dt}$$

Then:

$$C_m = \frac{q}{dV_m}$$

The parameter q represents the amount of charge required to generate I_c: experimentally, q was obtained by integrating I_c with respect to time (dt) (**fig. 18-lower trace**). The parameter dV_m is the voltage pulse commanded (- 10 mV) (**fig. 18-upper trace**).

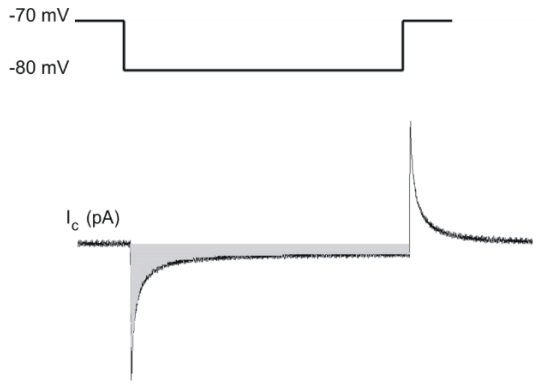

Fig. 18. Capacitive current (I_c) (lower trace) evoked by the administration of a negative potential step of -10 mV (upper trace) starting from -70 mV. The grey area represents the amount of charge (q) required to generate I_c and was estimated by integrating I_c with respect to time (dt).

Neuronal input resistance (R_{in}) is a passive membrane property that measures the opposition to current flow. R_{in} is inversely related to the number of ion channels expressed by the cell. Experimentally, R_{in} was calculated from the linear portion of the current-to-voltage (I-V)

relationship (**fig. 19B**) obtained in current-clamp mode by measuring steady-state voltage responses (**fig. 19A**) to hyperpolarizing and depolarizing current steps. The angular coefficient of the I-V curve represents the total conductance of the membrane (g_m). The reciprocal of g_m is R_{in} (**fig. 19B**).

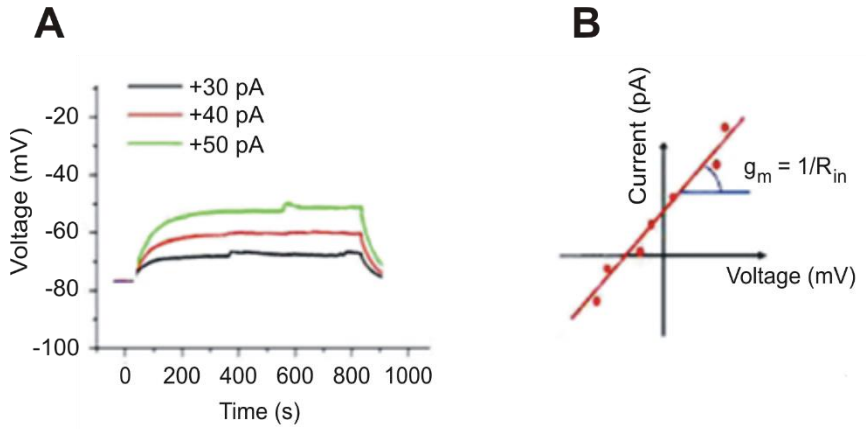

Fig. 19. (A) Representative depolarizing subthreshold voltage responses to the injection of positive current steps (+30, +40 and +50 pA). **(B)** The linear portion of the current-to-voltage (I-V) relationship, whose angular coefficient is the total conductance of the membrane (g_m). The reciprocal of g_m is input resistance (R_{in}).

4.3.3.2 Analysis of synaptic currents

Synaptic currents, also called 'phasic' currents, are mediated by receptors clustered opposite the release site or located in a perisynaptic position, just outside the postsynaptic density. In this work, spontaneous excitatory and inhibitory synaptic events were recorded in voltage-clamp mode during the application of protocols each lasting 50 s (long recordings protocols). The off-line analysis were performed using NeuroMatic, a collection of Igor Pro functions. Firstly, events were detected automatically, setting a detection threshold of 10 pA. Other parameters were empirically set to detect the maximum number of events that were clearly discernible from the background noise. Secondly, selected parts of the record were reviewed manually in order to eliminate artifacts and include previously undetected events. Finally, a quantitative analysis of the amplitudes and the intervals was performed using Microcal Origin 6.0. The amplitudes of spontaneous synaptic currents obeyed a lognormal distribution (**fig. 20B**) in all neurons tested. Accordingly, the mean amplitude was computed as the peak of the lognormal function used to fit the distribution. Intervals for spontaneous synaptic currents were distributed exponentially (**fig. 20A**) and the mean interval was computed as the tau (τ) value of the mono-exponential function that best fitted the distribution (**fig. 20A**).

This parameter represents the value of the interval at which the distribution is decreased exponentially to 37% of its initial value. The reciprocal of τ is the mean of the instantaneous frequencies of synaptic currents.

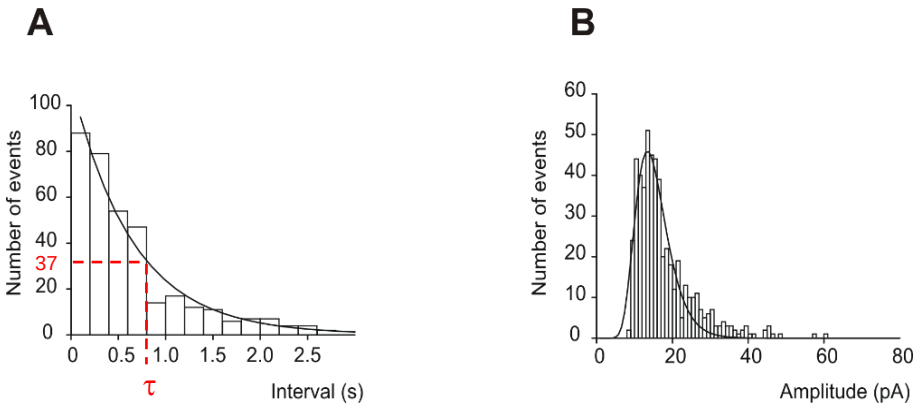

Fig. 20. (A) Representative exponential distribution of the intervals of spontaneous synaptic currents. The mean interval is τ that represents the value of the interval at which the distribution is decreased exponentially to 37% of its initial value. The reciprocal of τ is the mean of the instantaneous frequencies of synaptic currents. **(B)** Representative lognormal distribution of the amplitudes of spontaneous synaptic currents. The mean amplitude is the peak of the lognormal function.

In some experiments, a kinetic analysis of spontaneous synaptic currents was performed by measuring rise time and time constant of decay (τ). The former represents the time that current takes to activate to 90%, whereas τ represents the time that current takes to deactivate to 37% of its peak value. Experimentally, rise time was computed using a measurement in Clampfit; τ was obtained by the mono-exponential function that best fitted the decay phase of the current.

4.3.3.3 Analysis of extrasynaptic currents

Extrasynaptic currents, also called 'tonic' currents, are mediated by receptors located hundreds of nanometres away from the postsynaptic density. In this work, we investigated the presence of $GABA_AR$-mediated tonic currents in voltage-clamp mode by applying a saturating concentration of a specific $GABA_AR$ antagonist, bicuculline (10 μM), according to the standard method (**fig. 21**) [Bright & Smart, 2013]. As well as blocking synaptic currents, this treatment revealed a tonic inhibition by causing a shift in the 'baseline holding current' required to clamp the membrane potential of cells at a set value. In general, the direction of the shift depends on two parameters: the holding potential (V_h) of voltage-clamp

recordings and the Nernst equilibrium potential for Cl^- (E_{Cl^-}). The shift is outward if V_h is negative and E_{Cl^-} is set to be close to 0 mV [Bright & Smart, 2013] (**fig. 21A**), while is inward if V_h is positive and E_{Cl^-} is set to be close to the resting membrane potential. The quantitative analysis of the shift was performed by generating all-point histograms (**fig. 21B**) for two trace intervals, each lasting 10 s: one recorded in control conditions and one recorded during perfusion of bicuculline. Histograms were fitted with Gaussian curves, in agreement with literature data [Bright & Smart, 2013]. Peak values of the curves represented the mean currents recorded before and during drug perfusion. The difference between the mean currents (bicuculline - control) provided an estimation of the tonic current.

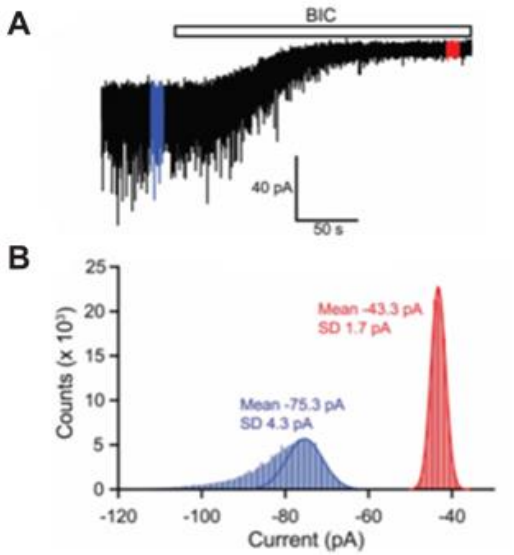

Fig. 21. (A) Representative current trace recorded from a thalamic relay neuron in control conditions and during the application of bicuculline (BIC). Note that bicuculline blocks all synaptic events and reveals a tonic $GABA_AR$-mediated current, causing an outward shift in the 'baseline holding current'. Blue and red boxes indicate the 10 s long intervals used to the construction of the all-point histograms. **(B)** Representative all-point histograms for the intervals shown in panel A (blue box: trace interval recorded in control conditions; red box: trace interval recorded during bicuculline perfusion). Peak values of histograms, fitted with Gaussian curves, represent the mean currents recorded before (-75.3 pA) and during (-43.3 pA) perfusion of bicuculline. The difference between the mean currents (bicuculline - control) provides the outward shift. Thus, this method gives a tonic current of -43.3 + 75.3= 32pA. Adapted from [Bright & Smart, 2013].

On this basis, the application of a molecule that increases tonic inhibition causes a shift whose direction is opposite to that described for $GABA_AR$ antagonist: indeed, the shift will be inward if V_h is negative and E_{Cl^-} is close to 0 mV and will be outward if V_h is positive and E_{Cl^-} is close to the resting membrane potential. In this thesis, a putative TGOT-mediated modulation of tonic inhibition was quantified by measuring the difference between the 'baseline holding current' recorded during perfusion of TGOT and that recorded in control conditions.

4.3.3.4 Analysis of cell excitability

Neuronal excitability was assessed during current-clamp experiments by recording voltage responses to the injection of depolarizing currents steps of increasing intensity (**fig. 22A**). The quantitative analysis of the responses were performed by measuring the firing frequency, computed as the number of action potential generated per unit time, at each current step. The values of frequency were used to construct the firing rate-to-injected current (F-I) relationship (**fig. 22B**), characterized by two parameters: the offset (i.e., the minimal intensity of injected current required to attain a response) and the gain (i.e., the slope of the relationship), according with literature [Brickley et al., 1996]. The offset was assessed during the experiment, adjusting the intensity of the injected current to evoke the action potential discharge at the lowest frequency. The gain was computed as the angular coefficient of the linear regression function that best fitted the F-I curve (**fig. 22B**).

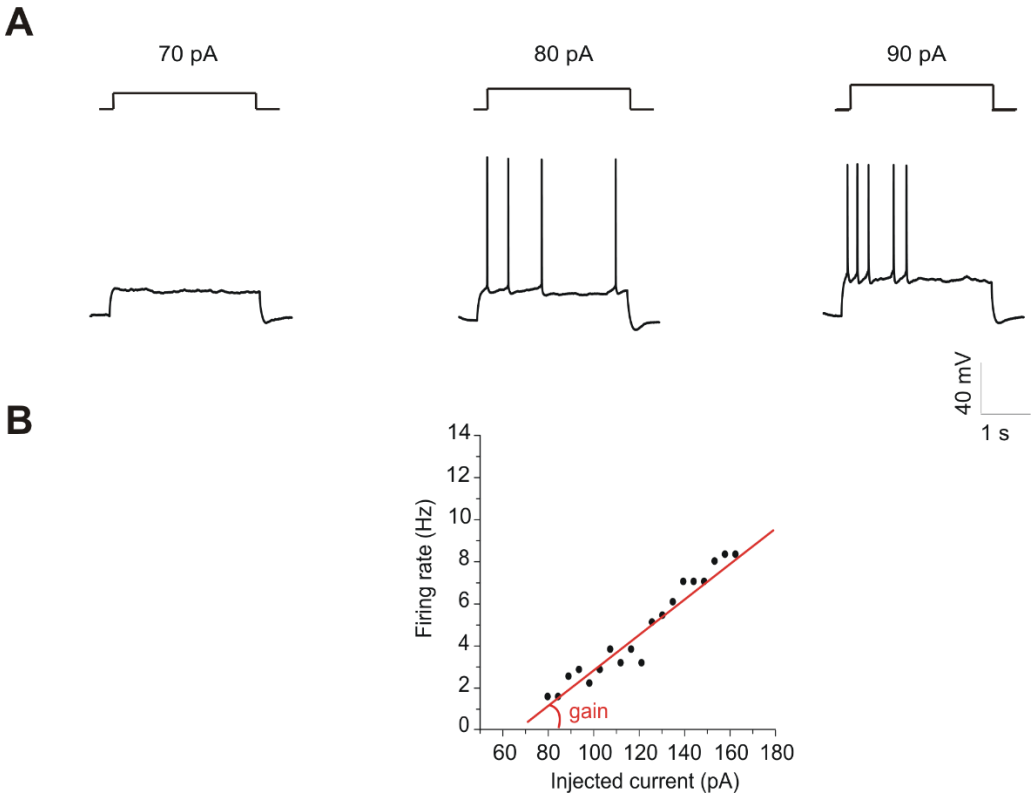

Fig. 22. **(A)** Representative voltage responses recorded from a CA1 hippocampal neuron after the injection of depolarizing current steps of increasing intensity (70, 80 and 90 pA). **(B)** Graph showing the firing rate-to-injected current (F-I) relationship referred to the traces of panel A. The experimental values (black dots) were fitted with a linear regression function (red line) whose angular coefficient represents the gain of the F-I curve.

5. RESULTS

Morphological and electrophysiological evidence indicate that the neuropeptide oxytocin (OT) acts as a neurotransmitter or neuromodulator in the central nervous system [Mühlethaler et al., 1983; Tiberiis et al., 1983; Mühlethaler et al., 1984; Raggenbass et al., 1989; Owen et al., 2013]. Indeed, the presence of binding sites for OT has been widely demonstrated in CA1 field and *subiculum* of the hippocampal formation by *in vitro* light microscopic autoradiography [Freund-Mercier et al., 1989; Tribollet et al., 1988; Barberis & Tribollet, 1996] and *in situ* hybridization [Yoshimura et al., 1993]. The first electrophysiological experiments, based on extracellular recordings from rat slices, have demonstrated that OT is able to excite a subpopulation of GABAergic interneurons (IN) located in CA1 *stratum pyramidale* [Mühlethaler et al., 1983; Mühlethaler et al., 1984; Raggenbass et al., 1989; Raggenbass, 2001]. Furthermore, Zaninetti and Raggenbass have shown that external perfusion of the selective OT receptor (OTR) agonist Thr^4,Gly^7-oxytocin (TGOT) causes an increase in the frequency and the amplitude of spontaneous inhibitory postsynaptic currents (sIPSC) recorded from CA1 pyramidal neurons (PYR) [Zaninetti & Raggenbass, 2000]. More recently, using whole-cell patch-clamp technique Owen and colleagues have shown that the increase in sIPSCs arises mainly from a specific class of GABAergic INs, fast-spiking, that respond to TGOT with a depolarization [Owen et al., 2013]. The molecular pathway underlying the TGOT-mediated depolarization is still unclear. Overall, the experiments performed on rats indicate that OT is able to target a selective population of hippocampal INs, leading to an increase in the level of the inhibitory synaptic transmission onto PYRs.

Taking the cue from those findings, our aim was to characterize in detail the neuromodulatory effect of OT in mouse. In order to exclude any interference from vasopressin receptors which may be present in the hippocampus [Audigier & Barberis, 1985], we also used the selective OTR agonist, TGOT (see "Material and methods"). In the first whole-cell patch-clamp experiments, performed by Dr. Paolo Spaiardi, we evaluated the effect of TGOT on spontaneous (sIPSC) and miniature (mIPSC) inhibitory postsynaptic currents recorded from CA1 PYRs in $Otr^{+/+}$ mice (i.e., animals that normally express OTRs, see "Material and methods"). By definition, spontaneous events are the consequence of the spontaneous release of neurotransmitter occurring when the presynaptic terminal fires

spontaneous action potentials, whereas miniature events are the result of a stochastic vesicular release. Accordingly, a comparison between the two types of events was helpful to elucidate the presynaptic mechanism underlying the TGOT-induced effect. Then, we evaluated the potential action of the agonist on spontaneous excitatory postsynaptic currents (sEPSC) in $Otr^{+/+}$ mice. Finally, in order to better investigate the involvement of OTRs in the TGOT-mediated responses, we performed a comparative analysis of both sIPSCs and sEPSCs between $Otr^{+/+}$ and $Otr^{-/-}$ mice (i.e., animals lacking OTRs in the entire body, see "Material and methods").

After having clarified the effect of TGOT on 'phasic' transmission, elicited by the activation of synaptic receptors, we wondered if the peptide could act also on 'tonically' elicited currents, mediated by extrasynaptic receptors that are widely described in CA1 PYRs [Banks & Pearce, 2000; Scimemi et al., 2005; Mortensen & Smart, 2006; Prenosil et al., 2006; Pavlov et al., 2009].

The next goal was to identify the neuronal target of TGOT, by investigating the effect of the agonist directly on the membrane potential of GABAergic INs in CA1. To recognize GABAergic cells, we used GAD67-GFP^{+} (Δneo) mice (see "Material and methods") whose GABAergic INs are constitutively labelled with Green Fluorescent Protein (GFP) [Tamamaki et al., 2003]. In addition, we performed some preliminary experiments aimed at understanding the putative ionic mechanism involved in the TGOT-induced effect.

Finally, we examined the effects of TGOT perfusion on the membrane potential of PYRs, enquiring if it was able to modulate their excitability: to this purpose, we evaluated how the agonist influenced the capability of the cells to generate action potentials in response to depolarizing current steps of increasing intensity.

5.1 Anatomical localization and electrophysiological properties of CA1 hippocampal neurons

Electrophysiological recordings described in this thesis were performed on 75 PYRs and 84 GABAergic INs located in CA1 *stratum pyramidale* of hippocampal brain slices (**fig. 23**). For the experiments, young (P17-P26) $Otr^{+/+}$, $Otr^{-/-}$ and GAD67-GFP^{+} (Δneo) mice were used (see "Materials and methods"). PYRs were visualized by infrared microscopy, whereas GABAergic INs were identified because of their GFP-dependent fluorescence (see "Materials and methods").

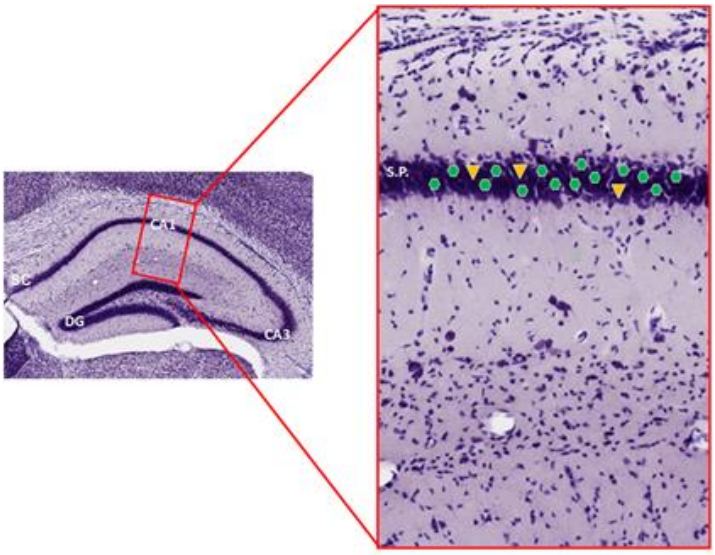

Fig.23. Schematic representation of a mouse brain slice (left). The regions of the hippocampal formation are shown. Abbreviations: DG, dentate gyrus; CA, Ammon's horn (with CA1 and CA3 fields); SC, subicular complex. Magnification of CA1 region of interest (red rectangle, right). The cell bodies of PYRs (yellow triangles) and GABAergic INs (green hexagons) subjected to electrophysiological analysis are shown. PYRs and INs are located in the *stratum pyramidale* (S.P.), easily recognized under the microscope because it appears more electrondense than surrounding layers.

First, we performed the analysis of passive membrane properties of neurons in order to assess their overall health. The mean values of membrane capacitance (C_m) and input resistance (R_{in}) of 46 PYRs in $Otr^{+/+}$, 29 PYRs in $Otr^{-/-}$ and 84 INs in GAD67-GFP^+ (Δneo) mice are summarized in **tab. 1A-B**. As regard the comparison between PYRs in $Otr^{+/+}$ and $Otr^{-/-}$ mice (**tab. 1A**), no significant differences in C_m and R_{in} were observed. Thus, although $Otr^{-/-}$ mice exhibit numerous behavioral deficits (see "Material and methods") [Lee et al., 2008; Sala et al., 2011], the intrinsic properties of hippocampal PYRs are not altered. Regarding the comparison between PYRs in $Otr^{+/+}$ and INs in GAD67-GFP^+ (Δneo) mice (**tab. 1B**), we found that C_m was significantly higher in PYRs, whereas R_{in} was significantly higher in INs (uncoupled two-tailed Student's t-test, $p<0.005$). These last data highlight the differences in cell dimensions and expression of ion channels between the two classes of cells, in accordance with literature data [Martina et al., 2013].

A

	C_m (pF)	R_{in} (MΩ)
PYRs from $Otr^{+/+}$ (N=46)	57.2 ± 3.2	115 ± 11
PYRs from $Otr^{-/-}$ (N=29)	50.9 ± 4.3	109 ± 6

B

	C_m (pF)	R_{in} (MΩ)
PYRs from $Otr^{+/+}$ (N=46)	57.2 ± 3.2	115 ± 11
INs from GAD67-GFP^+ (Δneo) (N=84)	42.9 ± 1.4 **	211 ± 14 **

Tab.1. (A) Summary of the mean values of membrane capacitance (C_m) and input resistance (Ri_n) obtained from 46 PYRs in $Otr^{+/+}$ and 29 PYRs in $Otr^{-/-}$ mice. No significant differences in C_m and R_{in} were observed. (**B)** Summary of the mean values of C_m and R_{in} obtained from 46 PYRs in $Otr^{+/+}$ and 84 INs in GAD67-GFP^+ (Δneo) mice. Significant differences in both C_m and R_{in} were detected (uncoupled two-tailed Student's t-test, **$p<0.005$).

The next experiments were targeted to understand in detail the neuromodulatory effect of TGOT on the hippocampal network.

5.2 Effect of TGOT on the synaptic transmission in CA1 field

In the first voltage-clamp recordings, performed by Dr. Paolo Spaiardi, we evaluated the action of TGOT on spontaneous inhibitory and excitatory synaptic transmission onto CA1 PYRs.

5.2.1 Effect of TGOT on spontaneous inhibitory postsynaptic currents (sIPSC) recorded from PYRs in $Otr^{+/+}$ mice

Spontaneous inhibitory postsynaptic currents (sIPSC) were recorded from 23 PYRs in $Otr^{+/+}$ mice, during the application of voltage-clamp protocols each lasting 50 s (long recordings) at a holding potential of 0 mV. Experiments were performed in control conditions, during perfusion of TGOT (1 μM) and during drug wash out. To exclude the activation of

glutamatergic receptors, sIPSCs were recorded in the presence of NBQX (10 μM) and CPP (30 μM) that block AMPA and NMDA receptors, respectively.

An example of how TGOT influenced the inhibitory synaptic input onto PYRs is shown in **fig. 24A-B**: in the presence of TGOT, both sIPSC frequency and amplitude increased. This effect was reversible, as during drug wash out the parameters tended to decrease towards their control values. A quantitative analysis of sIPSC interval (the reciprocal of the instantaneous event frequency) and amplitude was performed as well. Our data shown that TGOT caused a significant decrease in the sIPSC interval in 21 out of 23 PYRs examined (coupled two-tailed Student's t-test, $p<0.05$): on average the interval was 760 ± 137 ms in control conditions and 388 ± 61 ms during application of TGOT (**fig. 24C**). Furthermore, a significant increase in the sIPSC amplitude was measured in 20 out of 23 PYRs (coupled two-tailed Student's t-test, $p<0.05$): on average the amplitude was 13.0 ± 0.7 pA in control conditions and 16.7 ± 1.6 pA during perfusion with TGOT (**fig. 24D**).

The effect of TGOT was evident not only on the sIPSC frequency and amplitude but also on their kinetics properties (**fig. 25A**). Indeed, TGOT caused a significant increase in the sIPSC time constant of decay (τ) in 4 PYRs examined (coupled two-tailed Student's t-test, $p<0.05$): on average τ was 13.9 ± 1.8 ms in control conditions and 20.9 ± 3.1 ms during the application of TGOT (**fig. 25C**). No significant changes in the sIPSC rise time were observed: on average the rise time was 1.7 ± 0.2 ms in control conditions and 2.3 ± 0.5 ms in the presence of TGOT (**fig. 25B**).

The inhibitory currents modulated by TGOT were mediated by the activation of $GABA_A$ receptors ($GABA_AR$) expressed on PYRs: indeed, the perfusion of bicuculline (10 μM), a $GABA_AR$ antagonist, blocked all synaptic activity in 3 out of 3 cells (**fig. 26A**).

The confirmation that sIPSCs were carried by Cl^- flowing through $GABA_ARs$ was given by its reversal potential (E_{rev} = -64 mV), calculated from the current-to-voltage (I-V) relationship (**fig. 26B**). E_{rev} was very similar to the Nernst equilibrium potential for Cl^- (E_{Cl^-} = -68 mV) obtained from Cl^- intracellular and extracellular concentrations of 9 mM and 135 mM respectively (see "Materials and methods").

Finally, the effects elicited by TGOT on $GABA_AR$-mediated currents were highly dependent on the activation of OTRs: indeed, the co-administration of TGOT and SSR126768A (0.1 μM), an antagonist selective for the murine isoform of OTRs, was able to return the sIPSC interval and amplitude towards their control values (N=3) (**fig. 27**).

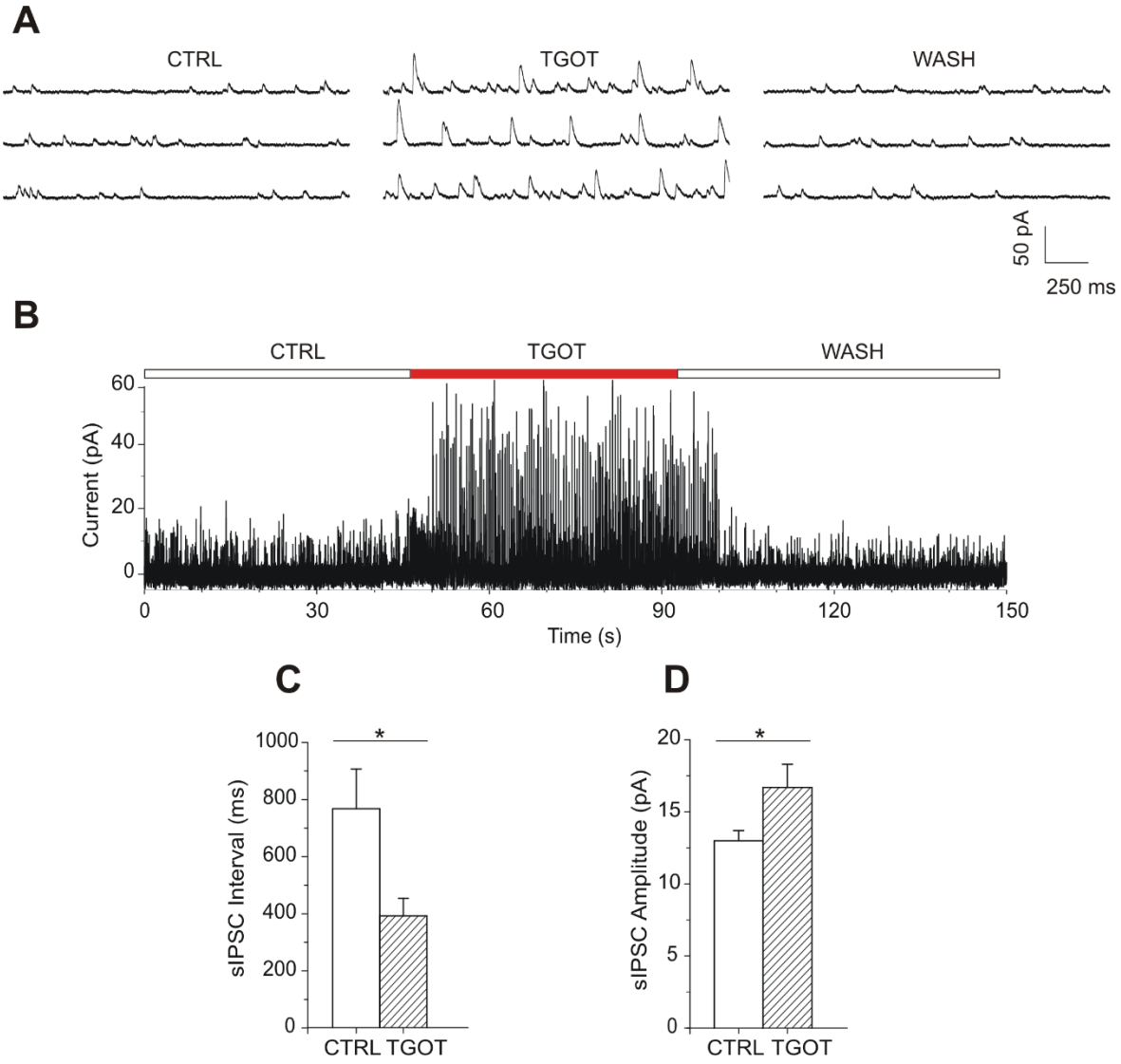

Fig. 24. (A) Representative current traces of sIPSCs recorded from CA1 PYR in the presence of glutamatergic synaptic blockers, NBQX (10 μM) and CPP (30 μM) at a holding potential of 0 mV, in control conditions (CTRL), during TGOT (1 μM) administration (TGOT) and during drug wash out (WASH). **(B)** Overview of the entire experiment that clarifies the effect elicited by TGOT on sIPSCs. **(C)** and **(D)** Histograms comparing the mean values of the sIPSC interval (N=21) and amplitude (N=20) obtained in control conditions and during TGOT administration. The agonist significantly decreased the interval (coupled two-tailed Student's t-test, *p<0.05) and increased the amplitude (coupled two-tailed Student's t-test, *p<0.05).

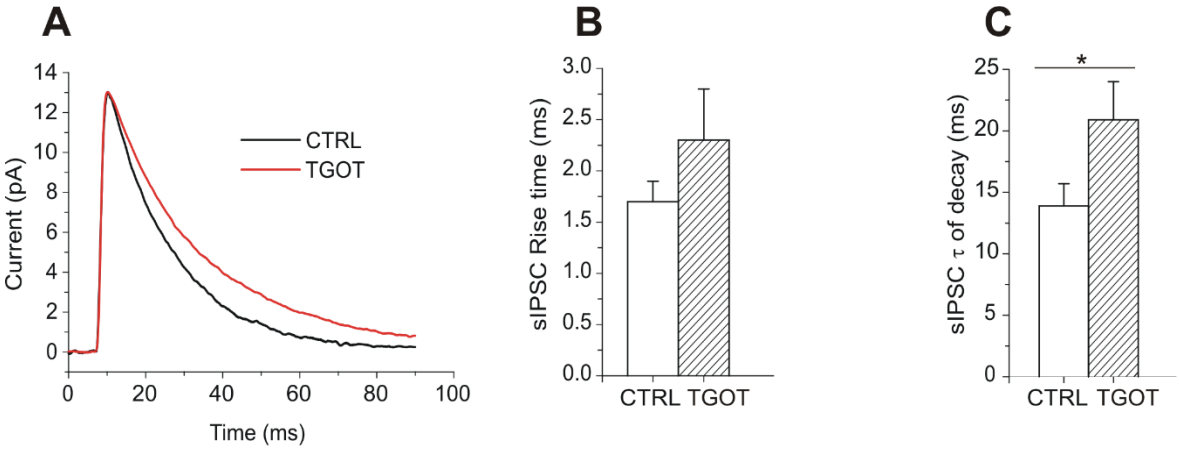

Fig. 25. (A) Superimposed average traces of sIPSCs (lined up according to the mid-point of their rise times) recorded from CA1 PYR in the presence of glutamatergic synaptic blockers at a holding potential of 0 mV. Currents were recorded in control conditions (CTRL: black line, average of 25 traces) and during the application of TGOT (TGOT: red line, average of 168 traces) and were normalized to the control. Note that TGOT was able to alter the sIPSC kinetics of decay but did not change the rise time. **(B)** and **(C)** Histograms comparing the mean values of the sIPSC rise time and time constant of decay (τ) obtained from 4 experiments under control conditions and during TGOT administration. The drug significantly increased τ of decay (coupled two-tailed Student's t-test, *p<0.05). No significant changes in the rise time were observed.

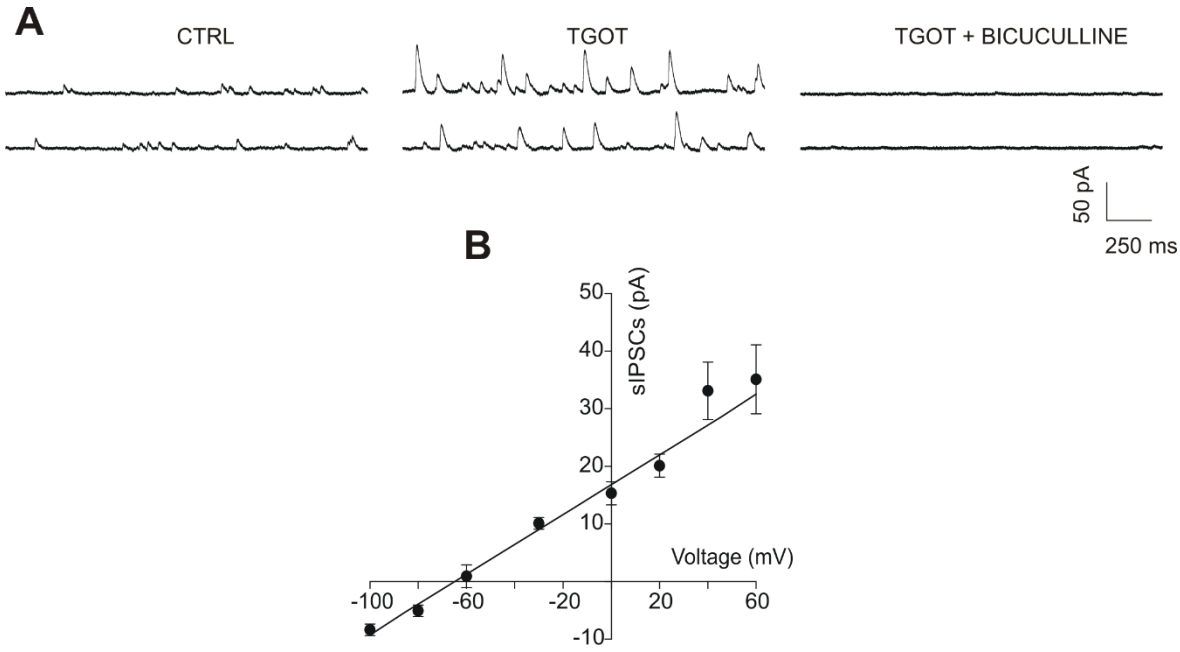

Fig. 26. (A) Representative current traces of sIPSCs recorded from CA1 PYR in the presence of glutamatergic synaptic blockers at a holding potential of 0 mV in control conditions (CTRL), during TGOT administration (TGOT) and during the co-administration of TGOT and bicuculline (10 μM), a $GABA_AR$ antagonist (TGOT + BICUCULLINE). Bicuculline blocked all synaptic activity. **(B)** Mean current-to-voltage (I-V) relationship of the sIPSC peak amplitudes, showing that E_{rev} was close to -60 mV.

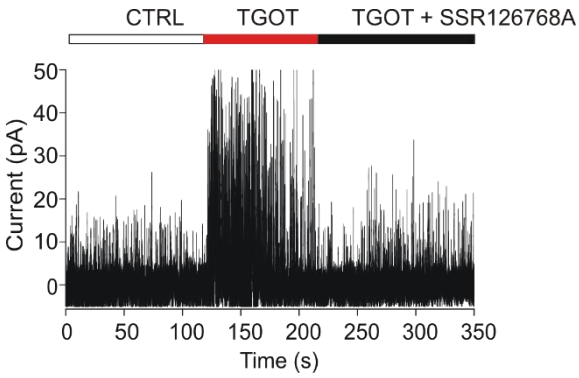

Fig. 27. Representative current trace of sIPSCs recorded from CA1 PYR in the presence of glutamatergic synaptic blockers at a holding potential of 0 mV in control conditions (CTRL), during TGOT administration (TGOT) and during the co-administration of TGOT and SSR126768A (0.1 μM), an antagonist selective for the murine isoform of OTRs (TGOT + SSR126768A). Note the complete abolition of the TGOT-mediated effects in the presence of the antagonist.

5.2.2 Effect of TGOT on miniature inhibitory postsynaptic currents (mIPSC) recorded from PYRs in Otr$^{+/+}$ mice

In order to understand the mechanism through which TGOT increases the level of the inhibitory synaptic transmission, we investigated the role of action potentials generated by the presynaptic GABAergic element. To this purpose, action potential firing was prevented using TTX (1 μM), a voltage-gated Na^+ channel blocker. Then, miniature inhibitory postsynaptic currents (mIPSC) were recorded from 3 Otr$^{+/+}$ PYRs held at 0 mV, in control conditions and during perfusion with TGOT. Our results shown that TGOT was not able to significantly modulate either the mIPSC interval or amplitude: on average the interval was 1054 ± 99 ms in control conditions and 1063 ± 141 ms in the presence of TGOT (**fig. 28A**), whereas the amplitude was 10.2 ± 0.2 pA in control conditions and 10.4 ± 0.1 pA during the application of TGOT (**fig. 28B**).

Furthermore, in contrast to what observed for sIPSCs, the mIPSC τ of decay was not significantly affected by TGOT (**fig. 29A**): on average τ was 13.0 ± 0.8 ms in control conditions and 14.3 ± 0.5 ms in the presence of TGOT (N=3) (**fig. 29C**). Similarly to sIPSCs, also the mIPSC rise time was not significantly altered by the agonist: on average the rise time was 2.2 ± 0.3 ms in control conditions and 2.3 ± 0.3 ms during perfusion of TGOT (N=3) (**fig. 29B**).

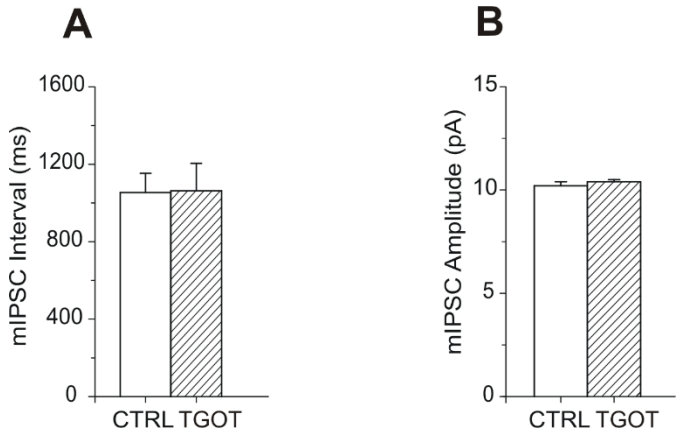

Fig. 28. (A) and **(B)** Histograms comparing the mean values of the mIPSC interval and amplitude obtained in 3 CA1 PYRs under control conditions and during perfusion of TGOT. mIPSCs were recorded at a holding potential of 0 mV, in the presence of glutamatergic synaptic blockers and TTX (1 μM), in order to prevent action potential firing. No significant differences in the interval and amplitude were observed.

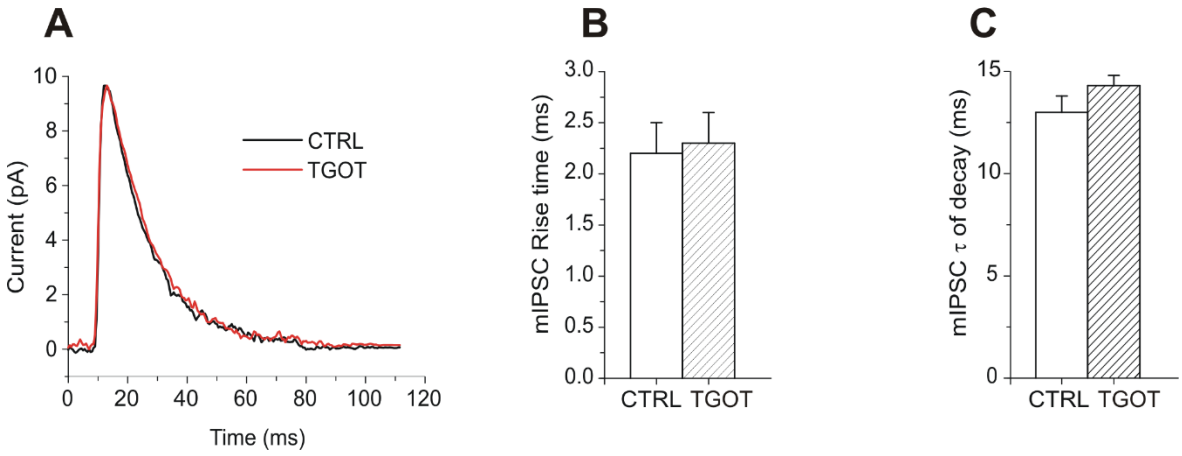

Fig. 29. (A) Superimposed average traces of mIPSCs (lined up according to the mid-point of their rise times) recorded from CA1 PYR in the presence of glutamatergic synaptic blockers at a holding potential of 0 mV. Currents were recorded in control conditions (CTRL: black line, average of 48 traces) and during the application of TGOT (TGOT: red line, average of 37 traces) and were normalized to the control. TGOT did not alter the kinetics properties. **(B)** and **(C)** Histograms comparing the mean values of the mIPSC rise time and time constant of decay (τ) obtained from 3 experiments under control conditions and during TGOT administration. No significant changes in the mIPSC rise time and τ of decay were observed.

Our data show that TGOT is able to modulate the $GABA_AR$-mediated synaptic transmission onto PYRs only when the presynaptic terminal generates action potentials. In other words, all the TGOT-mediated effect are closely dependent on the presynaptic firing activity.

The next step was to assess whether TGOT could have some action on the excitatory transmission.

5.2.3 Effect of TGOT on spontaneous excitatory postsynaptic currents (sEPSC) recorded from PYRs in Otr$^{+/+}$ mice

Spontaneous excitatory postsynaptic currents (sEPSC) were recorded from 7 PYRs in Otr$^{+/+}$ mice, during the application of voltage-clamp long recordings protocols at a holding potential of -70 mV. Experiments were performed in control conditions, during perfusion of TGOT and during drug wash out. To exclude the activation of GABAergic receptors, sEPSCs were recorded in the presence of bicuculline (10 μM) that blocks $GABA_A$Rs. In contrast to what observed for the sIPSCs, the excitatory transmission was not significantly affected by TGOT (**fig. 30A**). On average the sEPSC interval was 363 ± 123 ms in control conditions and 324 ± 115 ms during the application of TGOT (N=7) (**fig. 30B**), while the amplitude was 8.7 ± 1.0 pA in control conditions and 8.5 ± 1.0 pA during drug perfusion (N=7) (**fig. 30C**).

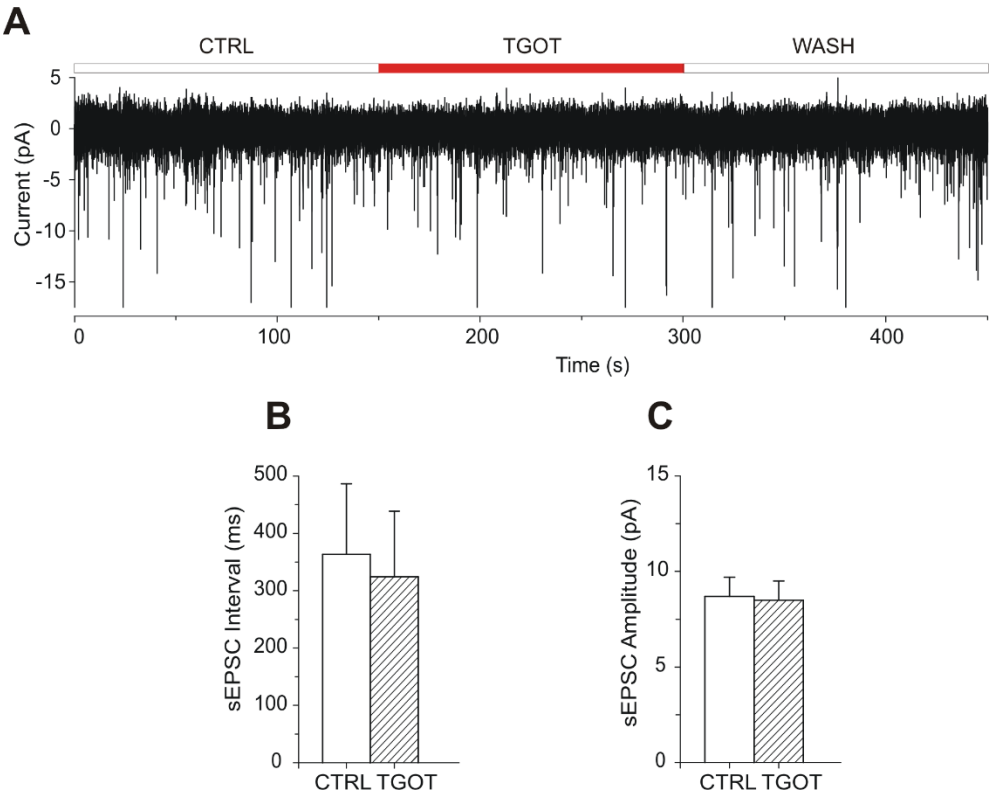

Fig. 30. (A) Representative current trace of sEPSCs recorded from CA1 PYR in the presence of GABAergic synaptic blocker bicuculline (10 μM) at a holding potential of -70 mV in control conditions (CTRL), during TGOT administration (TGOT) and during drug wash out (WASH). TGOT did not alter the excitatory transmission. **(B)** and **(C)** Histograms comparing the mean values of the sEPSC interval and amplitude obtained in 7 CA1 PYRs under control conditions and during perfusion of TGOT. No significant differences in the sEPSC interval and amplitude were observed.

5.2.4 Comparison of sIPSCs and sEPSCs between Otr$^{+/+}$ and Otr$^{-/-}$ mice

To better investigate the involvement of OTRs in the TGOT-mediated effects, sIPSCs and sEPSCs were recorded from Otr$^{-/-}$ mice as well (see "Materials and methods"). Animals were kindly donated by the lab of Dr. Bice Chini from the CNR Institute of Neuroscience in Milan. We first performed a comparative analysis of sIPSCs between Otr$^{-/-}$ and Otr$^{+/+}$ mice under control conditions (**fig. 31A**). We observed that the sIPSC interval was significantly lower in Otr$^{-/-}$ compared to Otr$^{+/+}$ mice (uncoupled two-tailed Student's t-test, $p<0.05$): on average the interval was 378 ± 47 ms in Otr$^{-/-}$ (N=15) and 760 ± 137 ms in Otr$^{+/+}$ mice (N=21) (**fig. 31B**). No significant differences in the sIPSC amplitude between Otr$^{-/-}$ and Otr$^{+/+}$ mice were observed: on average the amplitude was 13.4 ± 0.5 pA in Otr $^{-/-}$ (N=17) and 13.0 ± 0.7 pA in Otr$^{+/+}$ mice (N=20) (**fig. 31C**).

Subsequently, we tested the effect of TGOT on sIPSCs recorded from Otr$^{-/-}$ mice. In these animals, TGOT was not able to cause any significant variation in the sIPSC interval and amplitude: on average the interval was 378 ± 47 ms in control conditions and 345 ± 41 ms during the application of TGOT (N=15); the amplitude was 13.4 ± 0.5 pA in control conditions and 13.4 ± 0.5 pA during TGOT administration (N=17). Furthermore, TGOT did not influence the sIPSC kinetics (N=4): on average the rise time was 1.9 ± 0.2 ms in control conditions and 2.2 ± 0.6 ms in the presence of TGOT, whereas τ was 16.5 ± 1.5 ms in control conditions and 16.6 ± 0.5 ms during the application of TGOT.

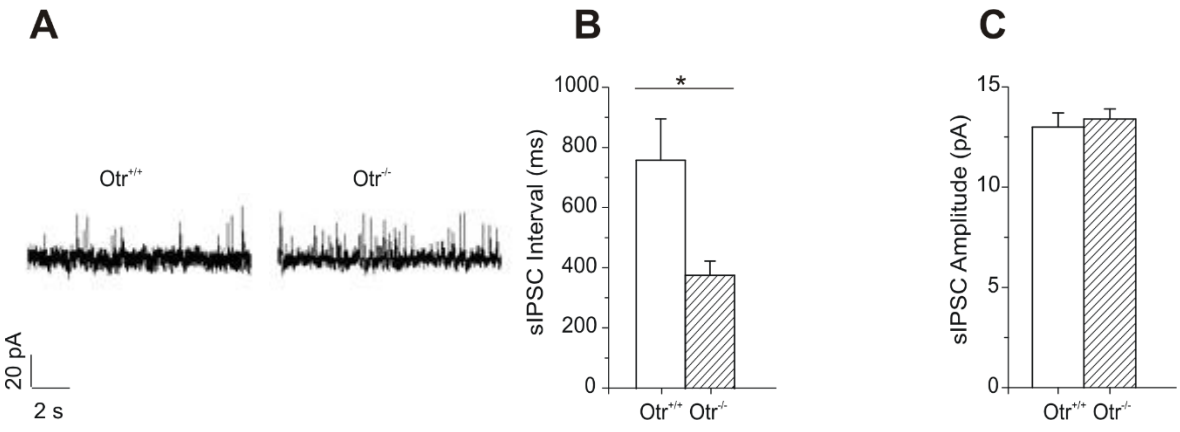

Fig. 31. (A) Representative current traces of sIPSCs recorded from CA1 PYR in the presence of glutamatergic synaptic blockers at a holding potential of 0 mV in control conditions in Otr$^{+/+}$ (left) and Otr$^{-/-}$ mice (right). **(B)** and **(C)** Histograms comparing the mean values of the sIPSC interval (N=21 in Otr$^{+/+}$ and N=15 in Otr$^{-/-}$ mice) and amplitude (N=20 in Otr$^{+/+}$ and N=17 in Otr$^{-/-}$ mice) obtained in control conditions. The interval was significantly lower in Otr$^{-/-}$ compared to Otr$^{+/+}$ mice (uncoupled two-tailed Student's t-test, *$p<0.05$). No significant differences in the amplitude between Otr$^{-/-}$ and Otr$^{+/+}$ mice were observed.

As regard excitatory synaptic transmission, we first recorded sEPSCs from PYRs in both $Otr^{-/-}$ and $Otr^{+/+}$ mice in control conditions (**fig. 32A**). We observed that the sEPSC interval was significantly higher in $Otr^{-/-}$ compared to $Otr^{+/+}$ mice (uncoupled two-tailed Student's t-test, $p<0.05$): on average the interval was 804 ± 178 ms in $Otr^{-/-}$ (N=8) and 363 ± 123 ms in $Otr^{+/+}$ mice (N=7) (**fig. 32B**). By contrast, no significant differences were observed in the sEPSC amplitude between $Otr^{-/-}$ and $Otr^{+/+}$ mice: on average the amplitude was 8.7 ± 1.0 pA in $Otr^{-/-}$ (N=9) and 8.7 ± 1.0 pA in Otr $^{+/+}$ mice (N=7) (**fig. 32C**).

Finally, we tested the effect of TGOT on sEPSCs recorded from $Otr^{-/-}$ mice. As expected, TGOT was not able to induce any significant variation either in the sEPSC interval or amplitude: on average the interval was 804 ± 178 ms in control conditions and 793 ± 159 ms during the application of TGOT (N=8); the amplitude was 8.7 ± 1.0 pA in control conditions and 8.6 ± 1.0 pA during TGOT administration (N=9).

Overall, the evaluation of sIPSCs and sEPSCs in $Otr^{-/-}$ mice highlights that in basal conditions the balance between excitation and inhibition is in favour of inhibition.

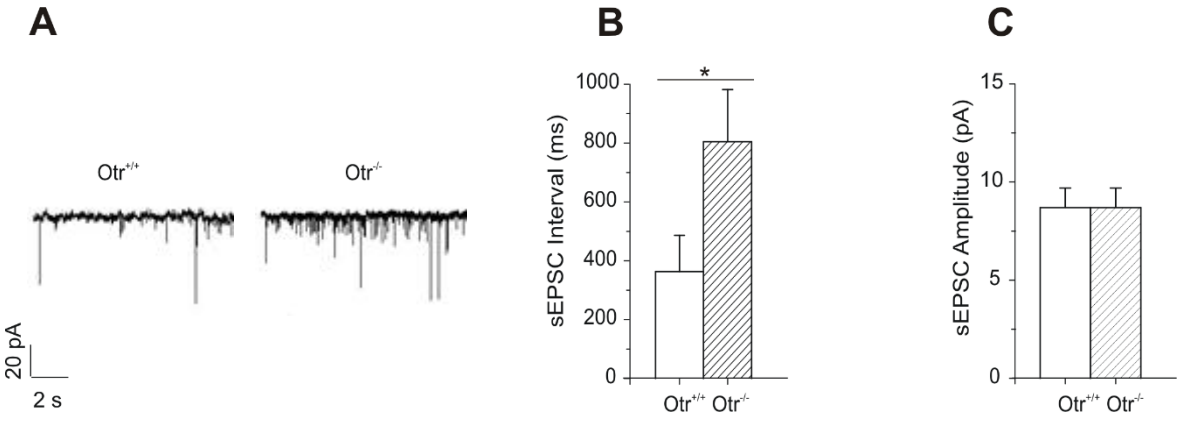

Fig. 32. (A) Representative current traces of sEPSCs recorded from CA1 PYR in the presence of GABAergic synaptic blocker at a holding potential of -70 mV in control conditions in $Otr^{+/+}$ (left) and $Otr^{-/-}$ mice (right). **(B)** and **(C)** Histograms comparing the mean values of the sEPSC interval (N=7 in $Otr^{+/+}$ and N=8 in $Otr^{-/-}$ mice) and amplitude (N=7 in $Otr^{+/+}$ and N=9 in $Otr^{-/-}$ mice) obtained in control conditions. The interval was significantly higher in $Otr^{-/-}$ compared to $Otr^{+/+}$ mice (uncoupled two-tailed Student's t-test, *$p<0.05$). No significant differences in the amplitude between $Otr^{-/-}$ and $Otr^{+/+}$ mice were observed.

The data described so far indicate that TGOT is able to modulate the inhibitory transmission in CA1 *stratum pyramidale*. In the hippocampus, the main source of inhibition onto PYRs is represented by GABAergic INs [Freund & Buzsaki, 1996] that release GABA in the extracellular space. GABA exerts its action by binding mainly $GABA_A$Rs that are expressed on the synaptic membrane of PYRs: the transient activation of these receptors gives rise to

inhibitory currents responsible for the so-called 'phasic' (or synaptic) inhibition [Farrant & Nusser, 2005]. However, GABA can escape from the synaptic cleft (a phenomenon termed 'spillover') and activate $GABA_A$Rs located in perisynaptic (i.e., just outside the postsynaptic density) [Wei et al., 2003] or extrasynaptic (i.e., hundreds of nanometres away from the edge of the nearest postsynaptic density) [Nusser et al., 1998] sites. In particular, the activation of extrasynaptic receptors gives rise to a persistent (or 'tonic') inhibition [Banks & Pearce, 2000; Scimemi et al., 2005; Mortensen & Smart, 2006; Pavlov et al., 2009].
After having clarified the effect of TGOT on phasic inhibitory currents, we enquired if the peptide could modulate also the tonic inhibition, mediated by the activation of extrasynaptic $GABA_A$Rs on CA1 PYRs.

5.3 Effect of TGOT on the extrasynaptic transmission in CA1 field

As a tool to evaluate the putative effect of TGOT on the extrasynaptic transmission, we used a widely described method consisting in the measurement of the 'baseline holding current' required to clamp cells at a given potential during voltage-clamp recordings (see "Materials and methods"). According to that standard method, cell perfusion with a molecule that is able to modulate the tonic inhibition should cause a shift in the 'baseline holding current' [Bright & Smart, 2013].

5.3.1 Effect of TGOT on the 'baseline holding current' recorded from PYRs in $Otr^{+/+}$ mice

First, the presence of extrasynaptic $GABA_A$R-mediated currents was assessed in 2 $Otr^{+/+}$ PYRs during the application of voltage-clamp long recordings protocols at a holding potential of 0 mV. Experiments were performed under control conditions and during perfusion of bicuculline at the concentration of 10 μM, in order to block both synaptic and extrasynaptic $GABA_A$Rs [Wlodarczyk et al., 2013]. In addition to recording sIPSCs, we also measured the 'baseline holding current' required to clamp the membrane potential of PYRs at 0 mV. As expected, bicuculline blocked all sIPSCs (**fig. 33A**) and caused an inward shift in the 'baseline holding current' (**fig. 33A**), consistent with the abolition of $GABA_A$R-mediated tonic currents, as described in literature [Bright & Smart, 2013]. It must be noted that the current shift was inward since E_{Cl^-} (-68 mV) was close to the resting membrane potential and the holding potential was 0 mV (see "Materials and methods"). A quantitative

analysis of current traces, performed by creating all-point histograms (see "Materials and methods") (**fig. 33B**), revealed a mean current shift of -8.3 ± 3.7 pA (N=2).

Subsequently, the putative action of TGOT on tonic currents was assessed in 25 PYRs. An example of how TGOT influenced the 'baseline holding current' is shown in **fig. 34A**: the peptide caused a reversible current shift, whose direction was opposite to that described for $GABA_AR$ antagonist. This outward shift is consistent with a positive modulation of tonic currents mediated by extrasynaptic $GABA_ARs$. The quantitative analysis of the traces, performed by generating all-point histograms (**fig. 34B**), revealed an outward current shift in 14 out of 25 PYRs examined: on average the shift was +46.4 ± 14.9 pA.

That action of TGOT was undoubtedly related to the presence of OTRs, since the agonist was not able to cause any significant change in the 'baseline holding current' in $Otr^{-/-}$ mice (N=15/15).

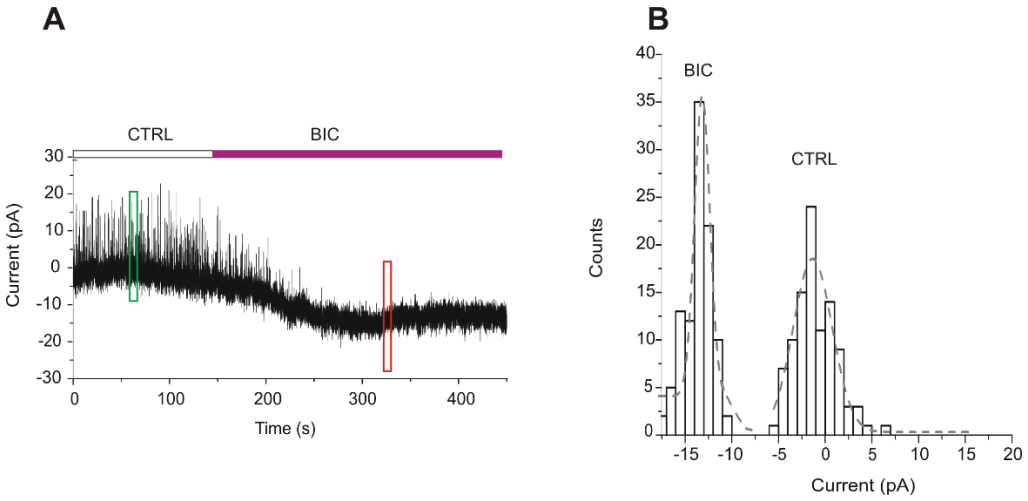

Fig. 33. (A) Representative current trace of sIPSCs recorded from CA1 PYR in the presence of glutamatergic synaptic blockers at a holding potential of 0 mV in control conditions (CTRL) and during perfusion of bicuculline (BIC). Note the complete abolition of the inhibitory synaptic activity and a decrease in the 'baseline holding current' during the application of bicuculline. Green and red boxes indicate the 10 s long intervals used to the construction of the all-point histograms. **(B)** Representative all-point histograms for the intervals shown in panel A (green box: trace interval recorded in control conditions; red box: trace interval recorded during bicuculline perfusion). Peak values of histograms, fitted with Gaussian curves, represent the mean currents recorded before (CTRL) and during (BIC) drug perfusion. The difference between the mean currents (BIC - CTRL) provides the inward shift, revealing the presence of tonically active currents mediated by extrasynaptic $GABA_ARs$.

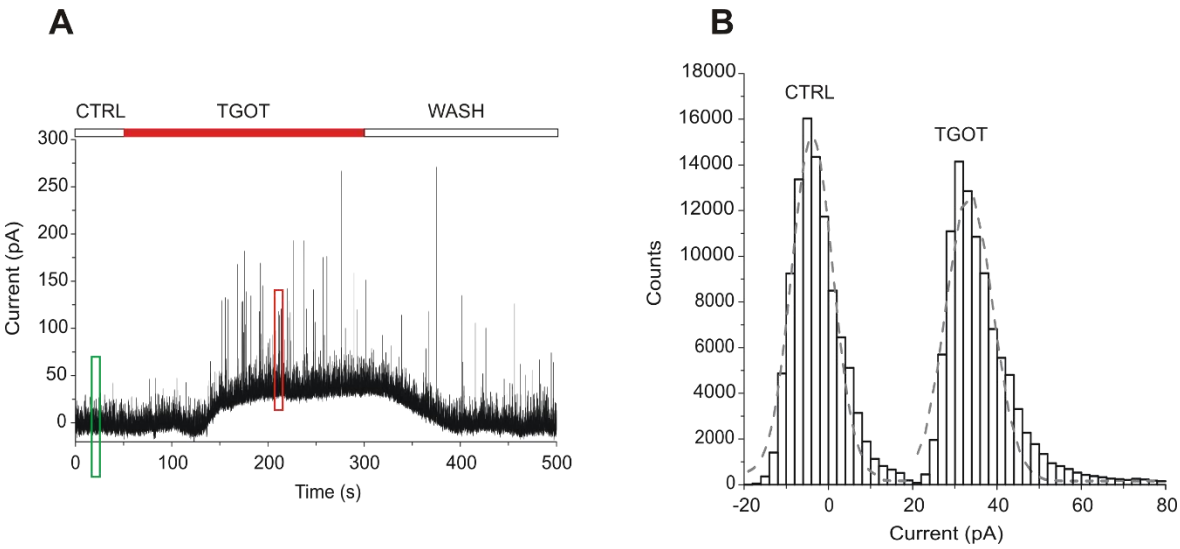

Fig. 34. (A) Representative current trace of sIPSCs recorded from CA1 PYR in the presence of glutamatergic synaptic blockers at a holding potential of 0 mV in control conditions (CTRL), during TGOT administration (TGOT) and during drug wash out (WASH). TGOT caused a reversible outward shift in the 'baseline holding current', together with an increase in both sIPSC frequency and amplitude. Green and red boxes indicate the 10 s long intervals used to the construction of the all-point histograms. **(B)** Representative all-point histograms for the intervals shown in panel A (green box: trace interval recorded in control conditions; red box: trace interval recorded during TGOT perfusion). Peak values of histograms, fitted with Gaussian curves, represent the mean currents recorded before (CTRL) and during (TGOT) drug perfusion. The difference between the mean currents (TGOT - CTRL) provides the outward shift, revealing a positive modulation of tonically active currents.

Overall, these results indicate that TGOT is able to increase not only the phasic (synaptic) but also the tonic (extrasynaptic) $GABA_AR$-mediated inhibition onto PYRs.

5.4 Effect of TGOT on the membrane potential of CA1 neurons

To better understand the hippocampal circuits involved in this oxytocinergic action, we tried to evaluate the effect of TGOT directly on the membrane potential of CA1 neurons. Our first goal was to investigate in detail the cell source of the TGOT-induced inhibition in CA1. To this purpose, the effect of TGOT on the membrane potential of CA1 GABAergic INs was studied first.

5.4.1 Effect of TGOT on the membrane potential of GABAergic INs in GAD67-GFP$^+$ (Δneo) mice

The effect of the agonist was evaluated in 84 INs recorded from GAD67-GFP$^+$ (Δneo) mice through the application of current-clamp long recording protocols. Voltage responses of cells were recorded in control conditions, during perfusion of TGOT and during wash out.

Experiments were performed both without glutamatergic and GABAergic synaptic blockers (N=71) and during synaptic isolation (N=13). Protocols were applied either starting from a membrane potential of -70 mV (N=58 without synaptic blockers; N=8 in the presence of synaptic blockers) or starting from spike threshold (N=13 without synaptic blockers; N=5 in the presence of synaptic blockers).

Our results show that in absence of synaptic blockers, about 50% of INs tested at -70 mV (N=31/58) responded to TGOT with a sustained depolarization (**fig. 35A**), whereas the remaining fraction of cells did not respond at all to the agonist. The mean depolarization, calculated using all-point histograms (**fig. 35B**), was +6.2 ± 0.8 mV. At threshold, in 13 INs examined TGOT caused a depolarizing response (on average: +2.5 ± 0.4 mV) (**fig. 36A**) together with a significant increase by a factor of 3.3 ± 1.2 in the firing rate (coupled two-tailed Student's t-test, $p<0.05$) (**fig. 36B**). Interestingly, the majority of responding INs were stuttering fast-spiking cells, characterized by a high frequency firing rate (**fig. 35A-inset**), whereas the majority of non-responding INs were regular firing, in agreement with literature data [Owen et al., 2013].

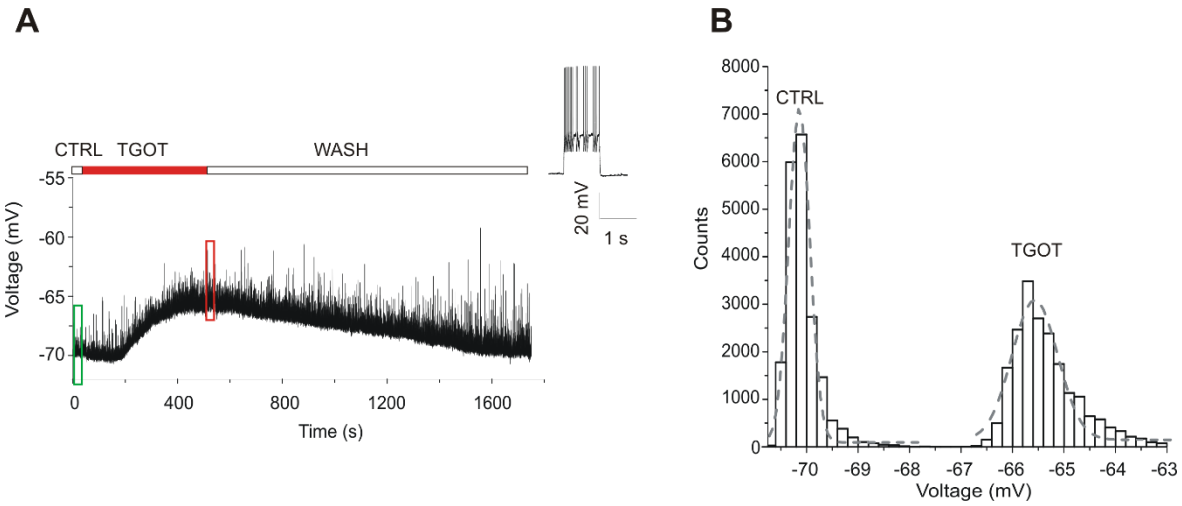

Fig. 35. (A) Representative voltage trace recorded from GABAergic IN without synaptic blockers, starting from membrane potential of -70 mV, in control conditions (CTRL), during TGOT administration (TGOT) and during drug wash out (WASH). TGOT caused a sustained depolarization primarily in a subpopulation of GABAergic INs, characterized by a high frequency firing rate (inset: stuttering fast-spiking). Green and red boxes indicate the 10 s long intervals used to the construction of the all-point histograms. **(B)** Representative all-point histograms for the intervals shown in panel A (green box: trace interval recorded in control conditions; red box: trace interval recorded during TGOT perfusion). Peak values of histograms, fitted with Gaussian curves, represent the mean membrane potentials recorded before (CTRL) and during (TGOT) drug perfusion. The difference between the mean potentials (TGOT - CTRL) provides the depolarization.

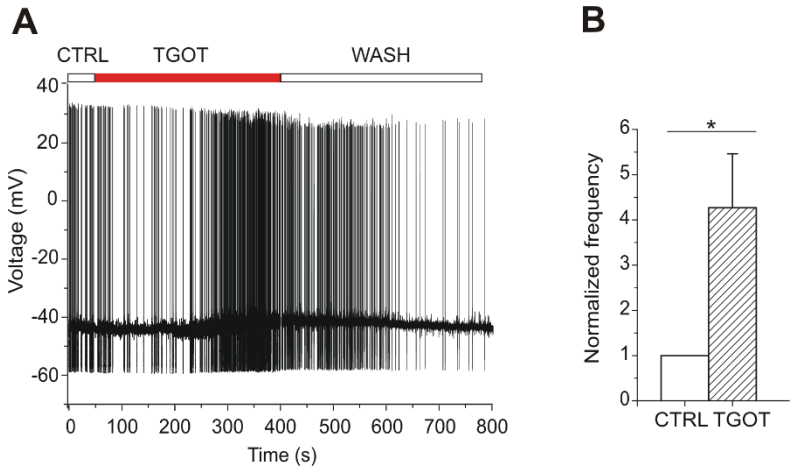

Fig. 36. (A) Representative voltage trace recorded from GABAergic IN without synaptic blockers, starting from spike threshold, in control conditions (CTRL), during TGOT administration (TGOT) and during drug wash out (WASH). TGOT caused a depolarization together with an increase in the firing rate. **(B)** Histogram comparing the firing frequency at threshold, normalized to control, obtained from 13 experiments in control conditions and during TGOT administration. The drug significantly increased the firing frequency (coupled two-tailed Student's t-test, *p<0.05).

Similar results could be obtained in the presence of glutamatergic and GABAergic synaptic blockers: indeed, 8 stuttering fast-spiking cells tested at -70 mV displayed a sustained depolarization (on average: +6.3 ± 1.1 mV) during TGOT perfusion (**fig. 37**). At threshold, 5 INs examined responded to the agonist with a depolarization (on average: +3.4 ± 1.0 mV) (**fig. 38A**) together with a significant increase by a factor of 3.4 ± 1.1 in the firing rate (coupled two-tailed Student's t-test, p<0.05) (**fig. 38B**).

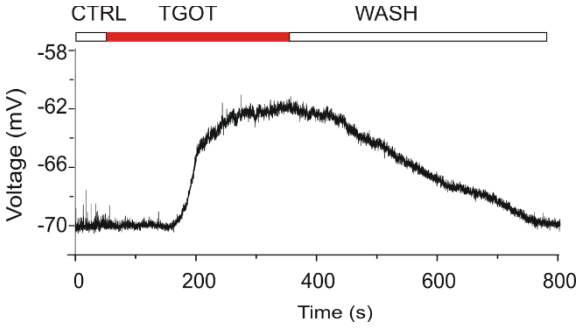

Fig. 37. (A) Representative voltage trace recorded from GABAergic IN in the presence of synaptic blockers, starting from membrane potential of -70 mV, in control conditions (CTRL), during TGOT administration (TGOT) and during drug wash out (WASH). Despite synaptic isolation, TGOT caused a sustained depolarization.

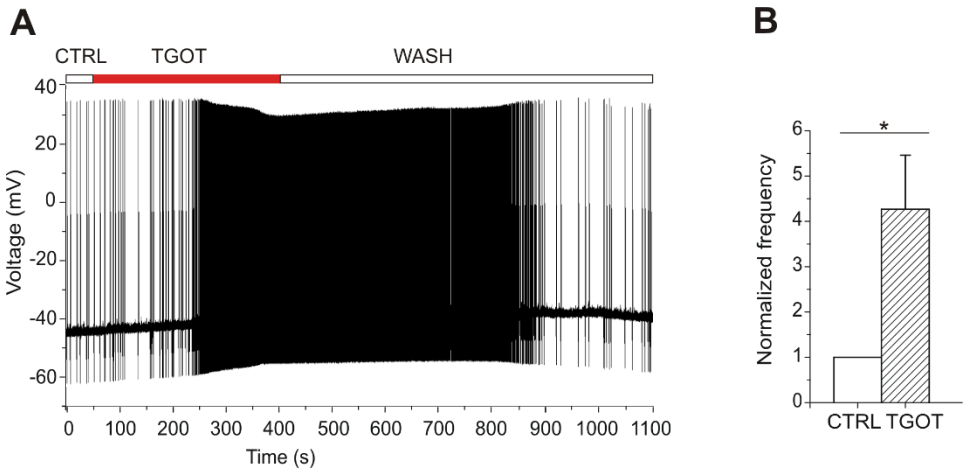

Fig. 38. (A) Representative voltage trace recorded from GABAergic IN in the presence of synaptic blockers, starting from spike threshold, in control conditions (CTRL), during TGOT administration (TGOT) and during drug wash out (WASH). Despite synaptic isolation, TGOT caused a depolarization together with an increase in the firing rate. **(B)** Histogram comparing the firing frequency at threshold, normalized to control, obtained from 5 experiments in control conditions and during TGOT administration. The drug significantly increased the firing frequency (coupled two-tailed Student's t-test, *p<0.05).

Our data indicate that TGOT is able to directly depolarize the membrane of a subpopulation of GABAergic INs. The observation that the TGOT-induced depolarization was elicited despite the synaptic blockade suggests that it was due (at least in good part) to a direct binding of TGOT to OTRs expressed in those cells and not secondary to any effect of TGOT on upstream neurons. To corroborate this conclusion, we recorded voltage responses of stuttering fast-spiking INs during the co-administration of TGOT and the selective OTR antagonist SSR126768A (0.1 μM) in order to block receptors. Our results shown that in the totality of the cells examined (N=6) the TGOT-mediated depolarization was completely abolished in the presence of the antagonist (**fig. 39**), supporting the direct interaction between TGOT and OTRs.

The expression of OTRs in a subpopulation of GABAergic INs was directly confirmed by single-cell reverse transcription (RT)-PCR experiments performed in the lab of Dr. Bice Chini in Milan. Briefly, after the electrophysiological experiment the cytoplasm of the recorded cell was gently aspirated into the patch pipette. The content of the pipette was inserted into a tube containing DEPC-treated water, used to avoid the degradation of the cytoplasmic mRNA. Samples collected were stored at -80°C and then used for the reverse transcription that allowed to obtain cDNA from mRNA. cDNA was then amplified through a PCR reaction, using primers complementary to a specific region of the Otr gene. Furthermore, primers complementary to a fragment of the constitutive gene GAPDH was

used as positive control. PCR products were loaded on a gel for the electrophoresis run that revealed two bands: a band of ~ 150 bp corresponding to cDNA coding for OTR and a band of ~ 550 bp corresponding to cDNA coding for GAPDH (**fig. 40**). These RT-PCR experiments shown the OTR band in 6 INs examined.

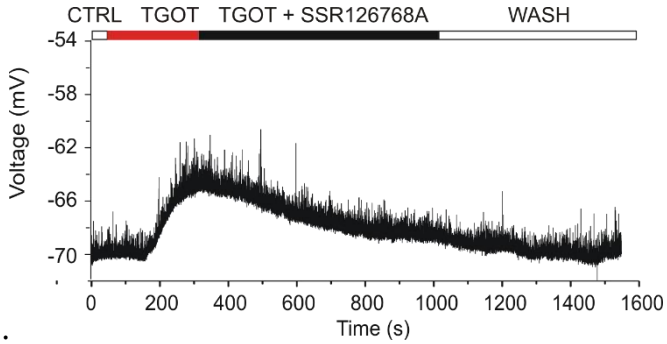

Fig. 39. Representative voltage trace recorded from stuttering fast-spiking GABAergic IN without synaptic blockers, starting from membrane potential of -70 mV, in control conditions (CTRL), during TGOT administration (TGOT), during the co-administration of TGOT and SSR126768A (0.1 μM), the antagonist selective for the murine isoform of OTRs (TGOT + SSR126768A), and during drugs wash out (WASH). Note the abolition of the TGOT-mediated depolarization in the presence of the antagonist.

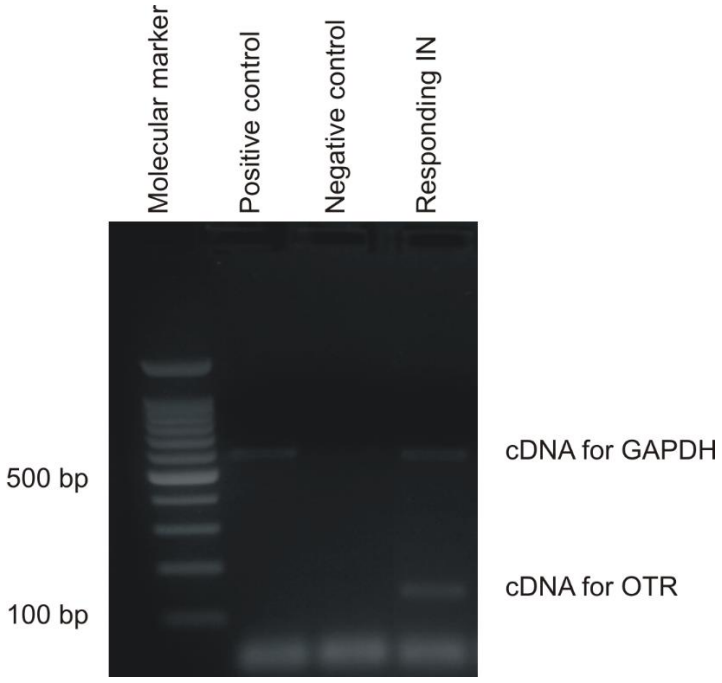

Fig. 40. Representative electrophoresis run of cDNA sample derived from the cytoplasm of a GABAergic IN that respond to TGOT. Molecular marker, negative control (DEPC-treated water) and positive control are indicated. The cytoplasm of responding IN displayed a band of ~ 550 bp that corresponds to cDNA coding for GAPDH and a band of ~ 150 bp that corresponds to cDNA coding for OTR. In the positive control, only cDNA for GAPDH is visible.

5.4.1.1 Putative ionic mechanism involved in the TGOT-mediated effect in GABAergic INs

After having identified the subpopulation of GABAergic INs that respond to TGOT and express OTRs, we started to explore the putative ionic mechanism involved in the TGOT-induced depolarization of those cells.

OTRs are defined 'promiscuous' G protein coupled receptors (GPCR) because of their ability to bind different G protein subtypes, such as G_i or $G_{q/11}$ [Chini et al., 2008; Manning et al., 2008]. In our study, we focused on the pathway activated by $G_{q/11}$ that can lead to the phosphorylation of different intracellular substrates, including L-type voltage-gated Ca^{2+} channels [Weiss et al., 2012; Satin, 2013]. To test the involvement of this pathway, we first recorded voltage responses of GABAergic INs in the presence of TGOT and then during the co-application of TGOT and nifedipine (5 μM), a selective blocker of L-type channels. Our results show that nifedipine was able to abolish the TGOT-induced depolarization in 8 out of 10 INs examined (**fig. 41**).

These preliminary results suggest that L-type Ca^{2+} channels could play a role in the membrane depolarization induced by OTR activation following TGOT binding. More detailed experiments have been planned in order to evaluate the effect of the agonist directly on the L-type current.

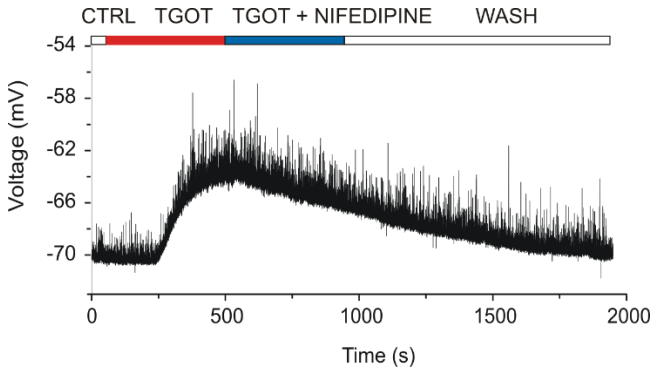

Fig. 41. Representative voltage trace recorded from GABAergic IN without synaptic blockers, starting from membrane potential of -70 mV, in control conditions (CTRL), during TGOT administration (TGOT), during the co-administration of TGOT and nifedipine (5 μM), the selective blocker of L-type voltage-dependent Ca^{2+} channels (TGOT + NIFEDIPINE) and during drugs wash out (WASH). Note the abolition of the TGOT-mediated depolarization in the presence of nifedipine.

5.4.2 Effect of TGOT on the membrane potential of PYRs in Otr$^{+/+}$ mice

In our lasts experiments, we examined the effects of TGOT on the membrane potential of PYRs. The action of the agonist was tested in 34 Otr$^{+/+}$ PYRs by applying current-clamp long recording protocols. Voltage responses were recorded under control conditions, during perfusion of TGOT and during drug wash out. Experiments were performed both without glutamatergic and GABAergic synaptic blockers (N=20) and during synaptic isolation (N=14). Protocols were applied either starting from a membrane potential of -70 mV (N=7 without synaptic blockers; N=8 in the presence of synaptic blockers) or starting from spike threshold (N=15 without synaptic blockers; N=6 in the presence of synaptic blockers).

Our results show that in absence of synaptic blockers the totality of PYRs did not respond to TGOT. Interestingly, at threshold in 10 out of 15 PYRs examined TGOT caused a hyperpolarizing response (on average: -3.0 ± 0.4 mV) (**fig. 42A**) together with a significant decrease by a factor of 0.7 ± 0.1 in the firing rate (coupled two-tailed Student's t-test, $p<0.005$) (**fig. 42B**).

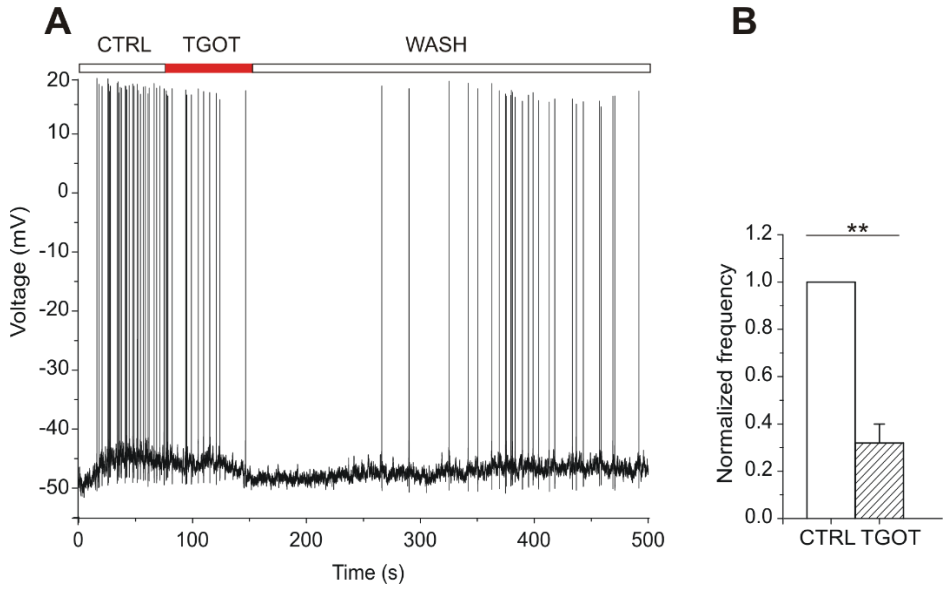

Fig. 42. (A) Representative voltage trace recorded from PYR without synaptic blockers, starting from spike threshold, in control conditions (CTRL), during TGOT administration (TGOT) and during drug wash out (WASH). TGOT caused a hyperpolarization together with a decrease in the firing rate. **(B)** Histogram comparing the firing frequency at threshold, normalized to control, obtained from 10 experiments in control conditions and during TGOT administration. The drug significantly decreased the firing frequency (coupled two-tailed Student's t-test, **p<0.005).

Also in the presence of synaptic blockers PYRs did not respond to TGOT (N=8/8). Surprisingly, at threshold the TGOT-mediated hyperpolarization was completely abolished during the application of blockers (N=6/6) (**fig. 43**).

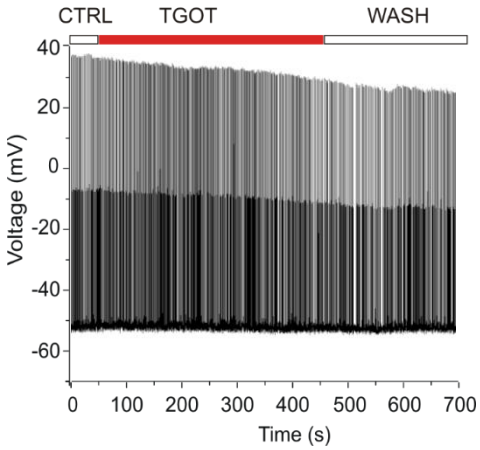

Fig. 43. Representative voltage trace recorded from PYR in the presence of synaptic blockers, starting from spike threshold, in control conditions (CTRL), during TGOT administration (TGOT) and during drug wash out (WASH). Note the complete abolition of the TGOT-induced hyperpolarization during the synaptic isolation.

This important result suggests that the effect elicited by TGOT on PYRs is not direct but is closely dependent on the activation of $GABA_A$Rs that mediate a hyperpolarizing current. Since the main consequence of the hyperpolarization is a reduction in cell excitability [Farrant & Nusser], we subsequently tested the effect of TGOT directly on the capability of PYRs to generate action potentials.

5.4.3 Effect of TGOT on the excitability of PYRs in $Otr^{+/+}$ mice

The effect of the agonist on cell excitability was evaluated in 7 $Otr^{+/+}$ PYRs, by recording voltage responses of neurons to depolarizing current steps of increasing intensity. Currents were applied starting from -70 mV both under control conditions and during perfusion of TGOT. An example of how TGOT influenced the capability of PYRs to generate action potentials is shown in **fig. 44A**: in the presence of the neuropeptide, the firing frequency was lower than that obtained under control conditions. The quantitative analysis of the responses was performed by measuring the firing frequency at each current step and then by plotting the firing rate vs the injected current (F-I relationship; see “Materials and methods”).

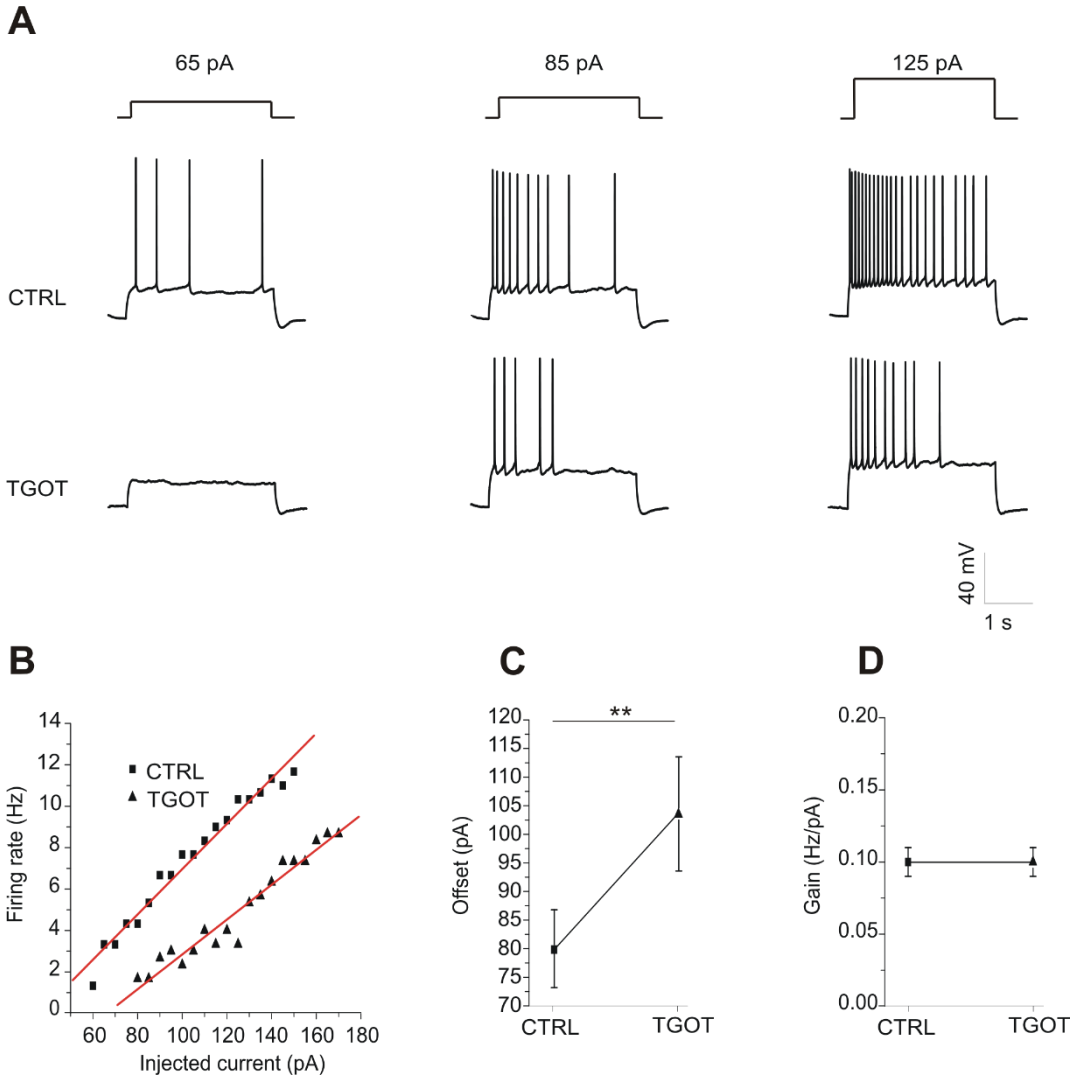

Fig. 44. (A) Representative voltage traces recorded from PYR starting from -70 mV, in response to the injection of depolarizing current steps of increasing intensity (65, 85 and 125 pA), in control conditions (CTRL) and in the presence of TGOT (TGOT). The firing frequency obtained during TGOT administration was lower than that obtained under control conditions. **(B)** Graph showing the firing rate-to-injected current (F-I) relationship referred to the traces of panel A. The experimental values (CTRL: black squares; TGOT: black triangles) were fitted with a linear regression function (red lines). The relationship obtained during perfusion of TGOT was shifted to the right compared to that one obtained under control conditions, indicating an increase in the offset (i.e., the minimal intensity of injected current required to attain a response). The gain (i.e., the slope of the curve) was not affected by TGOT. **(C)** and **(D)** Diagrams comparing the mean values of the offset and the gain obtained in 7 experiments in control conditions and during perfusion of TGOT. The agonist caused a significant increase in the offset (coupled two-tailed Student's t-test, **p<0.005) without changing the gain.

In the totality of PYRs the F-I curve obtained during perfusion of TGOT was shifted to the right compared to that one obtained under control conditions (**fig. 44B**), indicating that TGOT was able to cause a significant increase in the offset (i.e., the minimal intensity of injected current required to attain a response) (coupled two-tailed Student's t-test, $p<0.05$). Indeed, on average the offset was 80.0 ± 6.8 pA in control conditions and 104 ± 10 pA in the

presence of TGOT (**fig. 44C**). The gain (i.e., the slope) of the F-I relationship was not significantly modulated by TGOT: it was 0.10 ± 0.01 Hz/pA in control conditions and 0.10 ± 0.01 Hz/pA during the application of TGOT (**fig. 44D**). As described in literature, an increase in the offset is attributable to an increase in tonically active inhibitory currents: this would lead to a persistent reduction in the input resistance and therefore in cell excitability [Mithcell & Silver, 2003].

6. DISCUSSION

OT is a small neuropeptide that plays important neuromodulatory functions in the central nervous system, being involved in attachment, social recognition, social exploration, as well as anxiety and fear-related behaviour [Mühlethaler et al., 1983; Tiberiis et al., 1983; Mühlethaler et al., 1984; Raggenbass et al., 1989; Owen et al., 2013]. Among the brain areas in which binding sites for OT have been widely demonstrated there is the CA1 field of the hippocampal formation [Freund-Mercier et al., 1989; Tribollet et al., 1988; Barberis & Tribollet, 1996; Yoshimura et al., 1993]. Several electrophysiological studies have shown that OT is able to exert direct effects on specific neuronal populations in CA1 area [Mühlethaler et al., 1983; Mühlethaler et al., 1984; Raggenbass et al., 1989; Raggenbass, 2001]. In particular, Zaninetti and Raggenbass have demonstrated that TGOT, a selective OTR agonist, caused an increase in the frequency and the amplitude of sIPSCs recorded from PYRs. These events were mediated by the activation of $GABA_A$Rs, since were blocked by bicuculline [Zaninetti & Raggenbass, 2000]. Furthermore, Owen and colleagues have shown that TGOT was able to depolarize mainly a subpopulation of GABAergic INs displaying a fast-spiking pattern [Owen et al., 2013].
Overall, literature data indicate that the action of TGOT targets a selective population of CA1 INs, leading to an increase in the $GABA_A$R-mediated inhibitory transmission onto PYRs.

Taking the cue from those findings, we planned a series of experiments with the purpose to characterize in detail the mechanisms by which TGOT modulates the neuronal network in the hippocampal CA1 field. First, we evaluated the effect of TGOT on the inhibitory and excitatory synaptic transmission. Then, we tested the hypothesis of the activation of extrasynaptic receptors following GABA spillover, due to an increase in the neurotransmitter release during TGOT perfusion. We also tried to identify the neuronal target of TGOT and to understand the putative ionic mechanism involved in the cellular responses to the agonist. Finally, we attempted to clarify how TGOT influenced the excitability of PYRs and therefore their capability to generate action potentials in response to the injection of depolarizing current steps.

6.1 TGOT increases the synaptic $GABA_AR$-mediated inhibition onto CA1 PYRs in $Otr^{+/+}$ mice

The effect of TGOT was first assessed on sIPSCs recorded from CA1 PYRs in $Otr^{+/+}$ mice. Spontaneous events are the result of the release of neurotransmitter occurring when the presynaptic terminal fires spontaneous action potentials. sIPSCs were recorded in the presence of AMPA and NMDA receptor blockers during the application of long recording voltage-clamp protocols at a holding potential of 0 mV. From a quantitative analysis, it turned out that TGOT caused a reversible decrease in the sIPSC interval (the reciprocal of the instantaneous event frequency) and an increase in the amplitude, indicating a facilitation in the inhibitory transmission. This result is in agreement with electrophysiological experiments based on extracellular recordings performed on rats [Zaninetti & Raggenbass, 2000]. The effects elicited by TGOT on the inhibitory transmission are closely related to the activation of OTRs, widely described in CA1 area [Freund-Mercier et al., 1989; Tribollet et al., 1988; Barberis & Tribollet, 1996; Yoshimura et al., 1993]. Indeed, the perfusion of the antagonist selective for the murine isoform of OTRs returned the sIPSC interval and amplitude towards their control values.

The complete abolishment of sIPSCs during the application of bicuculline strongly suggested the involvement of $GABA_ARs$. It is known that binding of GABA to synaptic $GABA_ARs$, clustered opposite the release site, triggers the near-synchronous channel opening and thus the influx of Cl^- [Overstreet et al., 2002]. This mode of receptor activation is defined 'phasic' because of the short duration of the transient of GABA to which the synaptic $GABA_ARs$ are exposed [Farrant & Nusser, 2005].

Interestingly, we have shown that besides its effects on interval and amplitude of sIPSCs, TGOT also influenced the kinetic properties: in particular, the agonist was able to cause a significant increase in the sIPSC kinetics of decay. To interpret this surprising result, a brief digression is necessary. In general, the activation and deactivation kinetics of sIPSCs depend on the time constant of the synaptic GABA clearance and the biophysical properties of $GABA_ARs$ [Overstreet et al., 2002]. If the time course of the transients of GABA is short, the sIPSC decay is dominated by $GABA_AR$ deactivation, whose speed is greatly affected by their subunit composition and location [Jones & Westbrook, 1995]. For example, in the hippocampus, α5-containing $GABA_ARs$ that are located in a perisynaptic position (i.e., just outside the postsynaptic density) deactivate ~ 3-fold slower than synaptic receptors [Prenosil

et al., 2006]. This implies that the activation of perisynaptic $GABA_A$Rs generates sIPSCs slower than those generated by synaptic receptors.

On this basis, the slowing down of the kinetics of decay measured in a fraction of sIPSCs during TGOT application could be attributable to the activation of perisynaptic receptors. Generally, given their location and sensitivity to GABA reuptake inhibitors [Banks et al. 2000], perisynaptic $GABA_A$Rs are activated by spillover (i.e., the diffusion of the neurotransmitter far away from the synapse). The mechanism of spillover is promoted by the action potential-dependent release of multiple vesicles by the presynaptic terminal [Farrant & Nusser]: the higher is the firing activity of the presynaptic neuron, the higher is the neurotransmitter release and therefore the phenomenon of spillover. One possibility could be that TGOT would lead to the activation of perisynaptic $GABA_A$Rs by modulating the firing activity of GABAergic INs. Consistent with this hypothesis, the blockade of the action potential discharge in GABAergic cells was sufficient to prevent the effect elicited by TGOT on postsynaptic currents. In fact, during TGOT perfusion no significant changes could be measured in the time constant of decay of mIPSCs, recorded after having blocked the firing of INs. Furthermore, the absence of significant changes in the mIPSC interval and amplitude during TGOT perfusion strongly supported the involvement of presynaptic INs and the importance of TGOT in modulating their firing in the downstream effect.

Therefore, the proposed mechanism is the following: TGOT could induce GABAergic INs to release a larger amount of neurotransmitter in the synaptic cleft. Accordingly, GABA could bind a greater number of synaptic $GABA_A$Rs, thus explaining the increase in the sIPSC amplitude; moreover, because of the increase in neurotransmitter release, also the frequency of sIPSCs would increase, as observed. In addition, part of GABA could escape from the synapse and bind perisynaptic $GABA_A$Rs, whose deactivation is slower than that of synaptic receptors, explaining the slowing down of the sIPSC decay experimentally detected. All those effects are strictly dependent on the capability of INs to generate action potentials, since mIPSCs are not sensitive to TGOT.

In contrast to the inhibitory transmission, the glutamate receptor-mediated transmission was not significantly affected by TGOT, in agreement with literature [Tiberiis et al., 1983; Mühlethaler et al., 1984].

6.2 TGOT increases the extrasynaptic $GABA_AR$-mediated activity onto PYRs in $Otr^{+/+}$ mice

The data described so far indicate that TGOT is able to modulate the inhibitory transmission mediated by $GABA_ARs$ located at synaptic or perisynaptic sites on PYRs. In addition to synaptic and perisynaptic $GABA_ARs$, the presence of $GABA_ARs$ located in extrasynaptic sites has been reported [Song et al., 2011; Banks & Pearce, 2000; Scimemi et al., 2005; Mortensen & Smart, 2006; Pavlov et al., 2009]. The subunits of these receptors are associated to peculiar biophysical properties: for examples, in the hippocampus, α5-containing extrasynaptic $GABA_ARs$ have a higher affinity for GABA [Bohme et al., 2004] and desensitize more slowly [Caraiscos et al., 2004] than synaptic receptors. These properties allow them to respond to low levels of GABA present in the extracellular space [Bright & Smart, 2013], giving rise to a persistent (or 'tonic') inhibition of cells [Banks & Pearce, 2000; Scimemi et al., 2005; Mortensen & Smart, 2006; Pavlov et al., 2009]. The tonic activation of extrasynaptic $GABA_ARs$ was first identified in voltage-clamp recordings from rat cerebellar granule cells [Kaneda et al., 1995], where the perfusion of a saturating concentration of $GABA_AR$ antagonists not only blocked sIPSCs but also decreased the 'baseline holding current' required to clamp the cells at a given membrane potential. This current change was explained with an increase in the input resistance following $GABA_AR$ blockade: indeed, according to Ohm's law, when the input resistance increases, then the current must decrease to maintain the membrane potential at a set value in voltage-clamp mode. The standard method to estimate the tonic current is to quantify the shift as the difference between the 'baseline holding current' recorded during perfusion of a $GABA_AR$ antagonist and that recorded in control conditions. It is important to underline that the direction of the shift depends on two parameters: the holding potential (V_h) and the Nernst equilibrium potential for Cl^- (E_{Cl^-}). The shift is outward if V_h is negative and E_{Cl^-} is set to be close to 0 mV [Bright & Smart, 2013], while it is inward if V_h is positive and E_{Cl^-} is set to be close to the resting membrane potential. In our work, the presence of tonically active currents in CA1 PYRs was actually highlighted by an inward shift in the 'baseline holding current' elicited by bicuculline. The $GABA_AR$ antagonist was perfused at a concentration of 10 μM capable to block both synaptic and extrasynaptic $GABA_ARs$, in agreement with literature [Wlodarczyk et al., 2013].

In theory, the tonic current can be modulated by changes in GABA release or uptake and/or by changes in the number and properties of extrasynaptic $GABA_A$Rs [Farrant & Nusser, 2005]. For example, in GABAergic INs acetylcholine can facilitate the exocytosis of GABA leading to an increase in the external GABA concentration and therefore to the onset of tonic currents [Rossi et al., 2003]. Furthermore, kainate produces robust firing of GABAergic cells, causing an increase in extrasynaptic $GABA_A$R-mediated currents in CA1 PYRs [Frerking et al., 1999]. These examples clearly point out the correlation between the firing activity of GABA-releasing neurons and the magnitude of tonic currents: the link is given by GABA spillover that is promoted by a massive presynaptic activity and causes the activation of $GABA_A$Rs located in extrasynaptic sites [Farrant & Nusser, 2005]. As support of our hypothesis that TGOT could induce GABAergic INs to release a larger amount of neurotransmitter in the synaptic cleft, we explored the possibility that the agonist could be able to increase the magnitude of extrasynaptic $GABA_A$R-mediated currents onto PYRs. Indeed, a positive modulation of the tonic current was observed during TGOT perfusion, highlighted by an outward shift in the 'baseline holding current' recorded from PYRs, going exactly in the opposite direction to that evoked by bicuculline.
Overall, our results indicate that TGOT is able to increase not only the phasic (synaptic) but also the tonic (extrasynaptic) $GABA_A$R-mediated inhibition onto CA1 PYRs.

6.3 TGOT directly depolarizes a class of GABAergic INs

So far, our findings suggest a TGOT-mediated modulation of the inhibitory transmission in CA1. The next step was to investigate in detail the source of that increased inhibition onto PYRs. To this purpose, we tested the effect of TGOT directly on the membrane potential of CA1 GABAergic INs. Voltage responses were recorded starting either from a membrane potential of -70 mV or from spike threshold. We found that about 50% of INs examined at -70 mV responded to TGOT with a sustained depolarization, whereas the remaining percentage of cells did not respond to the agonist. Interestingly, the analysis of the firing pattern revealed that the majority of responding INs were stuttering fast-spiking cells, characterized by a high frequency firing rate, whereas the majority of non-responding INs were regular firing. This result is in agreement with data reported by Owen and colleagues [Owen et al., 2013]. In addition, we have shown that the totality of stuttering fast-spiking INs examined at their spike threshold displayed a depolarizing response to TGOT, together

with a significant increase in the firing rate. Accordingly, during perfusion of TGOT the number of action potentials generated per unit time was higher, leading to a likely increase in neurotransmitter release. These data clearly demonstrate that the facilitation in the $GABA_AR$-mediated transmission elicited by TGOT is due to an increase in the firing activity of a specific subpopulation of GABAergic INs.

Since the synaptic isolation of INs did not affect their ability to depolarize during TGOT administration, we can conclude that TGOT acts by binding directly OTRs expressed mainly by stuttering fast-spiking INs. This conclusion was corroborated by the observation that the blockade of OTRs was able to completely abolish the TGOT-induced depolarizing response. Furthermore, in neurons modulated by TGOT the presence of OTRs was confirmed by some single-cell reverse transcription (RT)-PCR experiments performed at the CNR Institute of neuroscience in Milan.

6.4 L-type voltage-gated Ca^{2+} channels may be involved in the TGOT-mediated effects in GABAergic INs

After having recognized the sub-population of GABAergic INs that respond to TGOT and express OTRs, we tried to identify the putative ionic mechanism involved in the TGOT-induced depolarization. OTRs are 'promiscuous' G protein coupled receptors (GPCR), being able to activate different G protein subtypes [Chini et al., 2008; Manning et al., 2008] coupled to different downstream pathways, in charge of different cell responses.

OTRs display high affinity for $G_{q/11}$ [Quian et al., 1998; Gimpl & Fahrenholz, 2001], whose activation stimulates phospholipase Cβ (PLCβ), leading to the production of inositol trisphosphate (IP3) and 1,2-diacylglycerol (DAG). IP3 triggers Ca^{2+} release from intracellular stores, whereas DAG stimulates protein kinase C (PKC) that in turn can phosphorylate different target proteins [Gimpl & Fahrenholz, 2001] including ionic channels. For example, the phosphorylation of L-type voltage-gated Ca^{2+} channels causes an increase in their current [Yang & Tsien, 1993; Weiss et al., 2012; Satin, 2013]. On this basis, it is reasonable to assume that an increase in the L-type current could be one of the mechanisms underlying the TGOT-induced depolarization. To test this hypothesis, we blocked the L-type channels using nifedipine: we found that nifedipine abolished the depolarization elicited by TGOT, indicating a putative involvement of the L-type current in the TGOT-mediated effect. It should be stressed that our recordings were performed starting

from -70 mV, a membrane potential at which the L-type currents are generally not active yet [Avery & Johnston, 1996]. However, some literature data report the presence of L-type channels whose activation occurs in a surprisingly negative range in the hippocampus [Avery & Johnston, 1996; Hasreiter et al., 2014], as well as in other brain regions [Regan et al., 1991; Koschak et al., 2001].

In order to better understand the role of this 'low threshold-activating' L-type current in the TGOT-mediated depolarization, more detailed experiments will be planned to evaluate the effect of the agonist directly on the current.

Finally, given the considerable heterogeneity of intracellular pathways activated by OTRs, we cannot exclude the involvement of other ionic currents modulated by TGOT that could contribute to generate the depolarization. For example, in our previous experiments performed on cell cultures we shown that the activation of OTRs could lead to the inhibition of inward rectifier potassium (IRK) channels. This action was mediated by a pertussis toxin-resistant G protein, presumably of the $G_{q/11}$ subtype, and by PLC [Gravati et al., 2010]. Therefore, TGOT could also inhibit IRK currents in CA1 GABAergic INs, thereby generating the depolarizing response.

6.5 TGOT decreases the excitability of PYRs in $Otr^{+/+}$ mice

In the last experiments, we proposed to investigate the consequences of TGOT perfusion on the membrane potential of PYRs.

Voltage responses of PYRs were recorded starting from -70 mV or starting from spike threshold: while at -70 mV PYRs did not respond to TGOT, at threshold most cells were hyperpolarized and their firing rate were significantly decreased. Interestingly, the hyperpolarizing response was completely abolished by the blockade of both $GABA_A$Rs and glutamatergic receptors. This fact implies that the TGOT-mediated effect is not direct but necessarily requires the activation of $GABA_A$Rs that mediate a hyperpolarizing current carried by Cl^-. Confirming the lack of a direct action on PYRs, the agonist was not able to modulate the excitatory transmission: this result clearly demonstrate that PYRs does not express OTRs. It should be stressed that in our experiments E_{Cl^-} was close to the resting membrane potential of PYRs: thus, at -70 mV the current flowing through $GABA_A$Rs was almost zero and consequently was not able to exert an evident hyperpolarizing effect. Conversely, at threshold, the driving force for Cl^- was increased and therefore the current

flowing through $GABA_A$Rs could hyperpolarize the cell. The long duration of the hyperpolarizing response suggests the involvement of extrasynaptic rather than synaptic $GABA_A$Rs: indeed, extrasynaptic $GABA_A$Rs give rise to a tonic inhibition that is much more prolonged than that mediated by synaptic $GABA_A$Rs [Farrant & Nusser, 2005]. Moreover, literature data clearly indicate that tonically active $GABA_A$Rs are able to hyperpolarize the membrane and reduce neuronal firing in many neurons [Walker & Kullmann]. A peculiar feature of tonic currents in CA1 PYRs is their marked outward rectification [Pavlov et al., 2009]: accordingly, the amplitude of currents is low at resting membrane potential, but it rapidly increases near threshold (-50 mV to -40 mV) [Pavlov et al., 2009]. Because of their outward rectification, tonic currents have a greater hyperpolarizing effect at threshold.

To sum up, TGOT causes a hyperpolarizing effect through the activation of extrasynaptic $GABA_A$Rs onto PYRs. The hyperpolarization becomes evident at threshold for two reasons: i) the membrane potential is far from E_{Cl^-} and this generates a driving force for Cl^- and ii) the amplitude of tonic currents carried by Cl^- rapidly increases as a result of their rectifying behavior.

Since the main consequence of the hyperpolarization is a reduction in cell excitability [Farrant & Nusser], we wondered if TGOT was able to alter the capability of PYRs to generate action potentials in response to depolarizing current steps. Our analysis revealed that in the presence of TGOT the firing frequency of PYRs was lower than that obtained in control conditions with the same current injection. This was also evident in the firing rate-to-injected current (F-I) relationship that was shifted to the right during perfusion of the agonist. The shift highlights an increase in the offset, i.e., the minimal intensity of injected current required to attain a response. As described in literature, an increase in the offset of the F-I curve (a subtractive operation) is attributable to an increase in tonically active inhibitory currents: this leads to a persistent reduction in the input resistance and therefore in cell excitability [Mithcell & Silver, 2003]. To note, the gain (i.e., the slope) of the F-I relationship was not influenced by TGOT in our experiments. This parameter is an index of the sensitivity of neurons to changes in the excitatory input [Pavlov et al., 2009]. The observation that TGOT caused a rightward shift in the curve without changing its slope is consistent with the effect on tonic currents: indeed, in hippocampal PYRs an increase in tonic inhibition modulates predominantly the neuronal offset and has minimal effect on neuronal gain [Pavlov et al., 2009].

7. CONCLUSIONS

The results of this work demonstrate that TGOT plays an important role on the hippocampal network, since it is able to modulate the inhibitory transmission onto PYRs located in CA1 *stratum pyramidale.*

The neuronal target of TGOT is represented mainly by stuttering fast-spiking GABAergic INs that respond to the agonist with a depolarization together with an increase in their firing rate. The action of TGOT on these cells is direct and is closely dependent on the presence of OTRs. One of the putative ionic mechanisms underlying the TGOT-induced depolarization could involve a peculiar L-type voltage-gated Ca^{2+} current, characterized by a 'low activation threshold'. However, given the considerable heterogeneity of intracellular pathways activated by OTR, we cannot exclude the involvement of other ionic currents that could contribute to generate the depolarization. Following the increase in their firing activity elicited by TGOT, stuttering fast-spiking INs release a greater amount of neurotransmitter in the extracellular space. Accordingly, GABA binds a greater number of synaptic $GABA_A$Rs with a higher probability, giving rise to wider and more frequent sIPSCs onto PYRs. In addition, part of neurotransmitter spreads outside the synapse and reaches perisynaptic $GABA_A$Rs located just outside the postsynaptic density: since these receptors desensitize more slowly than synaptic $GABA_A$Rs, it follows that their activation generates slower sIPSCs onto PYRs. When GABA spillover is massive, the neurotransmitter binds also extrasynaptic $GABA_A$Rs leading to an increase in the tonic current. This effect has direct consequences on PYRs: i) induces a prolonged hyperpolarization and ii) causes a persistent reduction in the input resistance. Together, these phenomena reduce the cell excitability and therefore the capability of PYRs to generate action potentials in response to excitatory inputs [Pavlov et al., 2009].

The proposed mechanism reveals that TGOT, by influencing the activity of hippocampal GABAergic INs, can regulate the operational modes of the downstream PYRs, possibly not only by modulating inhibition/disinhibition, but, eventually, also by inducing and maintaining network oscillation or by promoting plasticity [Freund & Buzsaki, 1996; Zaninetti & Raggenbass, 2000].

8. BIBLIOGRAPHY

ALBERI, S., DREIFUSS, J.J. & RAGGENBASS, M. (1997). The oxytocin-induced inward current in vagal neurons of the rat is mediated by G protein activation but not by an increase in the intracellular calcium concentration. *Eur J Neurosci* **9**, 2605-2612.

AMARAL, D.G. (1978). A Golgi study of cell types in the hilar region of the hippocampus in the rat. *J Comp Neurol* **182**, 851-914.

AMARAL, D.G., SCHARFMAN, H.E. & LAVENEX, P. (2007). The dentate gyrus: fundamental neuroanatomical organization (dentate gyrus for dummies). *Prog Brain Res* **163**, 3-22.

AMARAL, D.G. & WITTER, M.P. (1989). The three dimensional organization of the hippocampal formation: a review of anatomical data. *Neuroscience* **31**, 571-591.

ANDERSEN, P., MORRIS, R., AMARAL, D., BLISS, T. & O'KEEFE, J. (2007). The Hippocampus Book. Oxford University Press; New York.

AUDIGIER, S. & BARBERIS, C. (1985). Pharmacological characterization of two specific binding sites of neurohypophyseal hormones in hippocampal synaptic plasma membranes of the rat. *EMBO J* **4**, 1407-1412.

AVERY, R.B. & JOHNSTON, D.J. (1996). Multiple channel types contribute to the low-voltage-activated calcium current in hippocampal CA3 pyramidal neurons. *Neurosci* **16**, 5567-5582.

AZMITIA, E.C. & SEGAL, M. (1978). An autoradiography analysis of the differential ascending projections of the dorsal and the median raphe nuclei in the rat. *J Comp Neurol* **179**, 641-667.

BACCI, A., RUDOLPH, U., HUGUENARD, J.R. & PRINCE, D.A. (2003). Major differences in inhibitory synaptic transmission onto two neocortical interneuron subclasses. *J Neurosci* **23**, 9664-9674.

BANKS, M.I. & PEARCE, R.A. (2000). Kinetic differences between synaptic and extrasynaptic $GABA_A$ receptors in CA1 pyramidal cells. *J Neurosci* **20**, 937-948.

BANKS, M.I., WHITE, J.A. & PEARCE, R.A. (2000). Interactions between distinct $GABA_A$ circuits in hippocampus. *Neuron* **25**, 449-457.

BARBERIS, C., MOUILLAC, B. & DURROUX, T. (1998). Structural bases of vasopressin/oxytocin receptor function. *J Endocrinol* **156**, 223-229.

BARBERIS, C. & TRIBOLLET, E. (1996). Vasopressin and oxytocin receptors in the central nervous system *Crit Rev Neurobiol* **10**, 119-154.

BARBOUR, B. & HAUSSER, M. (1997). Intersynaptic diffusion of neurotransmitter. *Trends Neurosci* **20**, 377-384.

BARNARD, E.A., SKOLNICK, P., OLSEN, R.W., MOHLER, H., SIEGHART, W., BIGGIO, G., BRAESTRUP, C., BATESON, A.N. & LANGER, S.Z. (1998). International union of pharmacology. XV. Subtypes of γ-aminobutyric acid A receptors: classification on the basis of subunit structure and receptor function. *Pharmacol Rev* **50**, 291-313.

BELELLI, D., CASULA, A., LING, A. & LAMBERT, J.J. (2002). The influence of subunit composition on the interaction of neurosteroids with $GABA_A$ receptors. *Neuropharmacology* **43**, 651-661.

BIANCHI, M.T., HAAS, K.F. & MACDONALD, R.L. (2002). α1 and α6 subunits specify distinct desensitization, deactivation and neurosteroid modulation of $GABA_A$ receptors containing the δ subunit. *Neuropharmacology* **43**, 492-502.

BLOMFIELD, S. (1974). Arithmetical operations performed by nerve cells. *Brain Res* **69**, 115-124.

BOCKAERT, J. & PIN, J.P. (1999). Molecular tinkering of G protein-coupled receptors: an evolutionary success. *EMBO J* **18**, 1723-1729.

BOHME, I., RABE, H. & LUDDENS, H. (2994). Four amino acids in the α subunits determine the γ-aminobutyric acid sensitivities of $GABA_A$ receptor subtypes. *J Biol Chem* **279**, 35193-35200.

BOHUS, B., BORRELL, J., KOOLHAS, M., NYAKAS, C., BUWALDA, B., COMPAAN, J. & ROOZENDAAL, B. (1993). The neurohypophyseal peptides, and memory processing. *Ann NY Acad Sci* **689**,285-299.

BOILEAU, A.J., LI, T., BENKWITZ, C., CZAJKOWSKI, C. & PEARCE, R. A. (2003). Effects of γ2S subunit incorporation on $GABA_A$ receptor macroscopic kinetics. *Neuropharmacology* **44**, 1003-1012.

BORMANN, J. (2000). The 'ABC' of GABA receptors. *Trends Pharmacol Sci* **21**, 16-19.

BRICKLEY, S.G., CULL-CANDY, S.G. & FARRANT, M. (1996). Development of a tonic form of synaptic inhibition in rat cerebellar granule cells resulting from persistent activation of $GABA_A$ receptors. *J Physiol* **497**, 753-759.

BRICKLEY, S.G., CULL-CANDY, S.G. & FARRANT, M. (1999). Single channel properties of synaptic and extrasynaptic $GABA_A$ receptors suggest differential targeting of receptor subtypes. *J Neurosci* **19**, 2960-2973.

BRIGHT, D.P. & SMART, T.G. (2013). Methods for recording and measuring tonic $GABA_A$ receptor-mediated inhibition. *Front Neural Circuits* **7**, 193.

BROWN, N., KERBY, J., BONNERT, T. P., WHITING, P.J. & WAFFORD, K.A. (2002). Pharmacological characterization of a novel cell line expressing human α4β3δ $GABA_A$ receptors. *Br J Pharmacol* **136**, 965-974.

BRUSSAARD, A.B., KITS, K.S. & DE VLIEGER, T.A. (1996). Postsynaptic mechanism of depression of GABAergic synapses by oxytocin in the supraoptic nucleus of immature rat. *J Physiol* **497**, 495-507.

BUIJS, R.M., DE VRIES, G.J., VAN LEEUWEN, F.W. & SWAAB, D.F. (1983). Vasopressin and oxytocin: distribution and putative functions in the brain. *Prog Brain Res* **60**, 115-122.

BURKAT, P.M., YANG, J. & GINGRICH, K.J. (2001). Dominant gating governing transient $GABA_A$ receptor activity: a first latency and Po analysis. *J Neurosci* **21**, 7026-7036.

CARAISCOS, V.B., ELLIOTT, E.M., YOU-TEN, K.E., CHENG, V.Y., BELELLI, D., NEWELL, J.G., JACKSON, M.F., LAMBERT, J.J., ROSAHL, T.W., WAFFORD, K.A., MACDONALD, J.F. & ORSER, B.A. (2004). Tonic inhibition in mouse hippocampal CA1 pyramidal neurons is mediated by α*5* subunit containing γ-aminobutyric acid type A receptors. *PNAS (USA)* **101**, 3662-3667.

CHADDERTON, P., MARGRIE, T.W. & HAUSSER, M. (2004). Integration of quanta in cerebellar granule cells during sensory processing. *Nature* **428**, 856-860.

CHEN, L., WANG, H., VICINI, S. & OLSEN, R.W. (2000). The γ-aminobutyric acid type A ($GABA_A$) receptor-associated protein (GABARAP) promotes $GABA_A$ receptor clustering and modulates the channel kinetics. *PNAS (USA)* **97**, 11557-11562.

CHINI, B., MANNING, M. & GUILLON, G. (2008). Affinity and efficacy of selective agonists and antagonists for vasopressin and oxytocin receptors: an "easy guide" to receptor pharmacology. *Prog Brain Res* **170**, 513-517.

CHINI, B., MOUILLAC, B., ALA, Y., BALESTRE, M.N., TRUMPP, K.S., HOFLACK, J., ELANDS, J., HIBERT, M., MANNING, M., JARD, S., & BARBERIS, C. (1995). Tyr115 is the key residue for determining agonist selectivity in the V1a vasopressin receptor. *EMBO J* **14**, 2176-2182.

CHUNG, S.K., MCCABE, J.T. & PFAFF, D.W. (1991). Estrogen influences on oxytocin mRNA expression in preoptic and anterior hypothalamic regions studied by in situ hybridization. *J Comp Neurol* **307**, 281-295.

CLAIBORNE, B.J., AMARAL, D.G. & COWAN, W.M. (1986). A light and electron microscopic analysis of the mossy fibers of the rat dentate gyrus. *J Comp Neurol* **246**, 435-458.

COBB, S.R., BUHL, E.H., HALASY, K., PAULSEN, O. & SOMOGYI, P. (1995). Synchronization of neuronal activity in hippocampus by individual GABAergic interneurons. *Nature* **378**, 75-78.

COLQUHOUN, D. (1998). Binding, gating, affinity and efficacy: the interpretation of structure–activity relationships for agonists and of the effects of mutating receptors. *Br J Pharmacol* **125**, 924-947.

CONTRERAS, D. (2004). Electrophysiological classes of neocortical neurons. *Neural Networks* **17**, 633-646.

CRAIG, A. M., BLACKSTONE, C. D., HUGANIR, R.L. & BANKER, G. (1994). Selective clustering of glutamate and γ-aminobutyric acid receptors opposite terminals releasing the corresponding neurotransmitters. *PNAS (USA)* **91**, 12373-12377.

DANALACHE, B.A., GUTKOWSKA, J., SLUSARZ, M.J., BEREZOWSKA, I. & JANKOWSKI, M. (2010). Oxytocin-gly-lys-arg: a novel cardiomyogenic peptide. *PLoS ONE* **5**, e13643.

DELLER, T., MARTINEZ, A., NITSCH, R. & FROTSCHER, M. (1996). A novel entorhinal projection to the rat dentate gyrus: direct innervation of proximal dendrites and cell bodies of granule cells and GABAergic neurons. *J Neurosci* **16**, 3322-3333.

DE KOCK, C.P., BURNASHEV, N., LODDER, J.C., MANSVELDER, H.D. & BRUSSAARD, A.B. (2004). NMDA receptors induce somatodendritic secretion in hypothalamic neurones of lactating female rats. *J Physiol* **561**, 53-64.

DE WIED, D. (1965). The influence of the posterior and intermediate lobe of the pituitary and posterior peptides on the maintenance of conditioned avoidance response in rats. *Int J Neuropharmacol* **4**, 157-167.

DE WIED, D. (1991). The effects of neurohypophyseal hormones and related peptides on learning and memory processes. In: Frederickson, R. C., McGaugh, J. L., Felten, D. L., eds. Peripheral signalling of the brain. Toronto, Hogrefe and Hunter, pp. 335-350.

DONALDSON, Z.R. & YOUNG, L.J. (2008). Oxytocin, vasopressin and the neurogenetics of sociality. *Science* **322**, 900-904.

DURING, M.J. & SPENCER, D.D. (1993). Extracellular hippocampal glutamate and spontaneous seizure in the conscious human brain. *Lancet* **341**, 1607-1610.

ECCLES, J.C. (1969). The inhibitory pathways of the central nervous system. The Sherrington Lectures IX. Springfield, Ill. Charles C. Thomas.

FARINA LIPARI, E. & VALENTINO, B. (1993). Immunohistochemical research on vasopressin in the accessory hypothalamic nuclei. *Ital J Anat Embryol* **98**, 207-214.

FARINA LIPARI, E., VALENTINO, B. & LIPARI, D. (1995). Immunohistochemical research on oxytocin in the hypothalamic accessory nuclei. *Ital J Anat Embryol* **100**, 189-193.

FARRANT M. & NUSSER Z. (2005). Variations on an inhibitory theme: phasic and tonic activation of $GABA_A$ receptors. *Nat Rev Neurosci* **6**, 215-229.

FARRAR, S.J., WHITING, P.J., BONNERT, T.P. & MCKERNAN, R.M. (1999). Stoichiometry of a ligand-gated ion channel determined by fluorescence energy transfer. *J Biol Chem* **274**, 10100-10104.

FRERKING, M., PETERSEN, C.C.H. & NICOLL, R.A. (1999) Mechanisms underlying kainate receptor-mediated disinhibition in the hippocampus. *PNAS (USA)* **96**, 12917-12922.

FREUND, T.F. & ANTAL, M. (1988). GABA-containing neurons in the septum control inhibitory interneurons in the hippocampus. *Nature* **336**, 170-173.

FREUND, T.F. & BUZSAKI, G. (1996). Interneurons of the hippocampus. *Hippocampus* **6**, 347-470.

FREUND-MERCIER, M.J., PALACIOS, J.M., RIGO, M., WIEDERHOLD, K.H. & STOECKEL, M.E. (1989). Autoradiographic study of oxytocin specific binding sites in the human brain: characterization, distribution and modifications in some neurodegenerative diseases. *Eur J Neurosci Suppl* **2,** 123.

FRITSCHY, J.M., JOHNSON, D.K., MOHLER, H. & RUDOLPH, U. (1998). Independent assembly and subcellular targeting of $GABA_A$ receptor subtypes demonstrated in mouse hippocampal and olfactory neurons in vivo. *Neurosci Lett* **249**, 99-102.

GAINER, H., FIELD, R.L. & HOUSE, S.B. (2001). Vasopressin gene expression: experimental models and strategies. *Exp Neurol* **171**, 190-199.

GIMPL, G. & FAHRENHOLZ F. (2001). The oxytocin receptor system: structure, function, and regulation. *Physiol Rev* **81**, 629-683.

GIMPL, G., REITZ, J., BRAUER, S. & TROSSEN, C. (2008). Oxytocin receptors: ligand binding, signalling and cholesterol dependence. *Prog Brain Res* **170**, 193-204.

GOTTLIEB, D.I. & COWAN, W.M. (1973). Autoradiographic studies of the commissural and ipsilateral association connections of the hippocampus and dentate gyrus of the rat. *J Comp Neurol* **147**, 393-422.

GRAVATI, M., BUSNELLI, M., BULGHERONI, E., REVERSI, A., SPAIARDI, P., PARENTI, M., TOSELLI, M. & CHINI B. (2010). Dual modulation of inward rectifier potassium currents in olfactory neuronal cells by promiscuous G protein coupling of the oxytocin receptor. *J Neurochem* **114**, 1424-1435.

HAMANN, M., ROSSI, D.J. & ATTWELL, D. (2002). Tonic and spillover inhibition of granule cells control information flow through cerebellar cortex. *Neuron* **33**, 625-633.

HARA, Y., BATTEY, J. & GAINER, H. (1990). Structure of mouse vasopressin and oxytocin genes. *Brain Res Mol Brain Res* **8**, 319-324.

HASREITER, J., GOLDNAGL, L., BÖHM, S. & KUBISTA, H. (2014). Cav1.2 and Cav1.3 L-type calcium channels operate in a similar voltage range but show different coupling to Ca^{2+}-dependent conductances in hippocampal neurons. *Am J Physiol Cell Physiol* **306**, C1200-C1213.

HEINRICHS, M., VON DAWANS, B. & DOMES, G. (2009). Oxytocin, vasopressin, and human social behavior. *Front Neuroendocrinol* **30**, 548-557.

HEVERS, W. & LUDDENS, H. (1998). The diversity of $GABA_A$ receptors. Pharmacological and electrophysiological properties of $GABA_A$ channel subtypes. *Mol Neurobiol* **18**, 35-86.

HIRASAWA, M., SCHWAB, Y., NATAH, S., HILLARD, C.J., MACKIE, K., SHARKEY, K.A. & PITTMAN, Q.J. (2004). Dendritically released transmitters cooperate via autocrine and retrograde actions to inhibit afferent excitation in rat brain. *J Physiol* **559**, 611-624.

JENSEN, M.L., WAFFORD, K.A., BROWN, A.R., BELELLI, D., LAMBERT, J.J., & MIRZA, N.R. (2013). A study of subunit selectivity, mechanism and site of action of the δ selective compound 2 (DS2) at human recombinant and rodentnativeGABAA receptors. *Br J Pharmacol* **168**,1118-1132.

JIANG, L., SUN, S., NEDERGAARD, M. & KANG, J. (2000). Paired-pulse modulation at individual GABAergic synapses in rat hippocampus. *J Physiol* **523**, 425-439.

JOHNSTON, G.A. (2002). Medicinal chemistry and molecular pharmacology of $GABA_C$ receptors. *Curr Top Med Chem* **2**, 903-913.

JONAS, P., BISCHOFBERGER, J., FRICKER, D. & MILES, R. (2004). Interneuron diversity series: fast in, fast out-temporal and spatial signal processing in hippocampal interneurons. *Trends Neurosci* **27**, 30-40.

JONES, M.V. & WESTBROOK, G.L. (1995). Desensitized states prolong $GABA_A$ channel responses to brief agonist pulses. *Neuron* **15**, 181-191.

KAMINSKA, M., HARRIS, J., GIJSBERS, K., & DUBROVSKY, B. (2000). Dehydroepiandrosterone sulfate (DHEAS) counteracts decremental effects of corticosterone on dentate gyrus LTP. Implications for depression. *Brain Res Bull* **52**, 229-234.

KANEDA, M., FARRANT, M. & CULL-CANDY, S.G. (1995). Whole-cell and single-channel currents activated by GABA and glycine in granule cells of the rat cerebellum. *J Physiol* **485**, 419-435.

KAWAGUCHI, Y. (1993). Physiological, morphological, and histochemical characterization of three classes of interneurons in rat neostriatum. *J Neurosci* **13**, 4908-4923.

KIMURA, T., TANIZAWA, O., MORI, K., BROWNSTEIN, M.J. & OKAYAMA, H. (1992). Structure and expression of a human oxytocin receptor. *Nature* **356**, 526-529.

KISS A. & MIKKELSEN J.D. (2005). Oxytocin-anatomy and functional assignments: a minireview. *Endocr Regul* **39**, 97-105.

KLAUSBERGER, T. & SOMOGYI, P. (2008). Neuronal diversity and temporal dynamics: the unity of hippocampal circuit operations. *Science* **321**, 53-57.

KOCH, C. (1999). Biophysics of Computation. New York, Oxford University Press.

KOHLER, C., CHAN-PALAY, V. & WU, J.Y. (1984). Septal neurons containing glutamic acid decarboxylase immuno-reactivity project to the hippocampal region in the rat brain. *Anat Embryol* **169**, 41-44.

KOKSMA, J.J., VAN KESTEREN, R.E., ROSAHL, T.W., ZWART, R., SMIT, A.B., LÜDDENS, H. & BRUSSAARD, A.B. (2003). Oxytocin regulates neurosteroid modulation of $GABA_A$ receptors in supraoptic nucleus around parturition. *J Neurosci* **23**, 788-797.

KORSAKOV, S.S. (1889). Étude médico-psychologique sur une forme des maladies de mémoire. *Rev Philos* **28,** 501-530.

KOSCHAK, A., REIMER, D., HUBER, I., GRABNER, M., GLOSSMANN, H., ENGEL, J. & STRIESSNIG, J. (2001). Alpha 1D (Cav1.3) subunits can form L-type Ca^{2+} channels activating at negative voltages. *J Biol Chem* **276**, 22100-22106.

KULLMANN, D.M. (2000). Spillover and synaptic cross talk mediated by glutamate and GABA in the mammalian brain. *Prog Brain Res* **125**, 339-351.

KULLMANN, D.M. & SEMYANOV, A. (2002). Glutamatergic modulation of GABAergic signalling among hippocampal interneurons: novel mechanisms regulating hippocampal excitability. *Epilepsia* **43**,174-178.

KULLMANN, D.M., RUIZ, A., RUSAKOV, D.M., SCOTT, R., SEMYANOV, A. & WALKER, M.C. (2005). Presynaptic, extrasynaptic and axonal $GABA_A$ receptors in the CNS: where and why? *Prog Biophys Mol Biol* **87**, 33-46.

LEE, H.J., CALDWELL, H.K., MACBETH, A.H., TOLU, S.G. & YOUNG, W.S. (2008). A conditional knock-out mouse line of the oxytocin receptor. *Endocrinology* **149**, 3256-3263.

LEAO, R.M., MELLOR, J.R. & RANDALL, A.D. (2000). Tonic benzodiazepine-sensitive GABAergic inhibition in cultured rodent cerebellar granule cells. *Neuropharmacology* **39**, 990-1003.

LESTER, H.A., DIBAS, M.I., DAHAN, D.S., LEITE, J.F. & DOUGHERTY, D.A. (2004) Cys-loop receptors: new twists and turns. *Trends Neurosci* **27**, 329-336.

LOTURCO, J.J., OWENS, D.F., HEATH, M.J., DAVIS, M.B. & KRIEGSTEIN, A.R. (1995). GABA and glutamate depolarize cortical progenitor cells and inhibit DNA synthesis. *Neuron* **15**, 1287-1298.

LUDWIG, M. (1998). Dendritic release of vasopressin and oxytocin. *J Neuroendocrinol* **10**, 881-895.

LUDWIG, M. & LENG, G. (2006). Dendritic peptide release and peptide-dependent behaviours. *Nat Rev Neurosci* **7**, 126-136.

LUDWIG, M., CALLAHAN, M.F., NEUMANN, I., LANDGRAF, R. & MORRIS, M. (1994). Systemic osmotic stimulation increases vasopressin and oxytocin release within the supraoptic nucleus. *J Neuroendocrinol* **6**, 369-373.

LUSCHER, B. & KELLER, C.A. (2004). Regulation of $GABA_A$ receptor trafficking, channel activity and functional plasticity of inhibitory synapses. *Pharmacol Ther* **102**, 195-221.

MACCAFERRI, G. & MCBAIN, J.C. (1996). Long-term potentiation in distinct subtypes of hippocampal non-pyramidal neurons. *J Neurosci* **16**, 5334-5343.

MACCAFERRI, G. & LACAILLE, J.C. (2003). Interneuron diversity series: hippocampal interneuron classifications - making things as simple as possible, not simpler. *Trends Neurosci* **26**, 564-571.

MACLEAN, P.D. (1949). Psychosomatic disease and the "visceral brain": recent developments bearing on the Papez theory of emotion. *Psychosom Med* **11**, 338-353.

MANNING, M., STOEV, S., CHINI, B., DURROUX, T., MOUILLAC, B. & GUILLON, G. (2008). Peptide and non-peptide agonists and antagonists for the vasopressin and oxytocin V1a, V1b, V2 and OT receptors: research tools and potential therapeutic agents. *Prog Brain Res* **170**, 473-512.

MARKRAM, H., TOLEDO-RODRIGUEZ, M., WANG, Y., GUPTA, A., SILBERBERG, G., WU, C. (2004). Interneurons of the neocortical inhibitory system. *Nat Rev Neurosci* **5**, 793-807.

MARTINA, M., COMAS, T. & MEALING, G.A. (2013). Selective pharmacological modulation of pyramidal neurons and interneurons in the CA1 region of the rat hippocampus. *Front Pharmacol* **4**, 24.

MCCLELLAN, A.M. & TWYMAN, R.E. (1999). Receptor system response kinetics reveal functional subtypes of native murine and recombinant human $GABA_A$ receptors. *J Physiol* **515**, 711-727.

MCKERNAN, R.M. & WHITING, P.J. (1996). Which $GABA_A$-receptor subtypes really occur in the brain? *Trends Neurosci* **19**, 139-143.

MELLOR, J.R. & RANDALL, A.D. (2001). Synaptically released neurotransmitter fails to desensitize postsynaptic $GABA_A$ receptors in cerebellar cultures. *J Neurophysiol* **85**, 1847-1857.

MEYER-LINDENBERG, A., DOMES, G., KIRSCH, P. & HEINRICHS, M. (2011). Oxytocin and vasopressin in the human brain: social neuropeptides for translational medicine. *Nat Rev Neurosci* **12**, 524-538.

MILES, R., TOTH, K., GULYAS, A.I., HAJOS, N. & FREUND, T.F. (1996). Differences between somatic and dendritic inhibition in the hippocampus. *Neuron* **16**, 815-823.

MILLIGAN, C.J., BUCKLEY, N.J., GARRET, M., DEUCHARS, J. & DEUCHARS, S.A. (2004). Evidence for inhibition mediated by coassembly of $GABA_A$ and $GABA_C$ receptor subunits in native central neurons. *J Neurosci* **24**, 9241-9250.

MITCHELL, S.J. & SILVER, R.A. (2003). Shunting inhibition modulates neuronal gain during synaptic excitation. *Neuron* **38**, 433-445.

MODY, I. (2001). Distinguishing between $GABA_A$ receptors responsible for tonic and phasic conductances. *Neurochem Res* **26**, 907-913.

MODY, I., DE KONINCK, Y., OTIS, T.S. & SOLTESZ, I. (1994). Bridging the cleft at GABA synapses in the brain. *Trends Neurosci* **17**, 517-525.

MOLLEMAN, A. (2003). Patch clamping: an introductory guide to patch clamp electrophysiology. John Wiley & Sons, Ltd.

MORIMOTO, K. & GODDARD, G.V. (1985). Effects of thyrotropin-releasing hormone on evoked responses and long-term potentiation in dentate gyrus of rat. *Exp Neurol* **90**, 401-410.

MORTENSEN, M. & SMART, T.G. (2006). Extrasynaptic alpha beta subunit $GABA_A$ receptors on rat hippocampal pyramidal neurons. *J Physiol* **577**, 841-856.

MORTENSEN, M., EBERT, B., WAFFORD, K. & SMART, T.G. (2010). Distinct activities of GABA agonists at synaptic- and extrasynaptic-type $GABA_A$ receptors. *J Physiol* **588**, 1251-1268.

MORTENSEN, M., KRISTIANSEN, U., EBERT, B., FROLUND, B., KROGSGAARD-LARSEN, P. & SMART, T.G. (2004). Activation of single heteromeric $GABA_A$ receptor ion channels by full and partial agonists. *J Physiol* **557**, 389-413.

MÜHLETHALER, M., CHARPAK, S. & DREIFUSS J.J. (1984). Contrasting effects of neurohypophysial peptides on pyramidal and non-pyramidal neurones in the rat hippocampus. *Brain Res* **308**, 97-107.

MÜHLETHALER, M., SAWYER, W.H., MANNING, M.M. & DREIFUSS J.J. (1983). Characterization of a uterine-type oxytocin receptor in the rat hippocampus. *PNAS (USA)* **80**, 6713-6717.

NEELANDS, T.R., FISHER, J.L., BIANCHI, M. & MACDONALD, R.L. (1999). Spontaneous and γ-aminobutyric acid (GABA)-activated $GABA_A$ receptor channels formed by ε subunit-containing isoforms. *Mol Pharmacol* **55**, 168-178.

NEELANDS, T.R. & MACDONALD, R.L. (1999). Incorporation of the π subunit into functional γ-aminobutyric acid A receptors. *Mol Pharmacol* **56**, 598-610.

NEHER, E. & SAKMANN, B. (1976a). Single-channel currents recorded from membrane of denervated frog muscle fibres. *Nature* **260**,799-802.

NEHER, E. & SAKMANN, B. (1976b). Noise analysis of drug induced voltage clamp currents in denervated frog muscle fibres. *J Physiol* **258**, 705-729.

NUSSER, Z. & MODY, I. (2002). Selective modulation of tonic and phasic inhibitions in dentate gyrus granule cells. *J Neurophysiol* **87**, 2624-2628.

NUSSER, Z., CULL-CANDY, S. & FARRANT, M. (1997). Differences in synaptic $GABA_A$ receptor number underlie variation in GABA mini amplitude. *Neuron* **19**, 697-709.

NUSSER, Z., ROBERTS, J.D.B., BAUDE, A., RICHARDS, J. G. & SOMOGYI, P. (1995). Relative densities of synaptic and extrasynaptic $GABA_A$ receptors on cerebellar granule cells as determined by a quantitative immunogold method. *J Neurosci* **15**, 2948-2960.

NUSSER, Z., SIEGHART, W. & MODY, I. (1999). Differential regulation of synaptic $GABA_A$ receptors by cAMP-dependent protein kinase in mouse cerebellar and olfactory bulb neurones. *J Physiol* **521**, 421-435.

NUSSER, Z., SIEGHART, W. & SOMOGYI, P. (1998). Segregation of different $GABA_A$ receptors to synaptic and extrasynaptic membranes of cerebellar granule cells. *J Neurosci* **18**, 1693-1703.

O'MARA, S.M., COMMINS, S., ANDERSON, M. & GIGG, J. (2001). The subiculum: a review of form, physiology and function. *Prog Neurobiol* **64**, 129-155.

OKADA, M., ONODERA, K., VAN RENTERGHEM, C., SIEGHART, W. & TAKAHASHI, T. (2000). Functional correlation of $GABA_A$ receptor α subunits expression with the properties of IPSCs in the developing thalamus. *J Neurosci* **20**, 2202-2208.

OVERSTREET, L.S., JONES, M.V. & WESTBROOK, G.L. (2000). Slow desensitization regulates the availability of synaptic $GABA_A$ receptors. J Neurosci **20**, 7914-7921.

OVERSTREET, L.S., WESTBROOK, G.L. & JONES, M.V. (2002). In: Transmembrane Transporters, ed. Quick, M. W. , Wiley-Liss Inc., Hoboken, New Jersey, 2002, pp. 259-275.

OWEN, S.F., TUNCDEMIR, S.N., BADER, P.L., TIRKO, N.N., FISHELL, G. & TSIEN R.W. (2013). Oxytocin enhances hippocampal spike transmission by modulating fast-spiking interneurons. *Nature* **500**, 458-462.

OWENS, D.F., LIU, X. & KRIEGSTEIN, A.R. (1999). Changing properties of $GABA_A$ receptor-mediated signalling during early neocortical development. *J Neurophysiol* **82**, 570-583.

PAPEZ, J.W. (1937). A proposed mechanism of emotion. *Arch Neurol Psychiatry* **38**, 725-743.

PAVLOV, I., SAVTCHENKO, L.P., KULLMANN, D.M., SEMYANOV, A. & WALKER, M.C. (2009). Outwardly rectifying tonically active $GABA_A$ receptors in pyramidal cells modulate neuronal offset, not gain. *J Neurosci* **29**, 15341-15350.

PAWELZIK, H., HUGHES, D.I. & THOMSON, A.M. (2002). Physiological and morphological diversity of immunocytochemically defined parvalbumin- and cholecystokinin-positive interneurones in CA1 of the adult rat hippocampus. *J Comp Neurol* **443**, 346-367.

PAXINOS (2015). The rat nervous system (Fourth Edition) Elsevier-Academic Press.

PETRINI, E.M., MARCHIONNI, I., ZACCHI, P., SIEGHART, W. & CHERUBINI, E. (2004). Clustering of extrasynaptic $GABA_A$ receptors modulates tonic inhibition in cultured hippocampal neurons. *J Biol Chem* **279**, 45833-45843.

POSTINA, R., KOJRO, E. & FAHRENHOLZ, F. (1996). Separate agonist and peptide antagonist binding sites of the oxytocin receptor defined by their transfer into the V2 vasopressin receptor. *J Biol Chem* **271**, 31593-31601.

POUILLE, F. & SCANZIANI, M. (2001). Enforcement of temporal fidelity in pyramidal cells by somatic feed-forward inhibition. *Science* **293**, 1159-1163.

POULAIN, D.A. & WAKERLEY, J.B. (1982). Electrophysiology of hypothalamic magnocellular neurones secreting oxytocin and vasopressin. *Neuroscience* **7**, 773-808.

POW, D.V. & MORRIS, J.F. (1989). Dendrites of hypothalamic magnocellular neurons release neurohypophysial peptides by exocytosis. *Neuroscience* **32**, 435-439.

PRENOSIL, G.A, SCHNEIDER GASSER, E.M, RUDOLPH, U., KEIST, R., FRITSCHY, J.M. & VOGT, K.E. (2006). Specific subtypes of $GABA_A$ receptors mediate phasic and tonic forms of inhibition in hippocampal pyramidal neurons. *J Physiol* **96**, 846-857.

QIAN, A., WANG, W. & SANBORN, B.M. (1998). Evidence for the involvement of several intracellular domains in the coupling of oxytocin receptor to $G_{\alpha(q/11)}$. *Cell Signal* **10**, 101-105.

QIAN, H. & RIPPS, H. (1999). Response kinetics and pharmacological properties of heteromeric receptors formed by coassembly of GABA ρ- and γ2-subunits. *Proc R Soc Lond B* **266**, 2419-2425.

RAGGENBASS, M. (2001). Vasopressin- and oxytocin-induced activity in the central nervous system: electrophysiological studies using in-vitro systems. *Prog Neurobiol* **64**, 307-326.

RAGGENBASS, M., TRIBOLLET, E., DUBOIS-DAUPHIN, M. & DREIFUSS J.J. (1989). Correlation between oxytocin neuronal sensitivity and oxytocin receptor binding: an electrophysiological and autoradiographical study comparing rat and guinea pig hippocampus. *PNAS (USA)* **86**, 750-754.

RAMÓN Y CAJAL, S. (1893). Estructura del asta de Ammon y fascia dentata. *Ann Soc Esp Hist Nat* **22**.

RAO, V.V., LOFFLER, C., BATTEY, J. & HANSMANN, I. (1992). The human gene for oxytocin-neurophysin I (OXT) is physically mapped to chromosome 20p13 by in situ hybridization. *Cytogenet Cell Genet* **61**, 271-273.

RATHENBERG, J., KITTLER, J.T. & MOSS, S.J. (2004). Palmitoylation regulates the clustering and cell surface stability of GABAA receptors. *Mol Cell Neurosci* **26**, 251-257.

REGAN, L.J., SAH, D.W.Y. & BEAN, B.P. (1991). Ca^{2+} channels in rat central and peripheral neurons: high-threshold current resistant to dihydropyridine blockers and v -conotoxin. *Neuron* **6**, 269-280.

RIBAK, C.E., VAUGHN, J.E., SAITO, K. (1978). Immunocytochemical localization of glutamic acid decarboxylase in neuronal somata following colchicine inhibition of axonal transport. *Brain Res* **140**, 315-332.

RIBOT, T. (1881). Les maladies de la mémoire. Paris: Ballière.

ROSENBAUM, R.S., PRISELAC, S., KOHLER, S., BLACK, S.E., GAO, F., NADEL, L. & MOSCOVITCH, M. (2000). Remote spatial memory in an amnesic person with extensive bilateral hippocampal lesions. *Nat Neurosci* **3**, 1044-1048.

ROSSI, D.J., HAMANN, M. & ATTWELL, D. (2003). Multiple modes of GABAergic inhibition of rat cerebellar granule cells. *J Physiol* **548**, 97-110.

RUISSEN, M. & DE BRUIJN, E. (2015). Is it me or is it you? Behavioral and electrophysiological effects of oxytocin administration on self-other integration during joint task performance. *Cortex* **70**,146-154.

SALA, M., BRAIDA, D., LENTINI, D., BUSNELLI, M., BULGHERONI, E., CAPURRO, V., FINARDI A., DONZELLI, A., PATTINI, L., RUBINO, T., PAROLARO, D., NISHIMORI, K., PARENTI, M. & CHINI B. (2011). Pharmacologic rescue of impaired cognitive flexibility, social deficits, increased aggression, and seizure susceptibility in oxytocin receptor null mice: a neurobehavioral model of autism. *Biol Psychiatry* **69**, 875-882.

SATIN, J. (2013). The long and short of PKC modulation of the L-type calcium channel. *Channel (Austin)* **7**, 57-58.

SCIMEMI, A., SEMYANOV, A., SPERK, G., KULLMANN, D.M. & WALKER, M.C. (2005). Multiple and plastic receptors mediate tonic $GABA_A$ receptor currents in the hippocampus. *J Neurosci* **25**, 10016-10024.

SCOVILLE, W. & MILNER, B. (1957). Loss of recent memory after bilateral hippocampal lesions. *J Neurol Neurosurg Psychiatry* **20**, 11-21.

SEGAL, M. & LANDIS, S. (1974). Afferents to the hippocampus of the rat studied with the method of retrograde transport of horseradish peroxidase. *Brain Res* **78**, 1-15.

SEMYANOV, A., WALKER, M.C. & KULLMANN, D.M. (2003). GABA uptake regulates cortical excitability via cell type-specific tonic inhibition. *Nature Neurosci* **6**, 484-490.

SIEGEL, G.J., ALBERTS, R.W., BRADY, S. & PRICE D.L. (2006). Basic neurochemestry: molecular, cellular and medical aspects. 7th ed. Elsevier-Academic Press; San Diego, CA, pp. 267-290.

SIEGHART, W. & SPERK, G. (2002). Subunit composition, distribution and function of $GABA_A$ receptor subtypes. *Curr Top Med Chem* **2**, 795-816.

SIMON, J., WAKIMOTO, H., FUJITA, N., LALANDE, M. & BARNARD, E.A. (2004). Analysis of the set of $GABA_A$ receptor genes in the human genome. *J Biol Chem* **279**, 41422-41435.

SOFRONIEW, M.V. & WEINDL, A. (1978). Extrahypothalamic neurophysin-containing perikarya, fiber pathways and fiber clusters in the rat brain. *Endocrinology* **102**, 334-337.

SOMOGYI, P., FRITSCHY, J.M., BENKE, D., ROBERTS, J.D. & SIEGHART, W. (1996). The $\gamma 2$ subunit of the $GABA_A$ receptor is concentrated in synaptic junctions containing the $\alpha 1$ and $\beta 2/3$ subunits in hippocampus, cerebellum and globus pallidus. *Neuropharmacology* **35**, 1425-1444.

SOMOGYI, P.P. & KLAUSBERGER, T. (2005). Defined types of cortical interneurone structure space and spike timing in the hippocampus. *J Physiol* **562**, 9-26.

SONG, I., SAVTCHENKO, L. & SEMYANOV A. (2011). Tonic excitation or inhibition is set by $GABA_A$ conductance in hippocampal interneurons. *Nat Commun* **2**, 36.

SORIANO, E. & FROTSCHER, M. (1989). A GABAergic axo-axonic cell in the fascia dentata controls the main excitatory hippocampal pathway. *Brain Res* **503**, 170-174.

SPRUSTON, N., SCHILLER, Y., STUART, G. & SAKMANN, B. (1995). Activity dependent action potential invasion and calcium influx into hippocampal CA1 dendrites. *Science* **268**, 297-300.

STEWARD, O. (1976). Topographic organization of the projections from the entorhinal area to the hippocampal formation of the rat. *J Comp Neurol* **167**, 285-314.

STEWARD, O. & SCOVILLE, S.A. (1976). Cells of origin of entorhinal cortical afferents to the hippocampus and fascia dentata of the rat. *J Comp Neurol* **169**, 347-70.

STEWARD, O. & VINSANT, S.L. (1983). The process of reinnervation in the dentate gyrus of the adult rat: a quantitative electron microscopic analysis of terminal proliferation and reactive synaptogenesis. *J Comp Neurol* **214**, 370-386.

STOOP, R. (2012). Neuromodulation by Oxytocin and Vasopressin. *Neuron* **76**, 142-159.

STOOP, R. & PRALONG. E. (2000). Functional connections and epileptic spread between hippocampus, entorhinal cortex and amygdala in a modified horizontal slice preparation of the rat brain. *Eur J Neurosci* **12**, 3651-3663.

SZABÓ, G.G., HOLDERITH, N., GULYÁS, A.I., FREUND, T.F. & HÁJOS, N. (2010). Distinct synaptic properties of perisomatic inhibitory cell types and their different modulation by cholinergic receptor activation in the ca3 region of the mouse hippocampus. *Eur J Neurosci* **31**, 2234-2246.

TAMAMAKI, N., YANAGAWA, Y., TOMIOKA, R., MIYAZAKI, J., OBATA, K. & KANEKO T. (2003). Green fluorescent protein expression and colocalization with calretinin, parvalbumin, and somatostatin in the GAD67-GFP knock-in mouse. *J Comp Neurol* **467**, 60-79.

TENG, E. & SQUIRE, L.R. (1999). Memory for places learned long ago is intact after hippocampal damage. *Nature* **400**, 675-677.

TIA, S., WANG, J.F., KOTCHABHAKDI, N. & VICINI, S. (1996). Distinct deactivation and desensitization kinetics of recombinant $GABA_A$ receptors. *Neuropharmacology* **35**, 1375-1382.

TIBERIIS, B.E., MCLENNAN, H. & WILSON, N. (1983). Neurohypophysial peptides and the hippocampus. II. Excitation of rat hippocampal neurones by oxytocin and vasopressin applied in vitro. *Neuropeptides* **4**, 73-86.

TOMIZAWA, K., IGA, N., LU, Y.F., MORIWAKI, A., MATSUSHITA, M., LI, S.T., MIYAMOTO, O, ITANO, T. & MATSUI, H. (2003). Oxytocin improves long-lasting spatial memory during motherhood through MAP kinase cascade. *Nat Neurosci* **6**, 384-390.

TRETTER, V., EHYA, N., FUCHS, K. & SIEGHART, W. (1997). Stoichiometry and assembly of a recombinant $GABA_A$ receptor subtype. *J Neurosci* **17**, 2728-2737.

TRIBOLLET, E., BARBERIS, C., JARD, S., DUBOIS, D.M. & DREIFUSS, J.J. (1988). Localization and pharmacological characterization of high affinity binding sites for vasopressin and oxytocin in the rat brain by light microscopic autoradiography. *Brain Res* **442**, 105-118.

URBANOSKI, K., HARRIS, J., GIJSBERS, K. & DUBROVSKY, B. (2000). Effects of androsterone sulfate on the population spike of the rat dentate gyrus following tetanization. *Physiol Behav* **71**, 435-440.

VALEYEV, A.Y., CRUCIANI, R.A., LANGE, G.D., SMALLWOOD, V.S. & BARKER, J.L. (1993). Cl^- channels are randomly activated by continuous GABA secretion in cultured embryonic rat hippocampal neurons. *Neurosci Lett* **155**, 199-203.

VAN GROEN, T. & WYSS, J.M. (1990). Extrinsic projections from area CA1 of the rat hippocampus: olfactory, cortical, subcortical and bilateral hippocampal formation projections. *J Comp Neurol* **302**, 515-528.

VAN GROEN, T., VAN HAREN, F., WITTER, M.P. & GROENEWEGEN. H.J. (1986). Organization of the reciprocal connections between the subiculum and the entorhinal cortex in the cat. *J Comp Neurol* **250**, 485-497.

WAFFORD, K.A., VAN NIEL, M.B., MA, Q.P., HORRIDGE, E., HERD, M.B., PEDEN, D.R., BELELLI, D. & LAMBERT, J.J. (2009). Novel compounds selectively enhance delta subunit containing $GABA_A$ receptors and increase tonic currents in thalamus. *Neuropharmacology* **56**, 182-189.

WALKER, M.C. & KULLMANN, D.M. Tonic GABAA Receptor-Mediated Signaling in Epilepsy. Jasper's Basic Mechanisms of the Epilepsies [Internet]. 4th edition.

WALL, M.J. & USOWICZ, M.M. (1997). Development of action potential-dependent and independent spontaneous $GABA_A$ receptor-mediated currents in granule cells of postnatal rat cerebellum. *Eur J Neurosci* **9**, 533–548.

WANG, H., BEDFORD, F.K., BRANDON, N.J., MOSS, S.J. & OLSEN, R.W. (1999). GABA(A)-receptor-associated protein links GABA(A) receptors and the cytoskeleton. *Nature* **397**, 69-72.

WANG, Q., LIU, L., PEI, L., JU, W., AHMADIAN, G., LU, J., WANG, Y., LIU, F. & WANG, Y.T. (2003). Control of synaptic strength, a novel function of Akt. *Neuron* **38**, 915-928.

WEI, W., ZHANG, N., PENG, Z., HOUSER, C. R. & MODY, I. (2003). Perisynaptic localization of δsubunit-containing $GABA_A$ receptors and their activation by GABA spillover in the mouse dentate gyrus. *J Neurosci* **23**, 10650-10661.

WEISS, S., KEREN-RAIFMAN, T., OZ, S., BEN MOCHA, A., HAASE, H. & DASCAL N. (2012). Modulation of distinct isoforms of L-type calcium channels by $G_{(q)}$-coupled receptors in Xenopus oocytes: antagonistic effects of $G_{\beta\gamma}$ and protein kinase C. *Channel (Austin)* **6**, 426-437.

WERNICKE, C. (1881). Lehrbuch der Gehirnkrankheiten, vol 2. Berlin: Theodore Fischer.

WHITING, P.J. (2003). $GABA_A$ receptor subtypes in the brain: a paradigm for CNS drug discovery? *Drug Discov Today* **8**, 445-450.

WITTER, M.P. & AMARAL, D.G. (2004). Hippocampal Formation. The Rat Nervous System (Third Edition) Academic Press, Burlington, pp. 635-704.

WLODARCZYK, A.I., SYLANTYEV, S., HERD, M.B., KERSANTÉ, F., LAMBERT, J.J., RUSAKOV, D.A., LINTHORST, A.C., SEMYANOV, A., BELELLI, D., PAVLOV, I. & WALKER, M.C. (2013). GABA-independent $GABA_A$ receptor openings maintain tonic currents. *J Neurosci* **33**, 3905-3914.

WOHLFARTH, K.M., BIANCHI, M.T. & MACDONALD, R.L. (2002). Enhanced neurosteroid potentiation of ternary GABAA receptors containing the delta subunit. *J Neurosci* **22**, 1541-1549.

WYSS, J. M., SWANSON, L. W. & COWAN, W. M. (1979). A study of subcortical afferents to the hippocampal formation in the rat. *Neuroscience* **4**, 463-476.

YAMADA, J., YAMAMOTO, S., UENO, S., FURUKAWA, T. & FUKUDA, A. (2004). $GABA_A$ receptor-mediated tonic inhibition in rat somatosensory cortex. FENS Forum Abstr.2, A083.027.

YAMAMOTO, C. & MCILWAIN, H. (1966a). Potentials evoked in vitro in preparations from the mammalian brain. *Nature* **210**, 1055-1056.

YAMAMOTO, C. & MCILWAIN, H. (1966b). Electrical activities in thin sections from the mammalian brain maintained in chemically-defined media in vitro. *J Neurochem* **13**, 1333-1343.

YANG, J., TSIEN, R.W. (1993). Enhancement of N- and L-type calcium channel currents by protein kinase C in frog sympathetic neurons. *Neuron* **10**, 127-136.

YANG, M., WANG, W., ZHONG, M., PHILIPPI, A., OLIVIER LICHTARGE, O. & SANBORN, B.M. (2002). Lysine 270 in the third intracellular domain of the oxytocin receptor is an important determinant for G a(q) coupling specificity. *Mol Endocrinol* **16**, 814-823.

YOSHIMURA, R., KIYAMA, H., KIMURA, T., ARAKI, T., MAENO, H., TANIZAWA, O. & TOHYAMA M. (1993). Localization of oxytocin receptor messenger ribonucleic acid in the rat brain. *Endocrinology* **133**, 1239-1246.

ZANINETTI, M. & RAGGENBASS, M. (2000). Oxytocin receptor agonists enhance inhibitory synaptic transmission in the rat hippocampus by activating interneurons in stratum pyramidale. *Eur J Neurosci* **12**, 3975-3984.

ZINGG, H.H. & LAPORTE, S.A. (2003). The oxytocin receptor. *Trends Endocrinol Metab* **4**, 222-227.